THE COMPOUND JET

A NEW METHOD TO GENERATE FLUID JETS FOR INK JET PRINTING

BENGT HERMANRUD

1981

DEPARTMENT
OF
ELECTRICAL MEASUREMENTS

INSTITUTIONEN FÖR ELEKTRISK MÄTTEKNIK
LUNDS TEKNISKA HÖGSKOLA - LUNDS UNIVERSITET
LUND - SWEDEN

Digitized by the Internet Archive
in 2026

https://archive.org/details/IA41553201_0043

THE COMPOUND JET -
A NEW METHOD TO GENERATE FLUID JETS
FOR INK JET PRINTING

Bengt Hermanrud

Report 1/1981
Department of Electrical Measurements
Lund Institute of Technology

LUTEDX/(TEEM-1006)/1-143/(1981)

UNIV.
LEIDEN
BIBL.

CONTENTS

		Page
SUMMARY		1
1	INTRODUCTION	2
	1.1 The present use of ink jets	2
	1.2 Historical development of ink jet technology	2
	1.3 Ink problems in earlier systems	9
2	COMPOUND JET PRINCIPLE	11
	2.1 Description of a compound jet	11
	2.2 Instabilities. Comparison between compound and conventional jet	14
3	EXPERIMENTAL METHOD	17
	3.1 Compound jet assembly geometry	17
	3.1.1 Primary jet nozzle	17
	3.1.2 Secondary fluid chamber	20
	3.2 Compound jet fluid systems	24
	3.2.1 Primary jet	24
	3.2.2 Secondary fluid system	26
	3.3 Photographic methods	29
4	INVESTIGATION OF FLOW PATTERN IN THE STABLE COMPOUND JET	39
	4.1 Introduction	39
	4.2 Flow pattern inside secondary fluid	39
	4.3 Flow pattern at fluid/air boundary	46
	4.4 Flow pattern inside laminar compound jet	48
	4.5 Transfer of momentum inside the compound jet	57
	4.6 Qualitative discussion	59
5	INVESTIGATION OF FLOW PATTERN IN UNSTABLE COMPOUND JETS	63
	5.1 Introduction	63
	5.2 Varicose instability	63
	5.2.1 Normal liquids	63

Page

5.2.2 Non-mixable fluids 65
5.2.3 Non-Newtonian liquids 67
5.2.3.1 Addition of Polyethylene oxide 67
5.2.3.2 Influence of particles in the secondary fluid 69
5.3 Sinous instability 69
5.3.1 Examples of sinous instability 69
5.3.2 Discussion 72
5.4 Random instability 72
5.4.1 Examples of random instability 72
5.4.2 Discussion 76
5.4.3 Influence of polyethyleneoxide on random instability 77
5.5 Development of the instabilities 78
5.5.1 Instabilities caused by increase of secondary fluid 78
5.5.2 Instabilities caused by increase in primary fluid flow 81
5.5.3 Discussion 83
5.6 Pumping action of primary jet 83
5.6.1 Description of the pumping action 83
5.6.2 Pumping induced by Polyox in secondary fluid 84

6 DISCUSSION OF THE FLUID DYNAMICS OF COMPOUND JETS 86
6.1 Introduction 86
6.2 Liquid-in-liquid jets 88
6.2.1 Introduction 88
6.2.2 Velocity and momentum measurements in real jets 88
6.2.3 Velocity profiles in compound jets 91
6.2.4 Dependence of viscosity 95
6.2.5 Velocity profile at primary-secondary fluid interface 101
6.3 Compound jet in air 103
6.3.1 Introduction 103
6.3.2 Development of plug flow profile in a conventional jet 103

Page

6.3.3 Calculations of compound jet parameters 104
6.3.3.1 Momentum flux of the compound jet 104
6.3.3.2 Velocity of the compound jet 106
6.3.3.3 Acceleration of compound jet 107
6.3.3.4 Reynolds number of compound jet 108
6.3.3.5 Minimum fluid flow in primary jet 109
6.4 Molecular diffusion in a stable compound jet 110
6.5 Surface tension effects in a compound jet 111
6.5.1 Distance to compound jet drop formation 111
6.5.2 Pressure caused by surface tension 111
6.5.3 Surface tension between two non-mixable fluids 112

7 PRACTICAL APPLICATIONS 113
7.1 Compound jet in copying devices 113
7.1.1 Introduction 113
7.1.2 Experimental apparatus 113
7.1.3 Results 116
7.1.3.1 Dependence of jet velocity 116
7.1.3.2 Determination of upper frequency limit 118
7.2 Use of compound jet in computer controlled drafting machines 122
7.2.1 Introduction 122
7.2.2 Electrode systems 123
7.2.3 Principle of controlling ink jet line width 125
7.2.4 Experimental apparatus and procedures 128
7.2.5 Results 131
7.2.6 Spatter reducing technique 138

ACKNOWLEDGEMENTS 140

REFERENCES 141

SUMMARY

A new method for the generation of liquid jets is studied with respect to its physical properties as well as to its application for recording purposes. In contrast to ordinary jets the new jet emerges from the surface of a liquid. It is generated by submerging a nozzle in this liquid in such a way that a fluid jet ejected under high pressure from this nozzle is directed towards the surface of the liquid. On its way from the nozzle to the surface the jet entrains part of the surrounding liquid by viscous forces. Thus, when the jet breaks the surface and emerges into the air it consists of a central core formed by the original jet surrounded by a cylindrical sheath of the liquid entrained by the jet. Therefore this jet is called a compound jet. Normally the compound jet disintegrates into a train of drops at a point of drop formation due to a varicose instability in the same way as ordinary jets. Therefore the compound jet can be used for ink jet printing in the same way as ordinary jets but has the advantage that the choice of inks is much less critical. In extreme cases other types of instabilities can dominate the jet and then it cannot be used in ink jet printing applications.

After a general introduction the basic physical phenomena of the compound jet are demonstrated with the aid of microphotographs. Different flow patterns as well as instabilities are discussed. Physical parameters are calculated for the compound jet. Finally applications of the compound jet in recording of electrical signals are described using on-off intensity modulation.

1 INTRODUCTION

1.1 The present use of ink jets

During the last two decades fine jets of ink have been used increasingly for recording purposes. Several companies have made considerable efforts in developing specific ink jet products. Some of these products are working well today but many have failed due to great technological problems.

The main reason for the interest in ink jets is that the ever increasing use of computers has caused a growing demand for fast output devices. This includes alphanumerical printers, e.g., typewriters, line-printers, and address printing machines. Further, plotters, equipment for color graphics and facsimile printing have grown in importance since the alphanumerical method of presenting data becomes inconvenient if the amount of information is large. The third range of computer output devices includes equipment for bar code printing, textile printing, surface etching and other applications.

Because of their properties fine ink jets have often been found advantageous compared to other methods, e.g., electrostatic and mechanical x-y-plotters. Ink jets are electrically controllable, fast, silent, and can print on a variety of surfaces including ordinary paper. Ink jets can also provide different colors or shades of grey in high resolution.

Different methods for the control of ink jets have been described by Stemme et al. (1973), Sweet (1965), Winston (1962), and Hertz et al. (1972). The development of ink jet technology has generated a completely new graphic technique, due to both new demands and new possibilities as our knowledge of ink jets grows.

1.2 Historical development of ink jet technology

It has been known for more than a century that a cylindrical liquid jet is unstable. The continuously flowing jet from a nozzle will break up into droplets due to this instability. The length of the unbroken jet and the frequency of drop formation was studied by Savart who in 1833

suggested that the unbroken length of a jet is proportional to the square root of the jet veclocity and also proportional to the jet radius. He also indicated the possibility of controlling the drop formation frequency by means of applying acoustic energy to the jet.

Plateau calculated 1856 that if a cylindrical column of liquid was longer than its own circumference, it would be possible to divide the column into two separate drops whose total surface area was less than that of the column. Since the surface energy is proportional to the surface area, it is clear that the liquid cylinder would reach a lower state of energy if it was broken into droplets.

On these grounds Lord Rayleigh performed his analysis of the instability of liquid jets under the influence of surface tension. His first historical analysis (1878) concerned a non-viscous liquid jet travelling into a medium of negligible density. He assumed that an infinitesimal axisymmetrical variation of the diameter which is impressed on the jet could be represented by changes of the jet surface area. He then subtracted the surface energy of the disturbed jet from that of the undisturbed jet and obtained a difference in energy of the two configurations. He found that if the wavelength of the disturbance is greater than the circumference of the jet, the surface energy is smaller after the disturbance than before and hence the jet is unstable and will break up into droplets as shown in Figure 1.1.

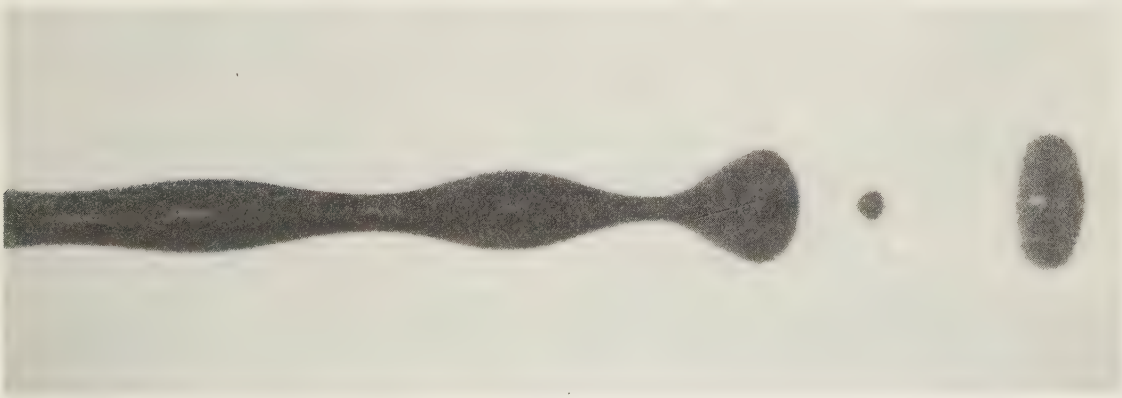

Figure 1.1. Spontaneous drop formation due to surface tension forces.

Lord Rayleigh further assumed that this axisymmetrical disturbance of the jet would grow exponentially. He calculated the kinetic and potential energy per unit length of the jet and found a maximum growth rate for the disturbance when the wavelength of the disturbance is equal to 4.51 jet diameters. This growth rate is thus expected to predominate and breaks the jet into separate droplets as shown in Figure 1.1. The break-up time could now be obtained by substituting the value of the maximum growth rate in the expression for the disturbance, giving the break-up length L of the cylindrical jet in vacuum, subject only to surface tension forces and an infinitesimal axisymmetrical disturbance δ. Lord Rayleigh obtained

$$L = 1.03\ v\ \left(\frac{d^3\rho}{\sigma}\right)^{1/2} \ln\left(\frac{d}{2\delta}\right) \qquad (1.1)$$

where ρ is the density of the fluid, σ the surface tension, v the speed and d is the diameter of the jet.

A. Haenlein 1931 found from experiments with water that

$$\ln\left(\frac{d}{2\delta}\right) = 12 \qquad (1.2)$$

meaning that the initial disturbance is approximately $3 \cdot 10^{-6}$ jet diameter. The break-up length is therefore not very sensitive for changes in the magnitude of δ.

Rayleigh also investigated the stability of a viscous jet (1872) but the theory resulted in a complicated expression for the growth rate of the disturbance. Weber made a further analysis of this problem (1931) which resulted in an expression for the break-up length of a viscous jet:

$$L = v\left[\left(\frac{d^3\rho}{\sigma}\right)^{1/2} + \frac{3\eta d}{\sigma}\right] \cdot \ln\left(\frac{d}{2\delta}\right) \qquad (1.3)$$

The viscosity η is thus adding an extra term accounting for an increase in L.

To summarize, it can be seen that the break up time is determined by the maximum growth rate of the disturbance. This is determined by the ra-

dius of the jet and the physical properties of the liquid in the jet but independent of the jet velocity. The jet breaks up once the disturbances attain the scale of the jet radius. This type of break-up was termed varicose by Rayleigh. Although varicose instability for liquid jets in air is related to surface tension, it must be pointed out that the lack of surface tension (as in a liquid jet into the same liquid) does not preclude varicose instability.

Under certain conditions it is found that the jet near the break-up point consists of almost spherical drops joined by ligaments of fluid. When the jet breaks up, two drops derive from this configuration, a preceding parent drop and a small satellite drop formed from the ligament (Figure 1.1). This satellite can either move faster than the parent drop, joining this drop downstream (forward merging) or move more slowly and be caught by the following drop (backward merging). This depends on whether the ligament breaks first near the parent drop or near the following drop. It is also possible that the ligament breaks at both ends simultaneously, causing the satellite to travel between parent drops, never to rejoin them.

The presence of satellite drops is not predicted by the theories mentioned. Later calculations concerning capillary instability of liquid jets using more refined non-linear models for the jet disturbance have tried to explain satellite drop formation (Chaudhary & Redekopp 1980). Since printing quality is often deteriorated by satellites it is desirable to find methods to avoid them.

It has been shown that high frequency mechanical vibrations can cause the jet to form drops in synchronism with the superimposed disturbance (Schneider & Hendricks 1964). This periodic disturbance is achieved by a piezoelectrical crystal which is in contact with the jet nozzle. If the vibration is large enough and of proper frequency compared to the size of the jet, it will control the drop formation. This will cause the drops to be of uniform size and the drop formation point to be situated at a constant distance from the nozzle. Chaudhary & Redekopp also suggested that the satellite drops could be controlled by adding a suitable harmonic to the fundamental vibration frequency. They have

reported a range of experimental results in order to demonstrate agreement with the theoretical calculations. The finer structure of the instabilities of a jet is, however, influenced by initial velocity distribution of the jet and other factors difficult to measure and control. Therefore, despite ambitious theoretical calculations many experimental results remain unexplained.

Controlling a continuously flowing jet with electric signals is possible in two principally different ways. Both methods comprise a charge electrode situated outside the ink jet nozzle. This electrode is usually a short metal tube which is placed close to or around the point of drop formation. If the charge electrode is connected to a voltage source and the ink is sufficiently conductive and on ground potential, the jet will be charged at the point of drop formation. The drops will then carry an electric charge trapped on them. By changing the voltage of the charge electrode at high rate it is possible to change the charge on different drops. This mechanism is used in both methods for the control of ink jets described below.

One of the methods is described by Sweet (1964). The method is based on giving each drop a certain charge to mass ratio (cf. Figure 1.2). A constant mass of the drops is achieved by vibrating the nozzle with a transducer T, thus forming drops of nearly the same size. The drop charge is then controlled by the signal voltage applied to the charge electrode E. Thereafter the charged drops pass through a high transversal electrostatic field maintained between two electrode plates P_1 and P_2. This field causes a deflection of the drops proportional to their charge, resulting in a vertical deflection (Figure 1.2). If a paper not shown in the figure moves continuously at right angles to the jet direction, this movement will produce the other axis of deflection.

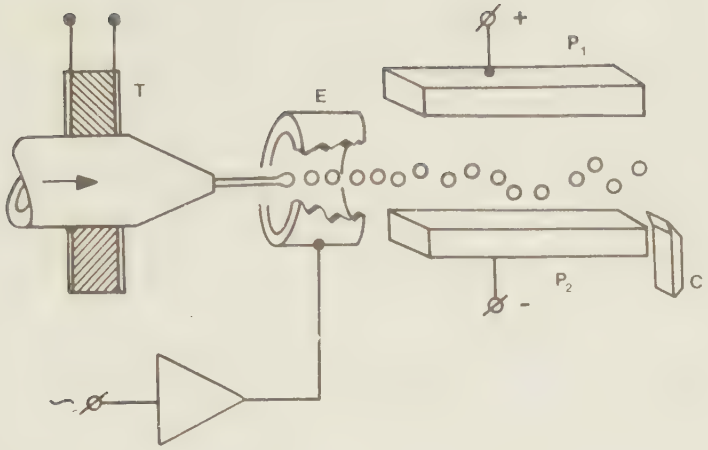

Figure 1.2. Sweet's modulating method where each drop is given a charge roughly proportional to the voltage of the tubular charge electrode E. The drop formation is controlled by the transducer T. The drops are deflected by the high voltage electrode plates P_1 and P_2. Uncharged drops hit the catcher C.

Uncharged drops will travel unaffected by the transverse field and hit a properly situated catcher C to save ink. Depending on their charge the charged drops will travel different paths to the printing surface. Thus each drop can be placed individually on a predetermined point of the printing surface by suitable control of the signal voltage.

The other way of modulating an ink jet with electrostatic forces is described by Hertz et al. (1967). A fine liquid jet can be transformed into a spray of fine droplets if the drops are sufficiently charged by the charge electrode E around the drop formation point as shown in Figure 1.3. Since the jet is dispersed, obviously no recording trace is obtained on the recording paper during the time the voltage of the charge electrode is maintained (Figure 1.3.b). Thus, by turning the

voltage on and off the ink jet can be switched between the spray and the linear jet mode. The phenomenon is explained by the fact that all drop charges are of the same sign and therefore give rise to a strong repulsion between the drops which breaks up the jet into a spray a few millimeters from the point of drop formation. This spray is easily separated from the linear jet consisting of uncharged drops by means of either a diaphragm or a transverse electrostatic field situated between the charging electrode and the printing surface (Figure 1.3.c).

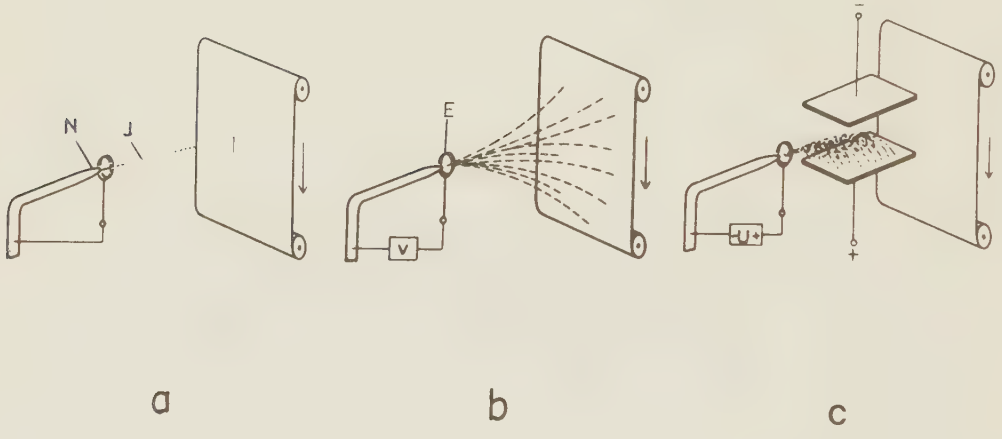

Figure 1.3. Hertz'modulating method where the fine jet is transformed into a spray of charged drops if a voltage V of sufficient magnitude is applied to the charge electrode E.

This modulation method is an intensity modulation method and can provide a grey scale if the drops are sufficiently small (10-20 microns).

Since the uncharged drops are used for printing, it is not necessary to keep the charge to mass ratio constant by means of an ultrasonic transducer as is essential with the Sweet method. Also there is no phasing problem between the moment of drop separation and the switching of the charge electrode voltage as in the Sweet method. The disadvantage of the Hertz method is that it only works with very fine jets as it is difficult to turn a larger jet into a spray. This causes less ink to reach the paper than with the Sweet method.

1.3 Ink problems in earlier systems

One of the main problems encountered in ink jet printing is clogging of the nozzle. To avoid this not too large particles are allowed in the ink and, further, the ink must not dry in the nozzle during shut-down periods.

Clogging the nozzle with particles can be prevented by introducing a filter in the ink conduit to the nozzle. However, the filter itself may also clog after long service. Therefore most ink jet systems use pure dye inks without pigment particles. Dye inks, however, present problems due to low contrast and light sensitivity. Further, as a rule they cannot be used for the printing of textiles and other materials.

Clogging the nozzle with dried ink can be prevented by using a non-drying ink. Even the residue of the ink must not dry in the nozzle or form a solid sediment with the dye. If it is essential to use a drying ink, e.g. for printing on a non-absorbing surface, clogging can be avoided by flushing the system after use with a non-drying liquid or applying a mechanical lid over the nozzle. Both of these solutions are inconvenient.

An increasing problem arises from health aspects. More and more dyes and additives are expected to be prohibited as they are found to cause allergies or cancer. This limits the choice of dyes that can be used for the production of ink.

The different demands on the ink concerning viscosity, surface tension

and conductivity further restricts the choice among available inks. Therefore the producers of ink jet equipment are often forced to develop their inks as well.

For the above reasons it would be desirable to have a greater tolerance in the ink parameters. This would also diminish the danger of changing the property of an ink during large scale production since a very small amount of faulty ink distributed to users of ink jet equipment could cause many machines to break down with the present systems. This paper will present a method to produce a fine ink jet without many of the ink problems which are inherent with existing systems.

2 COMPOUND JET PRINCIPLE

2.1 Description of a compound jet

Many of the problems experienced with present ink jet systems would be eliminated if it was possible to use really large nozzles. Nossles in the range of millimeters instead of microns would not clog with pigmented or drying ink. This means, however, very bad printing resolution with present systems. Therefore it would be desirable to get a very thin jet out of a large orifice in order to keep the high resolution of a small nozzle and gain the advantages of a large one.

This can be achieved in the following way. Figure 2.1 shows a fine nozzle submerged below the surface of a stationary fluid. By forcing a suitable "primary" fluid through this nozzle under high pressure a liquid-into-liquid jet is generated in the stationary fluid which in the following will be called the "secondary" fluid. Due to viscous forces the secondary fluid will be accelerated by the primary fluid close to the interface between the two fluids. Therefore, when the jet emerges into the air it will consist of a cylindrical core of primary fluid surrounded by a concentric layer of secondary fluid travelling at essentially the same speed. The jet emerging from the surface is therefore called a compound jet in the following. (This term is earlier used in literature to describe concentric flow of gases in a tube by Lennox and Pack 1962). After emerging into air compound jets spontaneously break up into drops due to axisymmetric varicose instabilities in the same way as conventional jets.

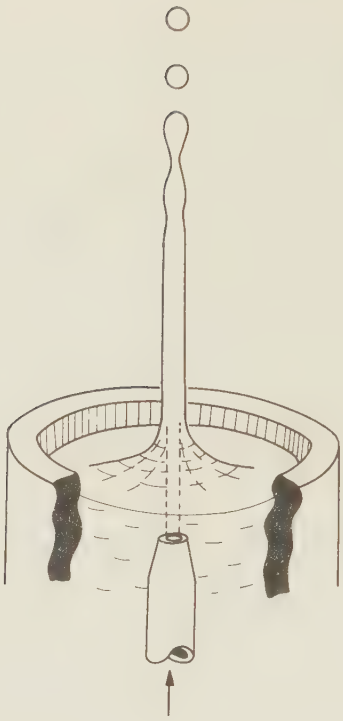

Figure 2.1. The compound jet formed by a fine high velocity primary jet entraining surrounding secondary fluid before breaking the surface.

This jet will have the desired properties of being reasonably small in order to retain high printing resolution and using a large orifice to allow the use of pigmented and other inks as a secondary liquid. The primary fluid can be any harmless and suitable fluid, for example a mixture of water and glycerine that will not clog the nozzle. Thus the compound jet arrangement will produce a fine liquid jet without many of the restrictions of any ordinary jet. Stable compound jets of this kind have been demonstrated with diameters from 15 μm to 1 mm.

In order to permit printing in all directions independent of gravity with the compound jet a certain restriction concerning the nozzle assembly has to be obeyed. While the secondary fluid surface from which the compound jet emerges in principle can be of any size, a small opening for this surface has the advantage that the surface tension prevents

secondary fluid from flowing out of the orifice due to gravity. Thus if the opening for the secondary fluid is of the size 1 to 4 square millimeters, it is possible to turn the nozzle assembly in any direction.

After emerging into air the compound jet behaves like a conventional jet. It can therefore be controlled with charging and deflecting electrodes using either Sweet's or Hertz' method.

The distance between the nozzle producing the primary jet and the surface of the secondary fluid determines the amount of liquid entrained from the secondary fluid. If the nozzle of the primary jet is situated deeper below the surface, the jet will entrain more secondary fluid into the compound jet. This distance thus determines the ratio of primary to secondary fluid content in the compound jet. Therefore it is possible to modulate the flow in the compound jet by varying the distance between the nozzle of the primary jet and the meniscus of the secondary fluid. Seen from another angle, if the secondary fluid is supplied at a constant flow rate, the distance between the nozzle and the meniscus of the secondary fluid will be fixed. Reducing the flow rate of the secondary fluid will cause the distance to decrease and vice versa.

Changing the viscosity of the primary or the secondary fluid means changing the viscous coupling between the primary jet and the secondary fluid. Since all momentum of the compound jet is supplied by the primary jet and the secondary fluid is essentially stationary, the momentum of the primary jet transferred to the secondary fluid will be determined by the viscous forces between the primary and the secondary fluids. This transfer rate will determine the distance between the nozzle and the secondary fluid meniscus, given a certain flow rate of the secondary fluid.

The possibility to change the flow rate of the secondary fluid as well as changing its viscosity opens great possibilities since the system is self-regulating. The higher the flow of secondary fluid, the more will be entrained by the primary jet, and the longer the distance will be between the nozzle and the meniscus. The higher the viscosity of the secondary fluid, the shorter the distance.

The fact that two different fluids are used for a single concentric jet opens possibilities to use non-mixing fluids as well as a conductive and a non-conductive fluid. Many ways of mixing liquids that are apt to react chemically with each other are open to the experimentator. The outer fluid can be pigmented, non-conductive and drying. It is also possible to change the flow of the secondary fluid, thus providing different flow rates of the compound jet as well as changing the fluid totally in any respect, even color.

2.2 Instabilities. Comparison between compound and conventional jet

The compound jet is expected to act as a normal jet produced by a nozzle. Increasing the speed of any jet, normal or compound, or reducing the viscosity of the jet causes the mass forces to prevail and turns the jet into an unstable one. Such a jet disintegrates into unevenly sized droplets long before the capillary instability due to the surface tension causes the jet to break up. This unwanted jet break-up is not due to surface tension forces but to eddies inside the jet causing radial velocity components of the liquid elements. As a result the point of drop formation is unstable and the drops break away in all directions causing a spray instead of the train of drops observed with a laminar jet. Such a jet is of course not suited for printing applications.

Since this unwanted instability occurs in an ordinary jet (Figure 2.2a and 2.2b) it is also expected to occur in the compound jet when changing jet velocity and the viscosity of the liquids used. A comparison between the ordinary jet and the compound jet also reveals a similar instability, shown in Figure 2.3a and 2.3b. It might even be expected that other forms of instability could show up in the compound jet when changing its parameters. The understanding of these instabilities and their origin is essential when using the compound jet in technical applications. Sometimes the instabilities of the jet can also be used to advantage.

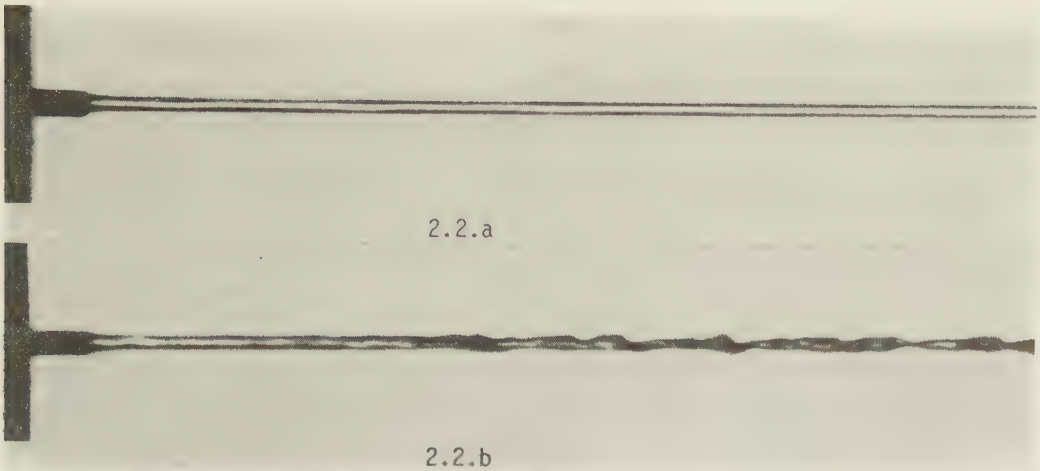

2.2.a

2.2.b

Figure 2.2a and 2.2b. Increasing the speed of the jet causes the ordinary jet to turn from laminar (2.2a) to turbulent flow (2.2b). 20% glycerin-water mixture ejected through a 75 μm nozzle with speed 8 m/s (2.2a) and 15 m/s (2.2b).

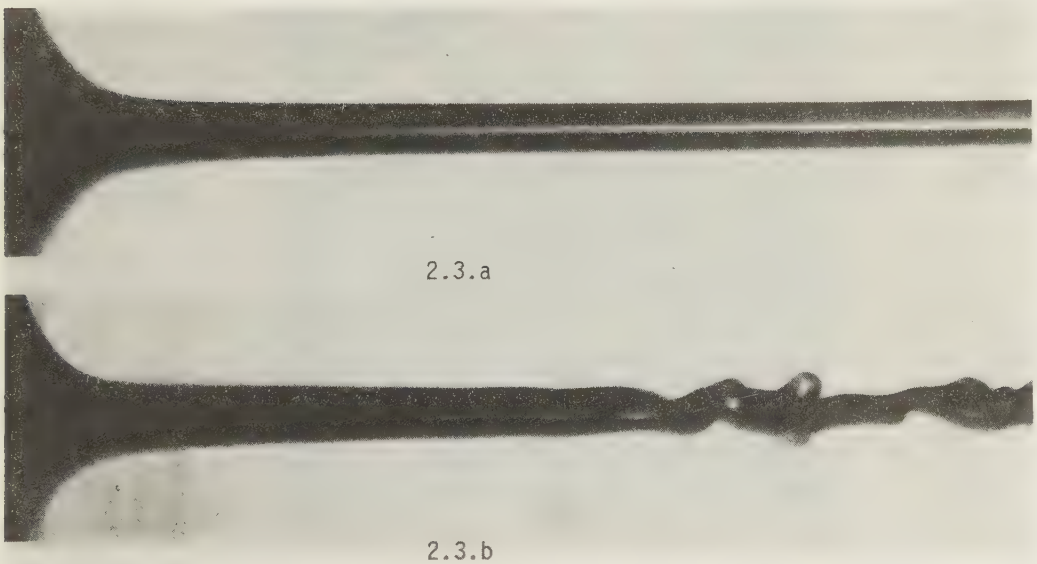

2.3.a

2.3.b

Figure 2.3a and 2.3b. Compound jet showing both laminar flow (2.3a) and undesired instabilities (2.3b) due to choice of liquids. Primary jet is 20% glycerin-water mixture ejected through a 75 μm nozzle with speed 8 m/s. Secondary fluid the same as primary fluid (2.3a) and water (2.3b).

A liquid jet emerging into a liquid is called a submerged jet. Theoretical calculations of the resulting flow patterns were first performed for turbulent flow by W. Tollmien (1926) and for laminar flow by H. Schlichting (1933). Since much of the flow patterns of the compound jet is similar to that of the submerged jet it could be expected that these calculations concerning axial and radial flow velocity distributions of the submerged jet could be applicable to the compound jet. There is, however, an important difference as the compound jet includes a meniscus between the secondary fluid and the air. Furthermore, the calculations mentioned above assume the submerged jet to consist of the same liquid as the one it is submerged into, while the compound jet is also meant to use liquids with quite different properties. Therefore, a more complicated flow pattern is expected than that calculated for the submerged jet.

Using pigmented ink in the secondary fluid means that special attention has to be paid to the effects of particles in the liquid. Pigment particles might cause sudden instabilities in the compound jet when they are accelerated into the sheath of secondary fluid surrounding the primary jet. Also fully soluble additives in the primary or secondary fluid cause complicated flow patterns in the compound jet, not seen in conventional jets as will be demonstrated below.

3 EXPERIMENTAL METHOD

3.1 Compound jet assembly geometry

3.1.1 Primary jet nozzle

The compound jet nozzle assembly comprises both a nozzle for the primary fluid and a chamber for the secondary fluid. The primary jet nozzle used consists of a glass capillary with an integrated filter situated upstream from the nozzle. The nozzles are manufactured by the Siemens-Elema company, Solna, Sweden, in almost any size to meet desired specifications. Since the nozzle diameters may be as small as 7 microns the filter of the capillaries are made to reject particles larger than 3 microns. The filter and capillary system represents a fluid resistance (Månsson 1972).

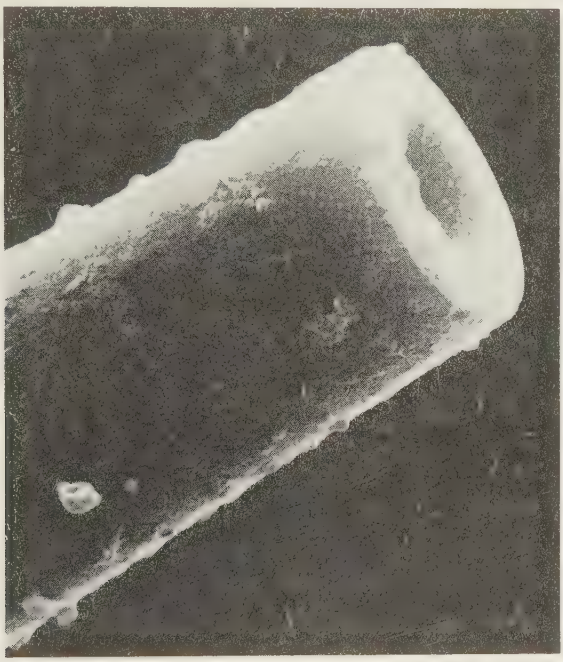

Figure 3.1. Scanning electron microscope picture showing the geometry of a 15-micron diameter glass nozzle used for the primary jet.

The wall thickness of the primary jet nozzle is about 10 microns (see Figure 3.1). The face of the nozzle is carefully ground. This is demonstrated by comparison with Figure 3.2 which shows a broken capillary. In a broken capillary the primary jet is apt to adhere to the longest part of the nozzle causing the jet to emerge at a different angle than it would from a finely ground capillary. Therefore broken nozzles cannot be used for ink jet applications.

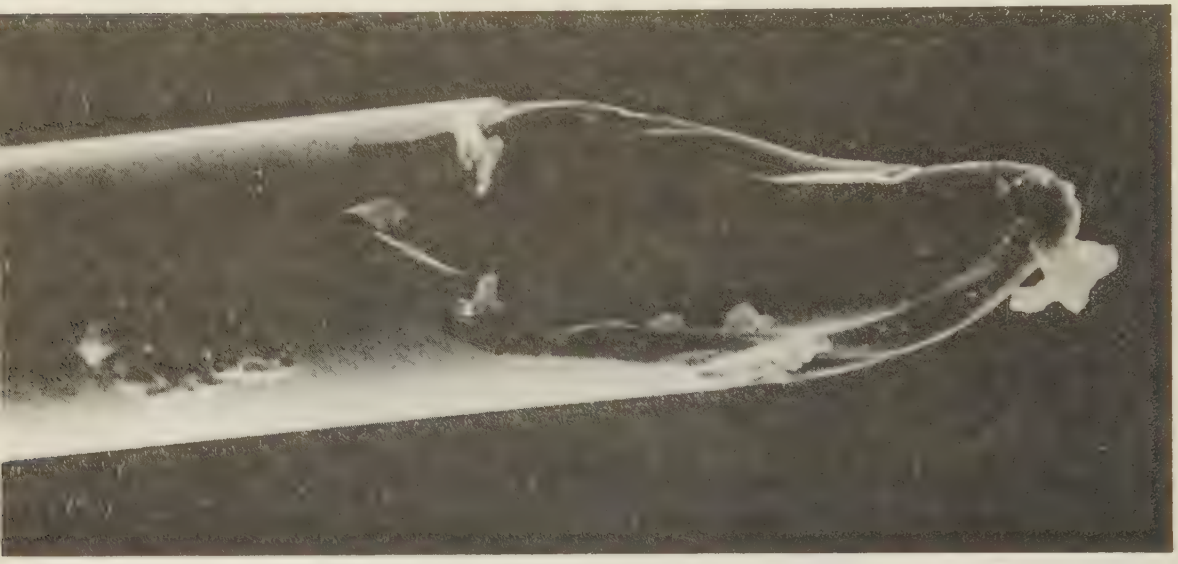

Figure 3.2. Scanning electron microscope picture showing the geometry of a roughly broken 80 μm diameter glass capillary used as a nozzle for a primary fluid.

In most of the experiments described below 75 microns glass nozzles were used to produce the primary jet. Such a nozzle is shown in Figure 3.3 both as a side view and a front view. Even these nozzles were ground carefully although the nozzle shown in Figure 3.3 shows some deficiencies.

Figure 3.3. Carefully ground 75 microns glass capillary with flaws photographed through a scanning electron microscope. Both front and side views are shown.

3.1.2 Secondary fluid chamber

In preliminary experiments a rectangular box was used as container for the secondary fluid. Here a horizontal capillary enclosed in a metal sheath was submerged in the box which was open at the top and filled with secondary fluid. The compound jet emerged through a hole in the wall opposite to the nozzle. Different shapes cause the velocity distribution of the secondary fluid to vary somewhat. Since, however, the area of these holes is large compared to both the primary nozzle and the compound jet (ratio range from 1:40000 with a 10 microns primary jet through a 2 mm orifice for the secondary fluid to at most 1:180 with a 75 microns primary jet through a 1 mm orifice), the influence of the shape of the orifice was found to be rather small as long as the area is large enough.

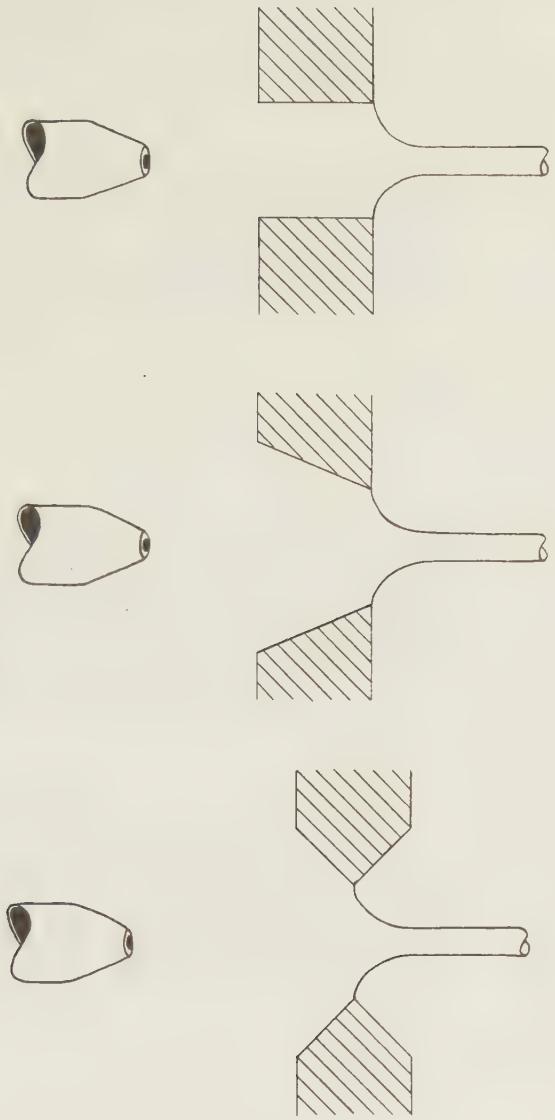

Figure 3.4. Different configurations of the compound orifice being a hole in a container wall. The shape of the hole is of less importance than its size.

Since no essential difference could be observed between compound jets produced through differently shaped holes, the final geometry used was chosen because of flow characteristics described more in detail in 3.2.2. Two of the final compound nozzle assemblies are shown in Figure 3.5a and 3.5b. The primary jet nozzles are glass capillaries. The capillary used in Figure 3.5b is equipped with a covering bronze sleeve from the manufacturer, providing a proper fitting against the plexiglass material in the nozzle assembly. In Figure 3.5a a watch jewel with a 100 µm hole was used to hold the glass capillary and close the chamber on its rear side.

The chamber for the secondary fluid and the capillary were drilled in plexiglass, thus it was possible to observe the fluid inside the assembly if the secondary fluid was transparent. (Different materials used in different secondary fluid chambers caused no change in the compound jet.) The bronze sleeve nozzle assembly automatically served as a ripple filter for the secondary fluid flow using the area between the bronze sleeve and the plexiglass housing as a flow restrictor element (cf. 3.2.2).

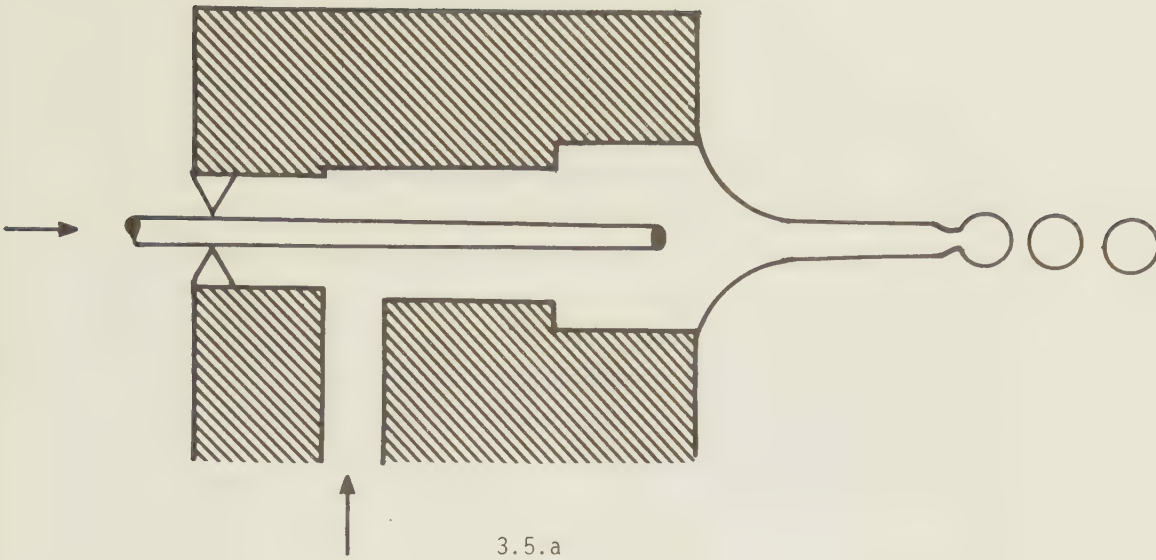

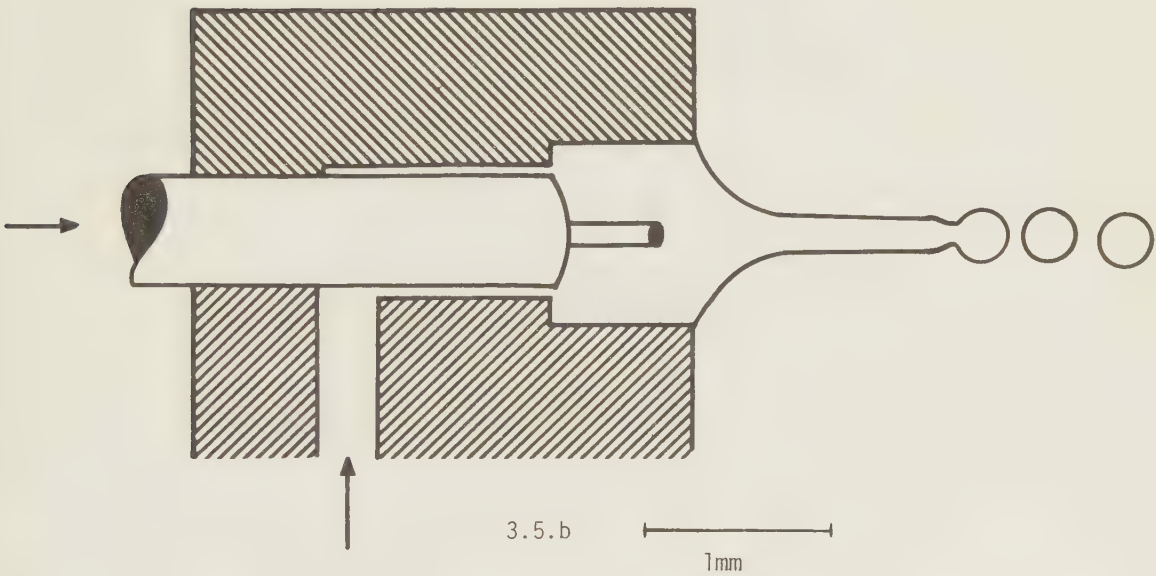

Figure 3.5. Final geometry of compound nozzle assembly with primary jet glass capillary held by a watch jewel (3.5a) or a bronze sleeve covered glass capillary (3.5b).

3.2 Compound jet fluid systems

3.2.1 Primary jet

The compound jet principle is based on transferring kinetic energy from the primary jet to the secondary fluid. The kinetic energy of the primary jet is produced by a high pressure pump supplying the primary fluid. This pressure must also overcome the pressure losses in the tubings, filter and nozzle, due to internal friction. It must furthermore supply surface energy to the jet. It has been shown (Månsson 1972) that the theoretically calculated velocity of a jet ejected from a glass capillary corresponds very well with experimental results assuming a pressure drop in the glass capillary according to the law of Hagen-Poiseuille for laminar flow. Since the theoretical calculation of the jet velocity is extremely sensitive to the internal diameter of the capillary, all jet speeds in this paper are measured by means of weighing the ink ejected from the nozzle per second assuming that no contraction of the jet takes place. The jet speeds measured with this method agree well with those obtained with other methods (cf. 7.1.4.1).

Since the size of the nozzles used ranges from 7 to 75 microns different primary fluid flows are required. The flow needed reaches from 2 to 50 µl/s and is supplied from five different systems.

1. Self priming Siemens-Elema continuous flow piston pump delivering from 0.7 to 5.0 MPa.
2. Crane-Chem continuous flow pump delivering up to 6 MPa.
3. Single stroke piston pump fabricated in the workshop of the Department of Electrical Measurements, delivering 4 ml of ink at up to 6.0 MPa.
4. ASF continuous flow selfpriming membrane pump type F120G delivering up to 1.0 MPa, suitable for larger flow rates.
5. Compressed air bottle delivering more than 10 MPa.

In all of the experiments described below it is of importance that the speed of the primary jet is constant. This implies that the pressure and the flow generated by the primary fluid pump is free from ripple which can be obtained only with the compressed air bottle system. However, this system is inconvenient to use. The ASF pump and the Crane-Chem

pump generated serious ripple and therefore were not used very much. The ripple produced by the Siemens-Elema pump and the piston pump is slight only, but the piston pump cannot supply a continuous flow of fluid during a longer period of time. Therefore the Siemens-Elema pump was used in most of the experiments, sometimes together with a ripple filter consisting of a fluid flow resistance of the Lee type (Figure 3.6) together with a receptacle in the form of a T-joint with some air inside. This ripple filter provides good filtering relatively independent of the viscosity of the fluid due to the geometry of the flow resistance. Figure 3.6 shows how the fluid is forced to frequent change in flow direction inside the flow resistance, thereby reducing the effect of viscosity.

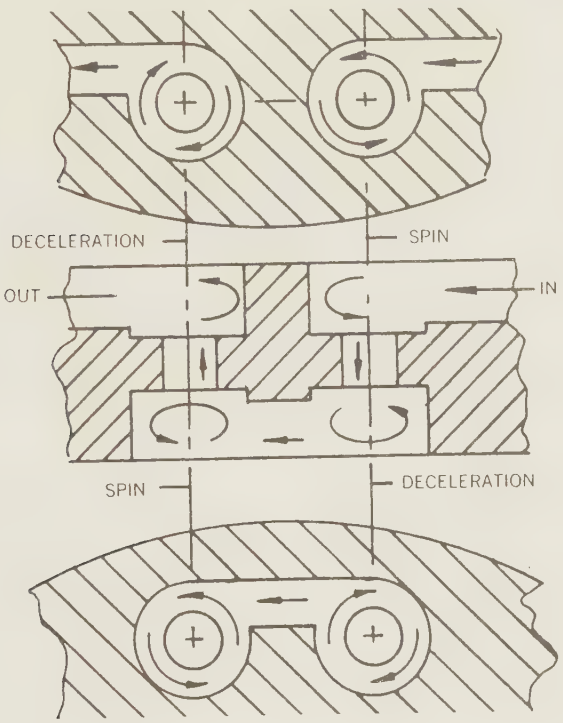

Figure 3.6. Fluid flow resistance element relatively independent of the viscosity of the fluid.

When turning off the pressure from the primary fluid, it was observed that a slight backward flow in the primary nozzle could occur. This flow is of no importance if the nozzle thus sucks air from the outside. If, however, the nozzle is submerged in a fluid containing particles, for example pigmented ink, these particles can clog the nozzle from the outside due to this backward flow. It is therefore sometimes advisable to use a check valve in the primary fluid flow system, situated immediately before the nozzle. Another possibility is to turn off the secondary fluid flow first, thus removing the secondary fluid from the vicinity of the nozzle before turning off the primary jet.

3.2.2 Secondary fluid system

The secondary fluid system with a hole in the wall of a container described in 3.1.2 involved several problems. The primary jet nozzle was situated a short distance behind the hole in the wall and this distance determined the amount of secondary fluid entrained. A very small change in this distance gave rise to a change in the primary to secondary fluid flow ratio. Removing the primary nozzle and replacing it with a new one situated at exactly the same distance behind the hole was practically impossible. Also a change in the viscosity of the secondary fluid (caused by e.g. a change in the surrounding temperature) would have the same effect as changing the distance between the primary jet nozzle and the hole in the wall of the container.

Because of the problems associated with the system described in 3.1.2 a compound jet assembly using constant secondary fluid flow was preferable. Therefore a system using constant secondary fluid flow was used in most of the experiments (cf. Figure 3.7). Since the primary jet entrains all the secondary fluid delivered to it, the primary to secondary fluid ratio can easily be controlled by controlling the secondary fluid flow. This is true independent of changes in viscosity or other parameters of the secondary fluid. Also positioning of a replacement primary jet nozzle becomes less critical since the primary to secondary flow ratio is not affected at all by positioning errors.

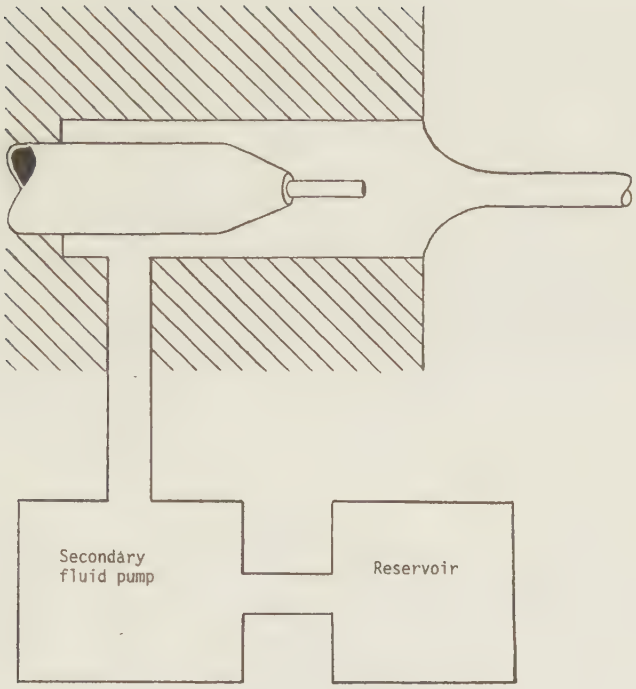

Figure 3.7. Compound jet nozzle assembly using constant secondary fluid flow supplied from a peristaltic pump.

A peristaltic pump (Gilson Minipuls II) was used as a constant flow source. Since it had interchangeable tubings and continuously adjustable speed, all flow rates required in the experiments could be obtained. Only the use of very small primary jet nozzles necessitated a miniature version of such a pump in order to obtain a constant flow under 10 µl/s. A small roller bearing was fixed to the shaft of a gearbox, directly coupled to a small DC-motor the speed of which could be controlled. Around the roller bearing a thin plastic tubing was fixed and pressed against it, causing it to work as a miniature peristaltic pump.

A ripple filter between the peristaltic pump and the orifice is always added. Otherwise the small strokes from the pump are seen as a movement of the meniscus back and forth, causing the flow in the compound jet to vary accordingly. A convenient way to arrange the ripple filter for the secondary fluid is to use a piece of hard plastic tubing with a wire inserted in it as a fluid flow resistance combined with a piece of soft tubing acting as a flow capacitor. This system is both easier to construct and cheaper than the one mentioned for the primary fluid and will function properly for the secondary fluid as long as the liquid does not contain too large particles which will more easily clog this tubing fluid resistor.

3.3 Photographic methods

Most of the investigations on the physics of the compound jet described here were conducted with the help of microphotographs. Since the speed of the jets was high and their diameters smaller than 0.1 mm high speed light sources had to be used to obtain sharp pictures.

In preliminary investigations a 35 mm camera with extension bellow accessory and 20 mm macro lens was used. This arrangement allowed a direct magnification of at most 12 times on the film. The general arrangement of the apparatus is shown in Figure 3.8. Since all the pictures were taken horizontally it was possible to investigate the gravitational influence on the horizontal jet.

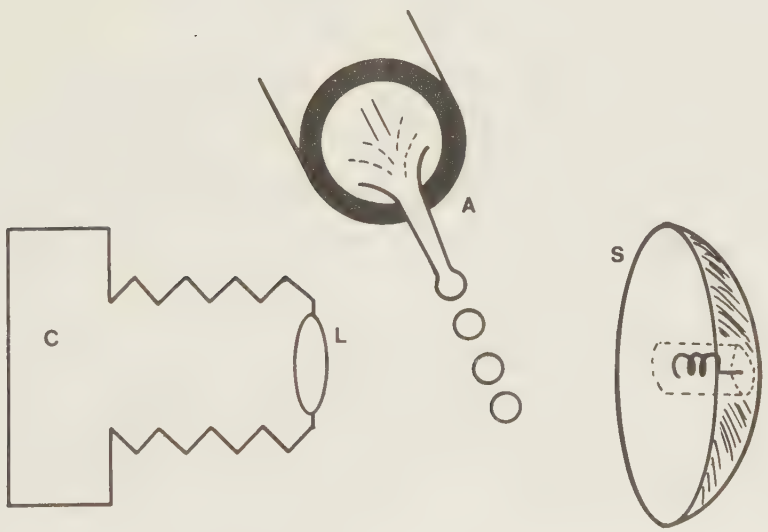

Figure 3.8. Arrangement of macrophotographic equipment in front of a horizontally situated compound jet.

The camera body C and the lens L are arranged directly in front of the compound jet nozzle assembly A. The nozzle is illuminated from behind by an electronic flashgun (exposure time 10^{-3} sec) or by a single flash from a stroboscope S (exposure time $5 \cdot 10^{-7}$ sec) depending on whether a stable situation is to be photographed or if single droplets or other fast moving objects are to be captured. The flashgun and the stroboscope are equipped with parabolic reflectors so that the beam from the light source represents a uniformly illuminated background for the nozzle and the jet. The beam was directed in such a way that its axis coincided with the optical axis of the camera lens. The benefit of this direct lighting into the lens with the photographed object between the lens and the light source compared with "indirect" lighting of the object is that the amount of light reaching the film is larger which allows shorter exposure times.

A General Radio 1538A stroboscope was used for the generation of single flashes. It was synchronized with the shutter of the camera.

In order to focus the camera on fast moving drops after the point of drop formation, the stroboscope was allowed to flash continuously. The short unsynchronized flashes produced successive, different sharp pictures in the camera eyepiece. Due to the relatively long time constant of the eye, this arrangement allowed focussing in spite of the short duration of the light pulses.

The total possible magnification of the photographic print was around 120 times with 12 times on the film and further 10 times with the enlarger. Using a primary jet originating from a 75 microns nozzle it was thus possible to obtain a final picture of the jet diameter not smaller than 10 mm.

Since it became essential for the understanding of the compound jet, a quite different nozzle assembly was designed.

This new nozzle assembly was intended for photographic purposes only whereas the drilled plexiglass nozzles worked as well in printing devices.

Since a closer investigation of the flow patterns inside the chamber also required a larger magnification a microscope was considered necessary. A suitable arrangement for microphotographic studies of the compound jet is shown in Figure 3.9. The microscope is situated above the compound nozzle assembly which is illuminated from below. The stroboscope is located on one side and the light from it is directed towards a mirror M and reflected by this upwards through the nozzle assembly in the microscope. Between the mirror and the nozzle it was possible to insert different light diffusers D and/or clear glass plates with black covering masks allowing special lighting arrangements (see below).

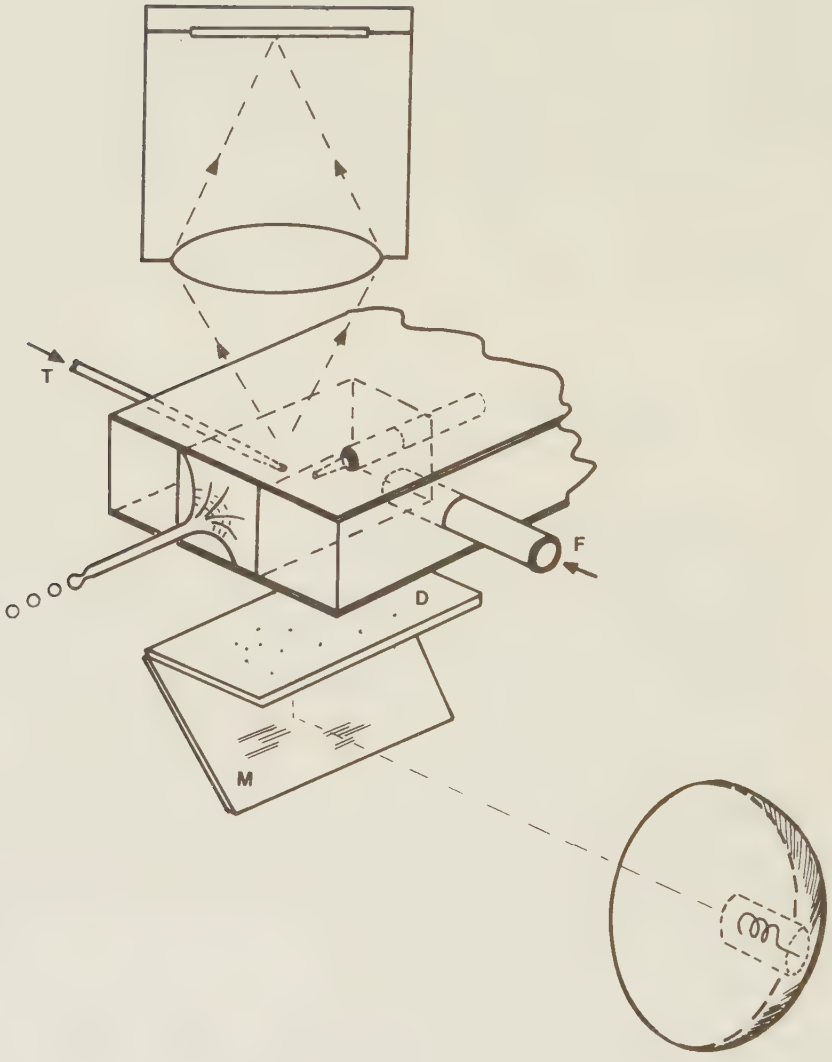

Figure 3.9. Experimental arrangement for microscopic photographs.

In order to make the interior of the compound nozzle assembly clearly visible two microscope cover glasses are used as wall material over and under the chamber. This causes the opening for the secondary fluid to be square-shaped which, however, does not seriously disturb the formation of the jet.

The secondary fluid inlet F is placed on one side of the nozzle. Directly opposite from this inlet is situated a capillary T through which it is possible to squirt a small amount of colored tracer fluid into the compound nozzle. The tracer fluid will move along with the secondary fluid and finally be accelerated into the compound jet. If the secondary fluid is transparent the streamlines of the flow will be revealed by this tracer fluid. Further, eddies and instabilities can be demonstrated at different places inside the chamber by moving the tracer fluid nozzle. This movement is effected with screws placed outside the area shown in Figure 3.9.

In order to get a sharp photographic picture of the primary jet through the secondary fluid in the chamber, the focus of the microscope has to be adjusted differently than when photographing the compound jet outside the chamber in the air. Therefore, it is impossible to obtain a picture with the interior of the chamber and the compound jet simultaneously in focus. The effect of this unavoidable focus shift depends on the size of the numerical aperture of the microscope lens and the overall microscope magnification. With a small aperture and small magnification the depth of the focus increases. With the stereoscopic microscope used the aperture is small and thus the focus shift effect minimized.

A Leitz Elvar largefield stereomicroscope is used for all microscopic pictures. This is a zoom microscope and therefore no specific aperture values are obtainable for different magnifications. A magnification up to 160 times can be obtained with an add-on lens.

The direct lighting method causes high contrast pictures. Therefore the grey shades of the photographed object may disappear as the film has too steep a gamma characteristic for the contrast. A method to decrease the contrast is to insert a light diffusor between the stroboscope and the object (D in Figure 3.9). The soft lighting, however, reduces the light

reaching the film as well. Therefore for many pictures the ultra high speed film Kodak 2484 developed at high temperature was used. This low contrast photographing method has produced pictures revealing the interior of both the compound jet and the drops (see below).

To allow photographing of the primary jet inside the compound assembly chamber the secondary fluid around the jet must be transparent. Since many experiments comprise similar primary and secondary fluids (cf. water-ethanol mixtures) it is difficult to see the transparent primary jet inside the secondary fluid. If, however, the refractive index is slightly different in the two fluids, a simple optical arrangement can produce a visible line of demarcation between the primary jet and the secondary fluid. This arrangement will be described in the following.

On the glass plate D in Figure 3.9 a black covering mask is attached. In this mask a slit is made exactly below and in the same direction as the jet axis. In this way light from the stroboscope illuminates the jet only and nothing else (cf. Figure 3.10).

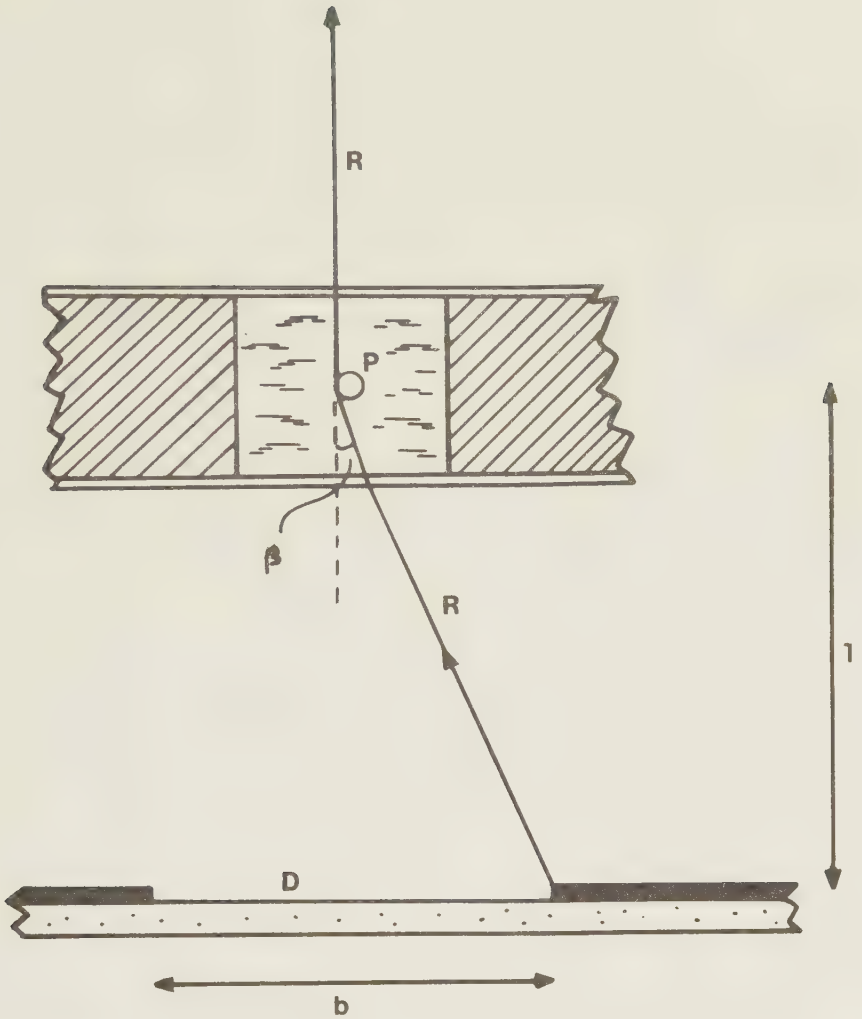

Figure 3.10. The compound assembly seen from the front. A black covering mask on the glass plate D allows only a narrow beam of light to reach the compound assembly and the primary jet P. The light from the edge of the mask is refracted as indicated by the ray R producing an optical black line of demarcation between the primary jet and the secondary fluid.

If the refractive index of the primary fluid is slightly larger than that of the secondary fluid the light ray R will be refracted into the primary jet and refraced again when exiting through the secondary fluid. Therefore the black mask will appear as a dark line on both sides of the primary jet when seen from above through the microscope. The slit acts as a light background for the jet producing sufficient contrast to show the borderline between the primary jet and the secondary fluid. (In Figure 3.10 the microscope is not shown).

The angle β in Figure 3.10 can be derived as follows:
Following from the law of refraction (cf. Figure 3.11)

$$n_1 \cdot \sin \alpha_1 = n_2 \cdot \sin \alpha_2$$

where n_1 and n_2 are refractive index of the primary and secondary fluid respectively, it is clear that a tangential ray will be refracted into the primary jet with angle

$$\alpha = \arcsin \frac{n_2}{n_1}$$

to the radius passing through the tangential point P_1 (see Figure 3.11). This is true if n_1 is larger than n_2.

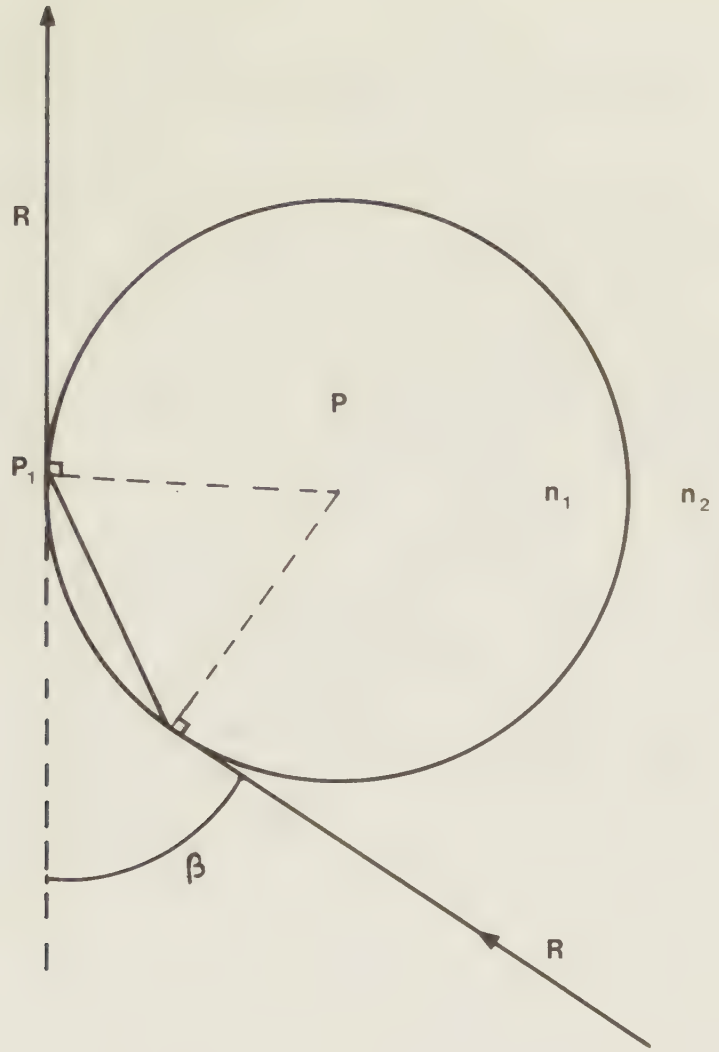

Figure 3.11. The light ray R is refracted by an angle β when passing through the primary fluid.

The ray from the edge of the black mask is therefore refracted by an angle

$$\beta = 180^{o} - 2 \arcsin \frac{n_2}{n_1}$$

Since all rays from the black mask are refracted in a similar way, they give rise to a dark border at the surface of the primary fluid. The abi-

lity to discover a jet which only slightly differs in refractive index from the surroundings can be demonstrated by the following calculation.

If the distance l in figure 3.10 between the mask and the jet is 10 mm and the slit b in the mask is 0.2 mm then

$$\beta = \text{arc tg} \frac{b}{2 \cdot l} = 0.57^{o}$$

making it possible to distinguish the primary jet when

$$\frac{n_2}{n_1} = 10^{-5}$$

By changing the mask from a single slit to other suitable configurations this method provides a simple means to discover borders between media with almost the same refractive index.

In the calculations above the refraction in the air-glass or glass-liquid border has been disregarded.

4 INVESTIGATION OF FLOW PATTERN IN THE STABLE COMPOUND JET

4.1 Introduction

By forcing the primary fluid through the stationary secondary fluid a complex flow pattern is generated. The jet emerging from the compound nozzle assembly can be either stable or unstable due to this pattern. In the following a jet breaking into droplets only due to the varicose instability described by Rayleigh (1878) is regarded as stable. The point of drop formation of such a jet always lies at the same place and the direction of drop propagation is the same. The drop formation point of an unstable jet moves back and forth and the drops have different radial velocity components, causing the jet to turn into a spray. This chapter describes experimental results for stable compound jets.

4.2 Flow pattern inside secondary fluid

The primary jet travelling through the secondary fluid is shown in Figure 4.1. The primary jet issues from a glass nozzle seen to the left and the compound jet emerges to the right. The meniscus of the secondary fluid is curved and is suspended at the edge of the cover glass of the compound assembly. The primary jet can be followed close to the edge of the cover glass.

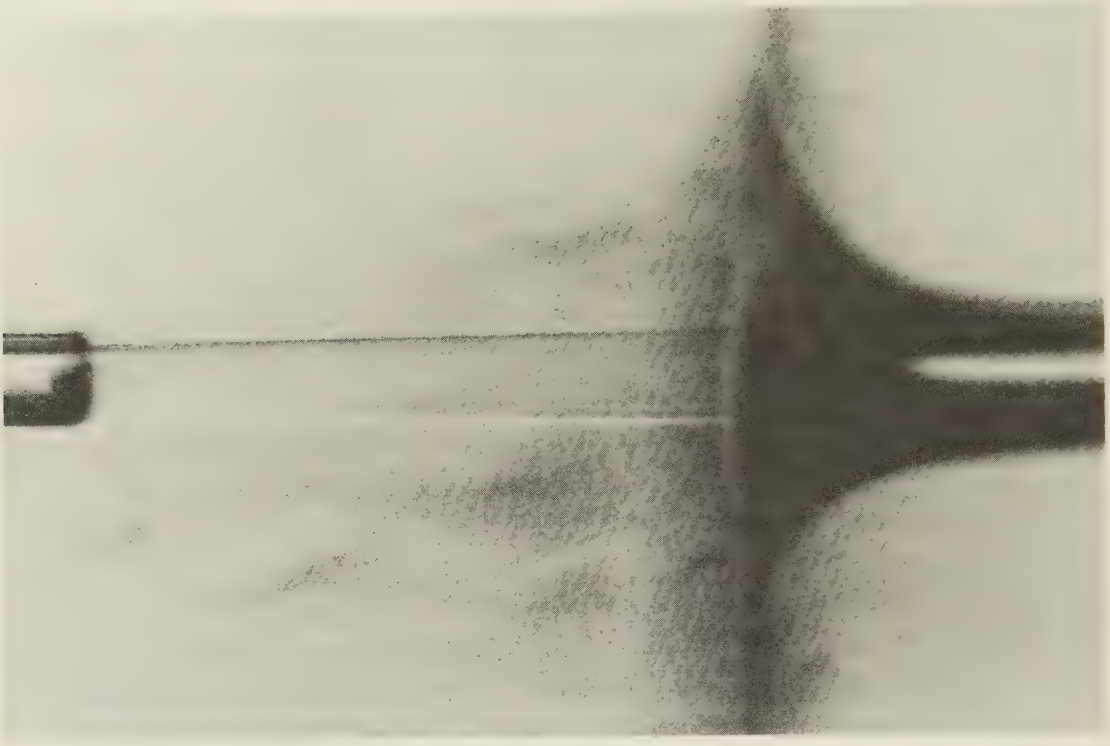

Figure 4.1. Compound jet formed from a primary jet (20% ethanol, 80% water) emerging from a 75 μm glass capillary through a clear secondary fluid (water) inside the compound nozzle assembly and through the water surface into air, thereby forming a compound jet (right). Primary jet velocity 11.5 m/s.

When entraining the secondary fluid the primary jet is slowed down. Since the flow of the primary fluid is the same at different distances from the primary nozzle, this retardation appears as a successive thickening of the primary jet.

From the dimensions in Figure 4.1 the retardation of the primary fluid can be calculated. The primary jet velocity v_1 at one point where the diameter of this jet is d_1 decreases to v_2 at another point with the increased primary jet diameter d_2. Following from the continuity of primary fluid flow Q_p we have

$$Q_p = v_1 \frac{\pi d_1^2}{4} = v_2 \frac{\pi d_2^2}{4}$$

If the retardation r is constant, the distance s travelled between the two points is

$$s = v_2 t + \frac{rt^2}{2}$$

since $v = v_2 + rt$

then $s = \frac{1}{2}(v_1 + v_2)t$

during the time t. From this the retardation r can be calculated if it is regarded as constant over the distance s.

$$r = \frac{v_1^2 - v_2^2}{2s} = \frac{v_1^2(1 - \frac{d_1^4}{d_2^4})}{2s}$$

Since v_1, d_1, d_2 and s can be measured from flow volume Q_p and microscope measurements respectively, r is calculated to $8 \cdot 10^4$ m/s^2 in Figure 4.1.

The retardation of the primary jet corresponds to an acceleration of the entrained secondary fluid. This acceleration continues inside the formed compound jet until a plug flow pattern is attained where the velocity of the primary jet is the same as the velocity of the secondary fluid.

The flow pattern of this acceleration inside the secondary fluid can be demonstrated by visualizing streamlines by introducing a tracer fluid. In Figure 4.2 this tracer fluid is added from above in the picture and is entrained and accelerated which explains the diminishing diameter of the tracer fluid.

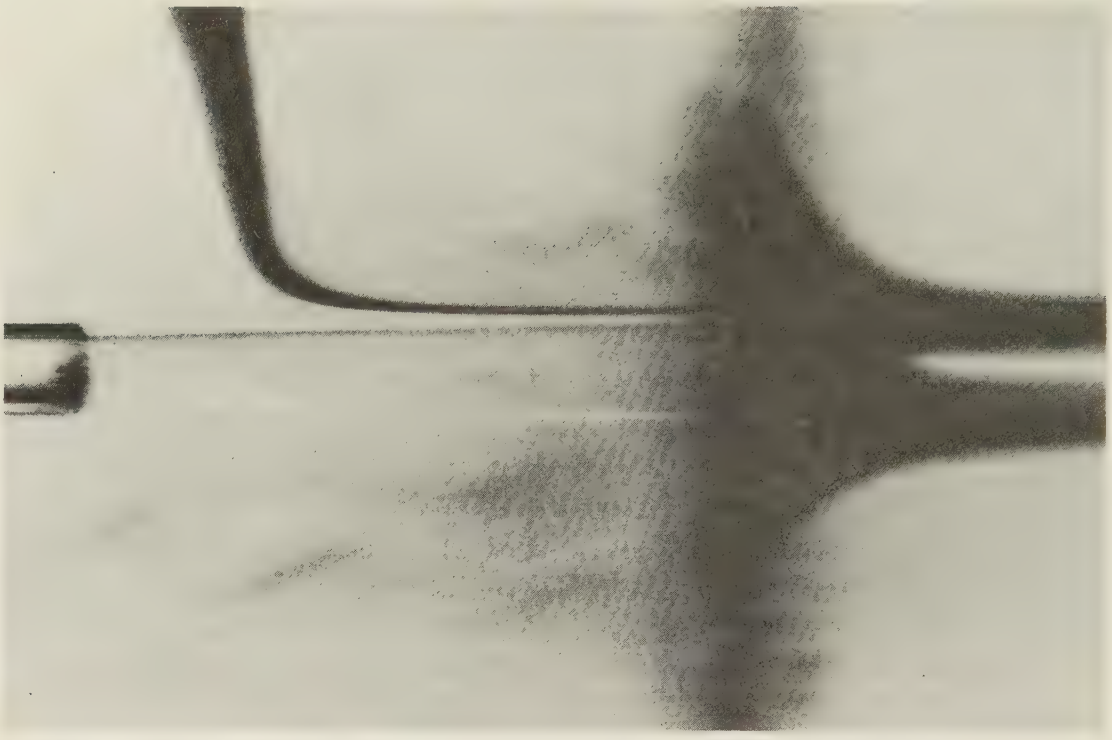

Figure 4.2. Microphotograph of compound jet generation. Dark tracer fluid added inside the compound nozzle assembly. The tracer fluid follows a streamline and is accelerated with the secondary fluid into the compound jet. Primary fluid is 20% ethanol, 80% water, secondary fluid is water. 75 μm primary jet, velocity 11.5 m/s.

When adding a tracer fluid at different places inside the secondary fluid different streamlines are revealed. Figure 4.3 shows a series of pictures where different streamlines are seen in different pictures, other parameters kept constant. The streamlines show first the acceleration of the secondary fluid. Further, they show the successive retardation of the inner part of the secondary fluid as the outer part is accelerated. This is demonstrated when the streamlines are first approaching the primary jet and then travelling parallel to the converging primary jet (cf. chapter 6).

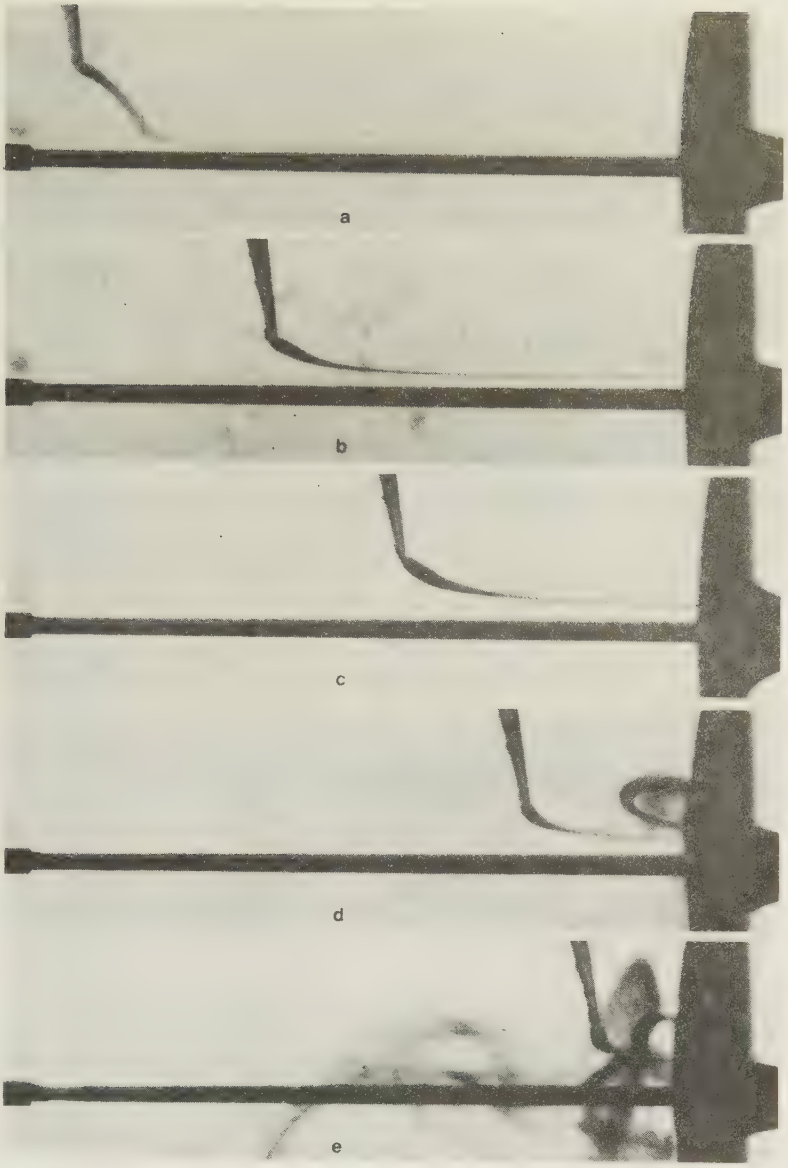

Figure 4.3. Streamlines in the secondary fluid shown by a colored tracer fluid which issues from a fine nozzle on top of the pictures. Accelerated but laminar flow is indicated for secondary fluid layers close to the primary jet. Eddies develop close to the secondary fluid/air boundary (4.3d and 4.3e). Primary jet diameter 75 µm, primary jet velocity 8.1 m/s, viscosity of primary fluid η_p = 1.9 cP and of secondary fluid η_s = 1.7 cP. Reynolds number of primary jet Re_p = 320. Flow of secondary fluid 65 µl/s.

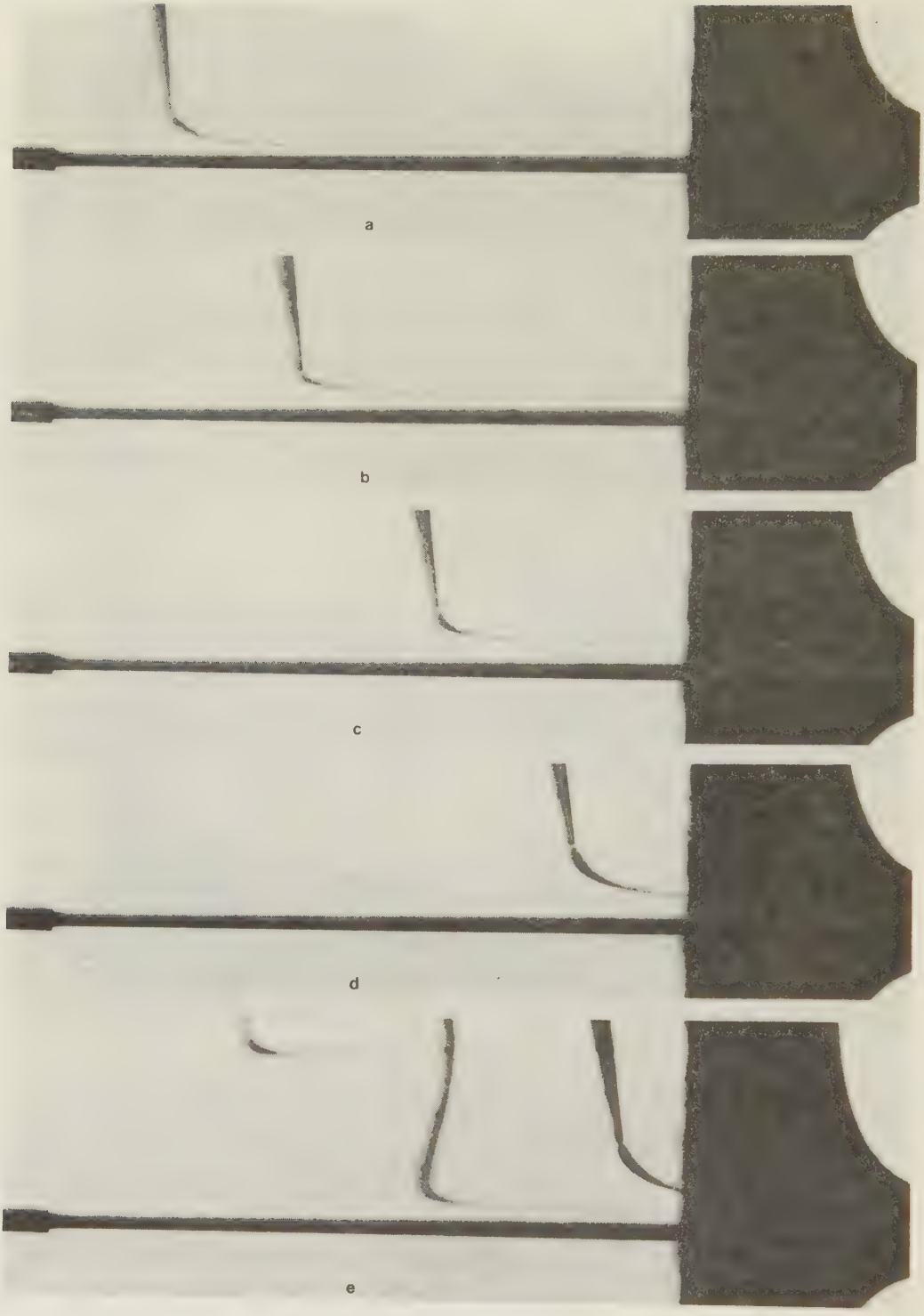

Figure 4.4. Streamlines in the secondary fluid. The flow of secondary fluid is increased compared to

(Figure 4.4 continued).

Figure 4.3. Primary jet diameter 75 μm, primary jet velocity 8.1 m/s, viscosity of primary fluid η_p = 1.9 cP and of secondary fluid η_s = 1.7 cP. Reynolds number of primary jet Re_p = 320. Flow of secondary fluid 82 μl/s.

Increasing the flow of the secondary fluid causes the distance between the primary jet nozzle and the meniscus of the secondary fluid to increase as seen in Figure 4.4. This series shows streamlines rather similar to those of Figure 4.3 despite increased secondary fluid flow. The eddies in the secondary fluid are seen to develop close to the secondary fluid/air boundary.

4.3 Flow pattern at fluid/air boundary

The irregularities of the flow in the secondary fluid close to the meniscus indicate that the flow close to this boundary is not only following the surface. Therefore a separation point in the boundary at the very meniscus can be expected. At such a separation point the viscous shear-forces are zero. Since this meniscus is also affected by the surface tension of the secondary fluid, the place of the separation point can be expected to vary if the surface tension of the fluid is changed. The separation point in the meniscus is demonstrated in Figure 4.5. Here a fine nozzle for tracer fluid is penetrating the meniscus from the inside. This nozzle is seen from the outside of the meniscus in the picture. The tracer fluid flows out from the nozzle, follows the outside of this nozzle back to the meniscus, where the tracer fluid is entrained by the secondary fluid flow in the surface. At the separation point (arrow) the tracer fluid turns inward from the surface and forms an eddy inside the secondary fluid. At low surface tension of the secondary fluid (Figure 4.5b) no separation point can be seen. Increasing the surface tension causes a separation point to appear close to the area where the compound jet is leaving the meniscus. Increasing the surface tension further causes the separation point to move backwards from the compound jet closer to the tracer fluid nozzle. The surfactant used is a tenside normally added to rinsing water to improve the drying of photographic film (Agfa Agepon). This indicates that the formation of the new surface of the compound jet happens slowly enough to allow the surfactant monolayer to form at the surface.

Similar results are obtained with other additives e.g. alcohol but these experiments offer no information about how fast the new surface of the compound jet is formed.

Figure 4.5. The meniscus and the compound jet seen from the outside. A fine tracer fluid nozzle penetrates the meniscus on top of the picture, 4.5a shows no tracer fluid, 4.5b shows a flow of tracer fluid in the meniscus, following it all the way to the compound jet. 4.5c shows a separation point (arrow) in the meniscus where the tracer fluid leaves the meniscus and flows into the secondary fluid, forming an eddy. In 4.5d the separation point has moved further away from the compound jet. The surface tension is increased from 4.5b to 4.5c and further increased in 4.5d by using diminishing concentrations of tenside in the secondary fluid.

4.4 Flow pattern inside laminar compound jet

In order to demonstrate the flow pattern inside the compound jet it is not possible to use a tracer fluid. Instead a mechanical arrangement outside the compound nozzle assembly was used (Figure 4.6). A sharp needle held in an adjustable fixture was mounted in the vicinity of the compound jet. The point of the needle was moved against the compound jet at different places between the compound nozzle assembly and the point of drop formation. When the needle was inserted a short distance into the jet as seen in Figure 4.6 it acted as a planing blade. The needle removed some fluid from one side of the compound jet and caused simultaneously a one-sided retardation of the flow speed thereby altering the jet direction.

Figure 4.6. The sharp point of a needle acting as a planing blade on the compound jet. Figure 4.6b shows a magnified part of the point of the needle planing off clear secondary fluid only, leaving the dark primary fluid undisturbed.

The compound jet photographed in Figure 4.6 is composed of a colored primary jet and a clear secondary fluid. The sheath of the secondary fluid is planed off as seen in Figure 4.6b where only clear fluid is seen to the right of the needle while the colored primary fluid is situated in the middle of the compound jet and thus left unaffected by the needle.

By inserting the needle at different places along the compound jet it has been demonstrated that the laminar compound jet consists of a cylindrical core of primary fluid enclosed by a coaxial sheath of secondary fluid. This configuration continues to the point of drop formation.

Of course it should be possible to demonstrate this jet geometry directly by simply photographing a compound jet consisting of a colored primary fluid and a translucent secondary fluid. However, the refraction of light in the secondary fluid makes it difficult to discern the primary fluid in a normal compound jet as explained in the following.

When the primary jet is seen through the sheath of clear secondary fluid its diameter is magnified due to the curved surface of the compound jet. Following from the law of refraction and Figure 4.7 the primary jet with radius r_p is apparently enlarged to the radius

$$r'_p = n_s \cdot r_p$$

where n_s is the refractive index of the secondary fluid.

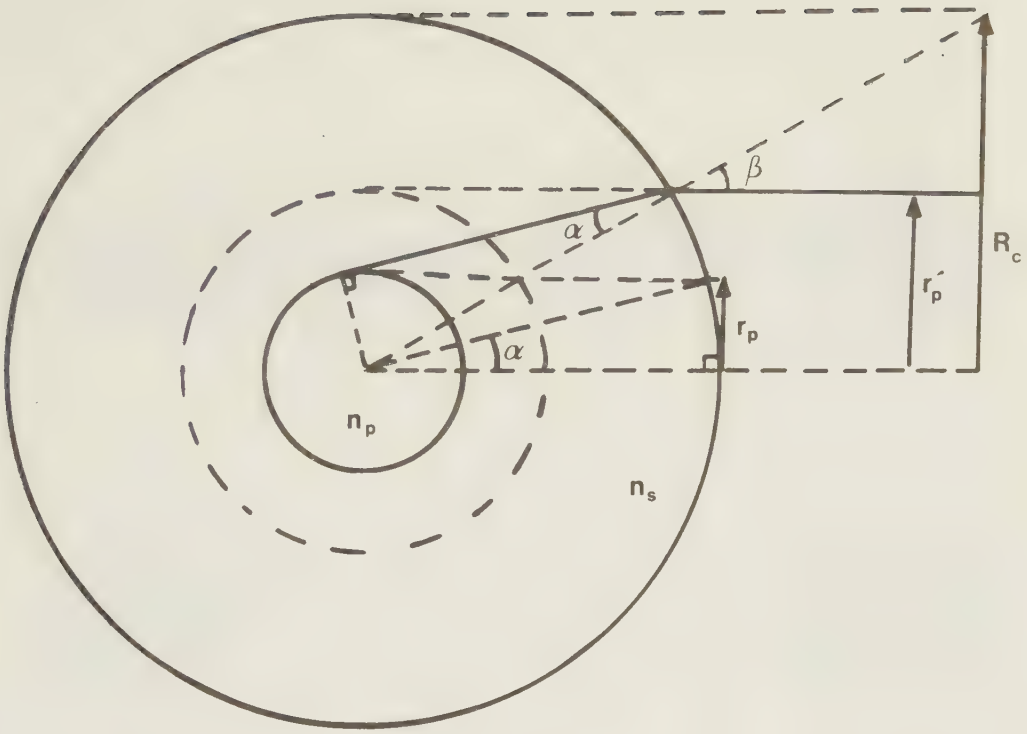

Figure 4.7. The primary jet with radius r_p is apparently enlarged by the curved surface of the compound jet causing the radius to look like r'_p from outside the jet.

$$\frac{r'_p}{r_p} = \frac{R_c \sin \beta}{R_c \sin \alpha} = n_s$$

Now, in an ordinary compound jet the secondary fluid flow approximately equals the flow of the primary jet. If the speed of the secondary fluid also equals the speed of the primary jet the diameter of the compound jet is 1.4 times the diameter of the primary jet. However, due to the magnification discussed above the actual compound jet diameter is only 1.04 times larger than the apparent primary jet diameter if the refractive index n_s is 1.35. This makes it difficult to observe the primary jet inside the compound jet. However, by strongly increasing the ratio of secondary to primary fluid flow it is possible to see the primary jet inside the compound jet.

In Figure 4.8 a colored primary jet is thus made visible inside a clear secondary fluid. Here the ratio of secondary to primary fluid was 3.2. The figure consists of a series of pictures ranging from the formation of the compound jet to the very drops formed from the jet. The picture was made possible by using the soft lighting method earlier mentioned (cf. chapter 3.3).

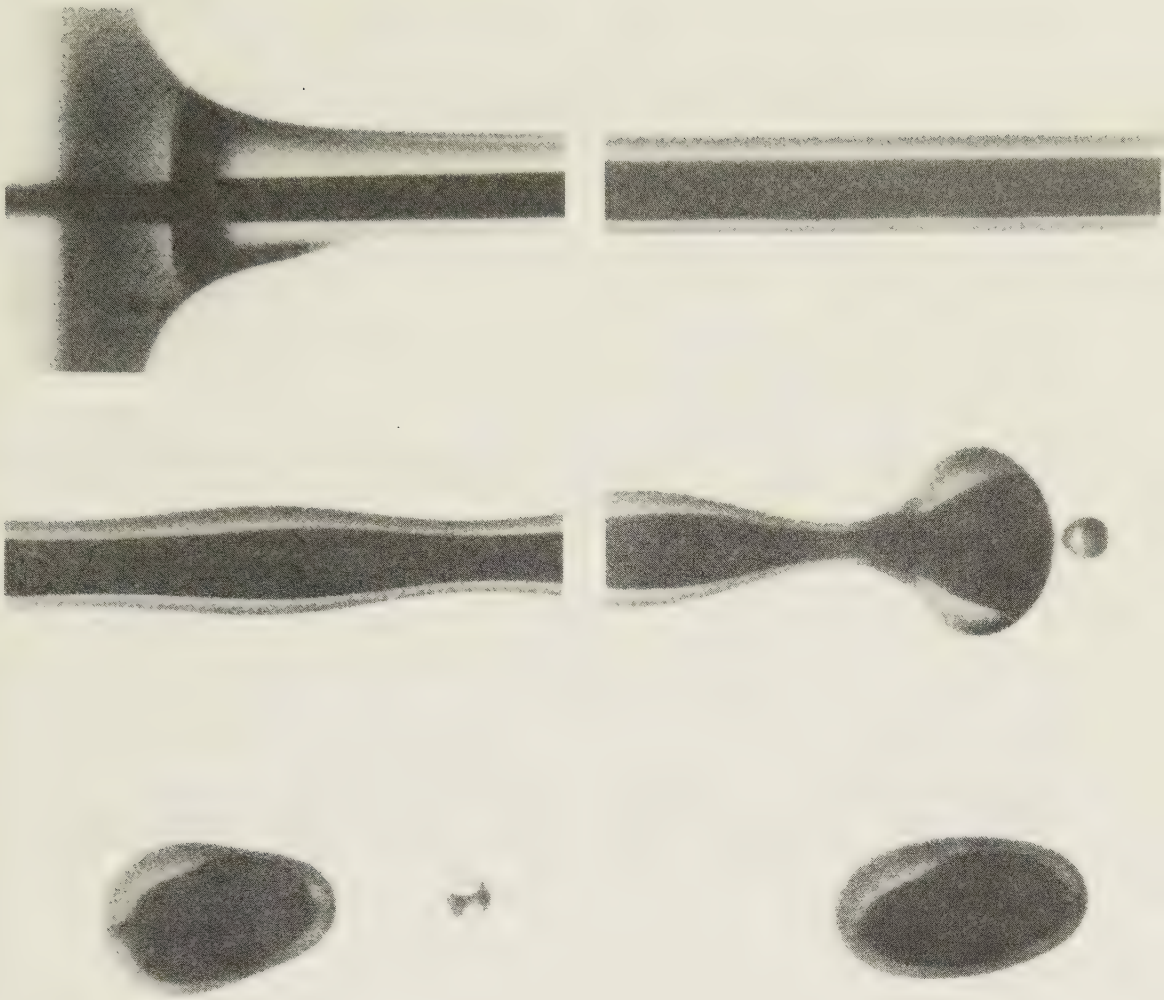

Figure 4.8. The formation of a laminar compound jet consisting of a core of colored primary fluid enclosed in a sheath of clear secondary fluid. Even the drops formed from the jet demonstrate a similar structure. Primary fluid flow 36 µl/s, secondary fluid flow 115 µl/s, primary and secondary fluid 80% water + 20% glycerine. Distance from nozzle to point of drop formation 22 mm.

It can be observed that the diameter of the primary jet is increased while the diameter of the compound jet is decreased as the speed of the primary and the secondary fluid is equalized. The sinusoidal disturbance causing the drop formation is formed in the compound jet-air surface causing a similar disturbance of equal wavelength in the primary jet inside. Closer to the point of drop formation the disturbance is growing in a non-sinous way much like an ordinary jet causing satellite drops as well as parent drops. The parent drops are formed with a sheath of secondary fluid as the jet itself. The satellite drops, however, show no tendency but are randomly formed from the ligament between the parent drops with both primary and secondary fluid.

The surface tension of the compound jet/air boundary is determining the drop formation of the compound jet itself. Likewise the surface tension between the primary and the secondary fluid can be expected to affect the propagation of the primary fluid inside the compound jet. This is most clearly visible when the primary and the secondary fluids are not mixable and the surface tension between the primary and the secondary fluid is different from that between the secondary fluid and air. This can be demonstrated by a water soluble primary fluid with high surface tension (70 dyn/cm) and an oil as secondary fluid with low surface tension (20 dyn/cm). Waterbased dye ink and clear silicone fluid comply with these specifications. Further silicone fluid is available with different viscosities making it easy to adjust this parameter without changing the low surface tension property.

In Figure 4.9 an example of a compound jet with unmixable primary and secondary fluids is shown. The dark primary fluid is a water soluble dye ink with surface tension of about 70 dyn/cm while the clear secondary fluid is a Midland Silicones MS 200 Dimethyl silicone fluid with surface tension of about 20 dyn/cm and viscosity 2 cP.

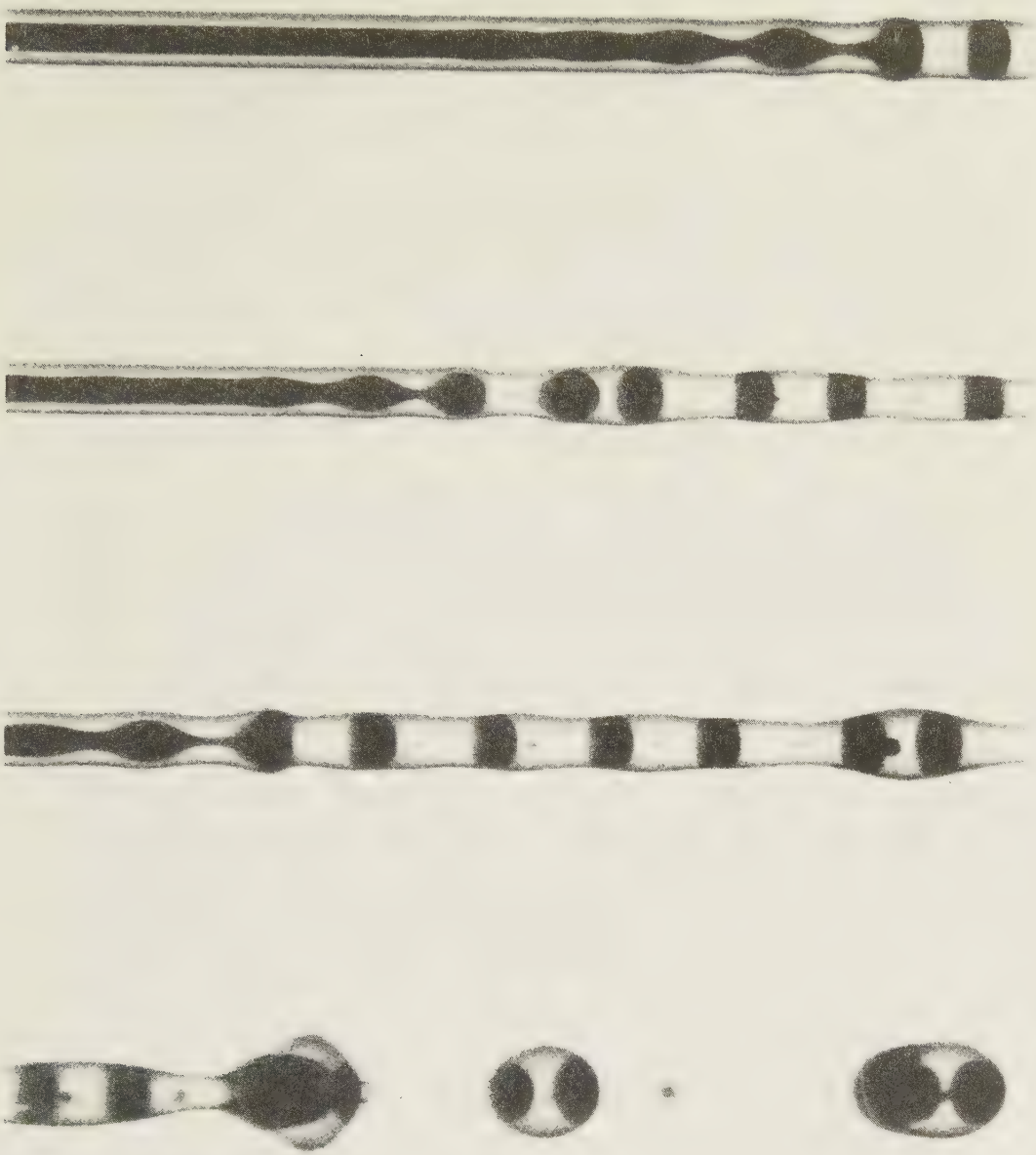

Figure 4.9. Water soluble primary fluid with high surface tension inside a sheath of low surface

tension silicone fluid. The two fluids are not mixable and demonstrate separate points of drop formation according to the different surface tensions of the two fluids. The primary jet forms parent drops as well as satellite drops inside the compound jet. The wavelength of the disturbance of the compound jet is larger than that of the primary jet causing more than one drop of primary fluid to be incorporated in each compound jet drop. The primary jet comes from a 75 µm glass capillary with primary fluid flow 35 µl/s. Secondary fluid flow 115 µl/s. Viscosity in primary and secondary fluid about the same (2 cP). Surface tension of primary fluid 70 dyn/cm, of secondary fluid 20 dyn/cm. Surface tension at interface primary-secondary fluid ≃ 50 dyn/cm. This causes drop formation of primary fluid column much earlier than dropformation of compound jet.

The surface tension between the primary and secondary fluid can be estimated by subtracting the respective surface tensions to air from each other. Since the difference is 50 dyn/cm this surface tension is larger than that of the compound jet to air surface tension (20 dyn/cm). Therefore a drop formation of the primary fluid inside the compound jet is expected before the compound jet itself disintegrates

The drop formation of the primary jet can be clearly seen in Figure 4.9 where both parent and satellite drops inside a sheath of secondary fluid are demonstrated. The compound jet itself is somewhat affected by this drop formation inside and disintegrates later into drops as shown in the figure. Since the wavelength of the disturbance of the compound jet is larger than that of the primary jet, the compound jet drops often contain two primary fluid drops. The satellite drops formed by the compound jet sometimes contain a separate primary jet satellite as seen in the figure.

Figure 4.9 also demonstrates a proof of early jet theories (Rayleigh 1878) concerning drop formation. Since the primary and secondary fluids travel with equal velocities the primary jet disintegrates into drops unaffected by jet movement in air as the surrounding secondary fluid is stationary relative to the primary fluid. Therefore the observed disturbance of the primary fluid can only be explained by the effects of surface tension be-

tween the fluids and the viscosities of the fluids and not by the velocity of the primary fluid.

The stability of the two different drop formation points shown in Figure 4.9 indicates conceivable applications for the use of non-mixable fluids in ink jet printing.

4.5 Transfer of momentum inside the compound jet

By supplying more secondary fluid to one side of the primary jet than to the other side the transfer of momentum inside the compound jet can be demonstrated.

Figure 4.10 shows a stable compound jet moving horizontally in air. The secondary fluid flow is chosen in such a way that a drop is suspended outside the nozzle assembly opening due to gravity. The primary jet ejected through the opening therefore entrains more secondary fluid from the lower side where the drop hangs than from the upper side (Figure 4.10a). Thereby the lower part of the primary jet also is retarded compared to the upper part causing the compound jet to turn downwards.

Due to viscosity a transfer of momentum takes place from the primary fluid to the more slowly moving secondary fluid. The upper part of the secondary fluid represents a thinner sheath than the lower and is therefore accelerated more quickly by the primary jet. When the lower part of the secondary fluid successively assumes a higher velocity this change can be regarded as a retardation of the whole upper part of the compound jet causing it to turn upwards again as can be seen in Figure 4.10b.

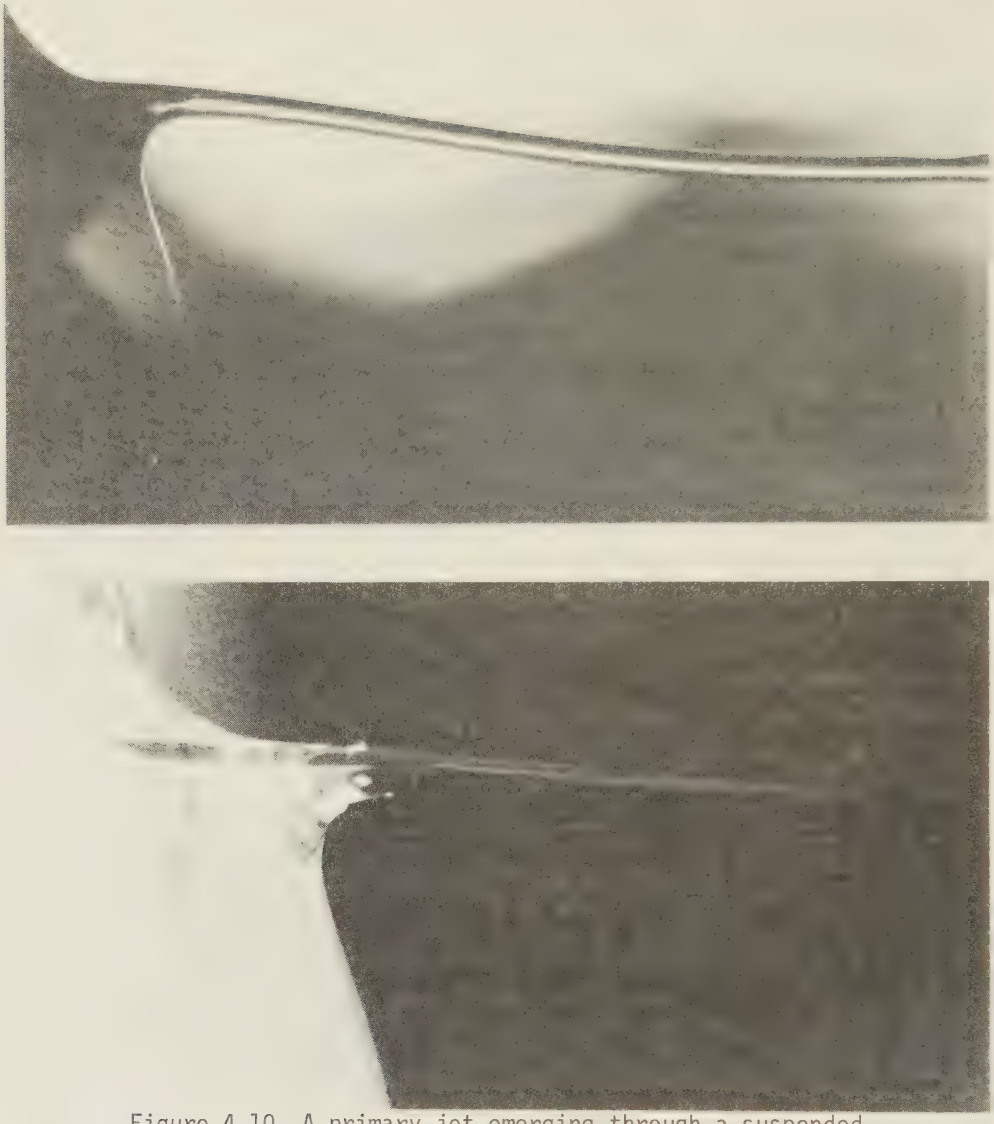

Figure 4.10. A primary jet emerging through a suspended drop of secondary fluid causing the jet to entrain more fluid on the lower side than on the upper one (4.10a). This causes an asymmetrical velocity distribution resulting in a downwards and later upwards bending of the compound jet (4.10b). The primary jet emerges from a 75 µm glass capillary with primary fluid flow 28 µl/s. Secondary fluid flow is controlled by adjusting the position of the primary jet nozzle while the secondary fluid is supplied from an open container. Viscosity in primary and secondary fluid about the same (2 cP).

4.6 Qualitative discussion

The formation of a laminar compound jet is caused by transfer of momentum from the retarding primary jet to the accelerating secondary fluid. Figure 4.11 shows a qualitative picture of the streamlines and the velocity distribution inside the secondary fluid demonstrating this acceleration. The successive retardation of the inner parts of the flow causes the flow to diverge, thereby causing the possibility of backward flow in the outer part of the secondary fluid (Prandtl and Tietjens 1934). This backward flow results in eddies indicated in Figure 4.11.

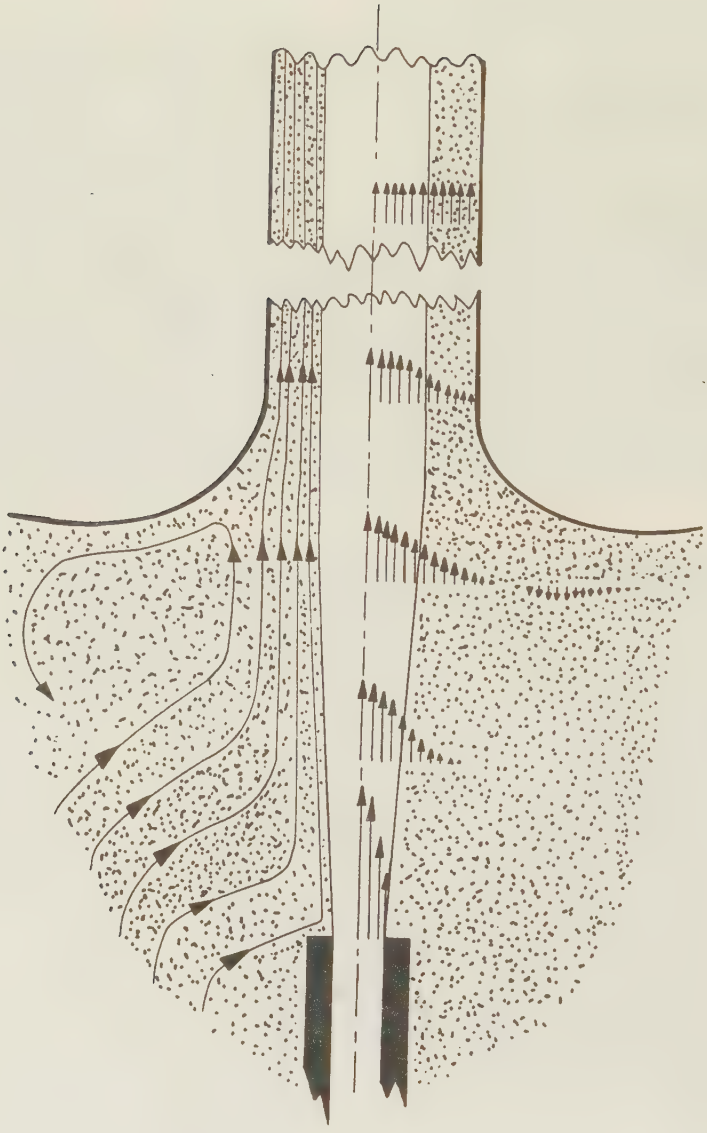

Figure 4.11. Qualitative picture of streamlines in the secondary fluid and velocity distribution in a laminar compound jet. The primary fluid is retarded while the secondary fluid is accelerated in a diverging flow also causing eddies.

As seen in the pictures a plug flow velocity profile cannot be assumed for the compound jet when emerging from the surface of the secondary fluid. The flow profile, however, flattens out more and more in the same way as a normal jet with a parabolic profile when exiting from the nozzle. The length l of such a jet until plug flow is attained can be approximated to

$$l = 0.025 \ Re \cdot d \qquad (4.1)$$

where Re is the Reynolds number for the flow and d is the diameter of the jet according to Brun and Lienhard (1968).

The redistribution of the flow profile in a compound jet can be observed in Figure 4.10. Here the primary jet enters the compound jet in an extremely excentric mode (Figure 4.10a). As a result of this the compound jet bends downward since the velocity in the compound jet at the exit from the meniscus not only varies strongly with radius but the flow profile is strongly assymmetrical. After about 12 jet diameters the jet begins to change its direction again, whereafter the direction is constant.

The fact that the direction is constant after the second bending can be explained by the assumption that plug flow is attained here. This assumption is supported by comparing this jet with a conventional jet, the relaxation length of the flow profile is given by equation (4.1).

Since the primary jet velocity in Figure 4.10 is 6.3 m/s, primary fluid viscosity 2 cP and density 10^3 kg/m^3 the Reynolds number can be calculated (cf. chapter 6)

$$Re = \frac{6.3 \cdot 75 \cdot 10^{-6} \cdot 10^3}{2 \cdot 10^{-3}} \approx 240$$

Since the densities and viscosities of the primary and secondary fluids are about the same the Reynolds number is also about the same for the primary and the compound jet (cf. chapter 6).

According to this a plug flow profile should have developed at about $0.025 \cdot 240 = 6$ compound jet diameters. However, from Figure 4.10b we find

that the distance between the bends in the jet is about 12 jet diameters. This discrepancy can be explained by the fact that the flow profile at the meniscus is also strongly asymmetric which accounts for a longer relaxation time for the flow profile. Remembering this the agreement between theory and experiment is acceptable.

5 INVESTIGATION OF FLOW PATTERN IN UNSTABLE COMPOUND JETS

5.1 Introduction

It has been pointed out earlier (cf. chapter 2) that the compound jet may become unstable. Except for the varicose instability leading to drop formation observed in conventional jets two other types of instabilities can be demonstrated in the compound jet. Beside the varicose instability there exists a sinous instability and a random instability in the compound jet. While the varicose instability gives rise to a stable, axisymmetric point of drop formation, the other instabilities cause the point of drop formation to change position in an irregular manner and the drops to travel in different directions.

Since all the instabilities are initiated by small disturbances, their respective speed of growth determines which of the three instabilities will develop fastest and thus visibly dominate the jet. The speed of growth depends on the jet parameters.

The sinous and random instabilities are related to velocity and viscosity profiles inside the jet resulting in energy redistribution as the jet moves along. Also aerodynamic forces are involved in these types of instabilities as they are in secondary atomization of ordinary jets as described by McCarthy and Molloy (1974).

In the following the three different instabilities will be discussed more in detail.

5.2 Varicose instability

5.2.1 Normal liquids

The theory for varicose jet instability due to surface tension forces was given by Rayleigh (1878) and was improved by Weber (1931) by including the viscosity of the fluid into the calculations. Lately Chaudhary and Redekopp (1980) were able to explain the formation of satellite drops between the main drops in the jet break-up process.

As shown in Figure 4.8 the drop formation in the compound jet due to varicose instability is the same as in the conventional jet. More examples

of compound jet drop formation are given in Figure 5.1 where the parameters of the primary and secondary fluids are essentially equal to those in Figure 4.8.

Figures 4.8 and 5.1 show clearly that no visible instabilities exist on the primary fluid column on its way to the point of drop formation.

Even during drop formation no mixing of secondary and primary fluid occurs as indicated by the well defined boundary between primary and secondary fluid in both parent and satellite drops. Thus, in this case, varicose instabilities dominate over the instabilities described below leading to normal drop formation. Satellites are formed as in conventional jets. However, satellite formation is influenced by the choice of primary and secondary fluid viscosity. Preliminary observations indicated that satellite formation decreases with increasing viscosity of primary fluid.

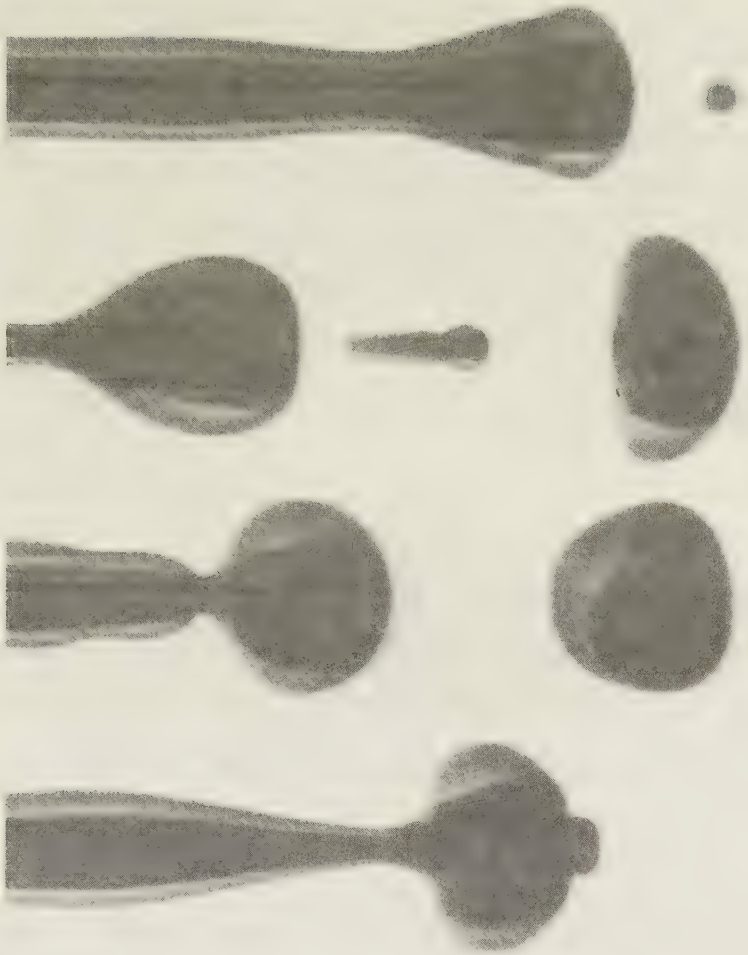

Figure 5.1. Different examples of compound jet drop formation due to varicose instability. No separate instability is seen in the primary jet or inside the parent or satellite drops. Primary flow 36 µl/s, secondary flow 115 µl/s, primary and secondary fluid 80% H_2O + 20% glycerine. Distance from nozzle to point of drop formation 22 mm.

5.2.2 Non-mixable fluids

In chapter 4, Figure 4.9 a compound jet was demonstrated consisting of two non-mixable fluids, i.e. essentially water and silicon fluid. The drop

formation of the primary jet occurs before the compound jet breaks up. There exists also another difference between the two points of drop formation. By comparing the three photographs of the same jet in Figure 5.2 it is demonstrated that while the place of the primary jet drop formation is reasonably stable, the compound jet drop formation moves back and forth and produces unevenly sized drops with no, one or several primary fluid drops inside.

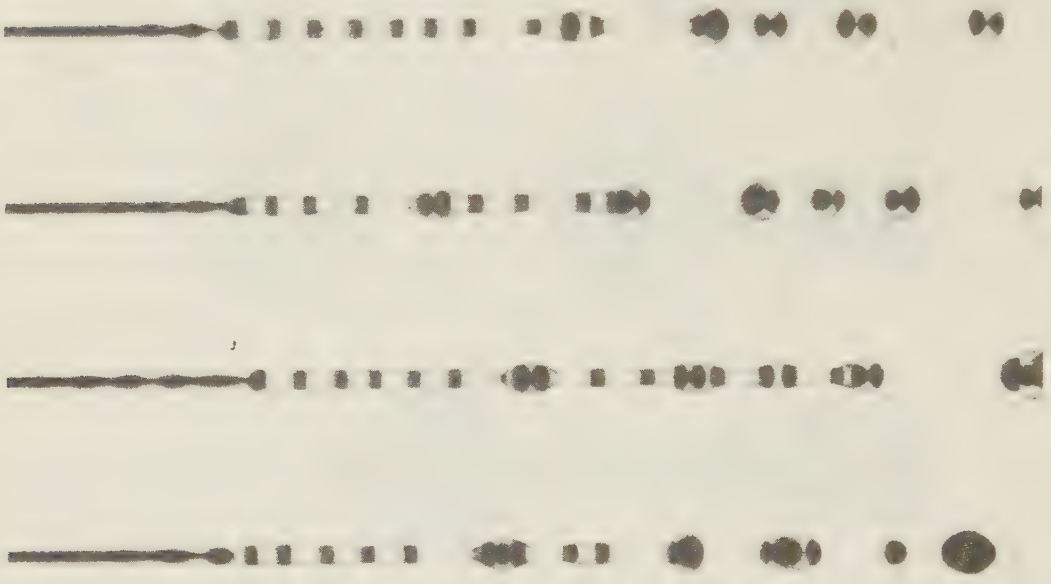

Figure 5.2. Water soluble primary jet fluid breaks up due to varicose instability inside a compound jet, the secondary fluid consists of silicon fluid. The different photographs show a stable primary jet drop formation and a less stable compound jet drop formation.

The varicose instability of the primary jet results in both a drop formation in the primary jet and a redistribution of the secondary fluid causing an instability of the compound jet. The surface tension of the secondary fluid-air boundary causes another, varicose instability of the compound jet.

These two instabilities of the compound jet become superimposed and the jet break-down is the final result of this. If the flow disturbance caused by the primary jet break-down is much larger than the surface disturbance existing in the secondary fluid-air boundary, the final compound jet break-down will be determined by the primary jet break-down. In Figures 4.9 and 5.2, however, the secondary fluid flow is large compared to primary fluid flow and therefore the flow disturbance caused by the primary jet break-down is small and comparable to the varicose instability in the compound jet surface. The final drop formation point is randomly determined from moment to moment.

5.2.3 Non-Newtonian liquids

Liquids where the viscosity is not independent of shear forces are called non-Newtonian liquids. In the following two such liquids will be discussed.

5.2.3.1 Addition of Polyethylene oxide

Some additives reduce drag tendencies in fluid flow in extremely low concentrations due to special viscous shear response. They are usually long synthetic molecules that are randomly formed like a ball of yarn by thermal motion. The time to form this ball from a stretched molecule is called "relaxation time". This time can be measured for different molecules and range from 10^{-13} s for water to $2 \cdot 10^{-4}$ s for the long polyethylene oxide molecules used in experiments described below (Bark 1978).

Since the polyethylene oxide molecules (Polyox) can pass the filters fitted to the primary jet nozzles, this additive can be used in both primary and secondary fluid. For the development of varicose instability described here no difference is noticed as to where the Polyox is added.

Bruce (1976) describes the effect of Polyox additives as decreasing the stability of a liquid jet. However, his criterion for stability is the magnitude of the signal voltage that has to be used on a piezoelectric transducer to control the drop formation and override the spontaneously developing varicose instability of the jet. According to his definition the smaller the signal necessary to control the drop formation, the more

stable the jet. This of course is a matter of definition but a jet with a very stable spontaneous drop formation is not easily disturbed by an external disturbance and can therefore be regarded as "stable". This definition is used in this paper.

Polyox additives to the fluids of a compound jet cause the point of drop formation to move away from the origin of the jet. With increasing concentration the additive tends to keep the drops linked with thin liquid threads as shown in Figure 5.3. It was also found that addition of polyox prevented other instabilities from forming, i.e. the instabilities described in 5.3. and 5.4. The additive does not encourage other instabilities (cf. 5.4.2).

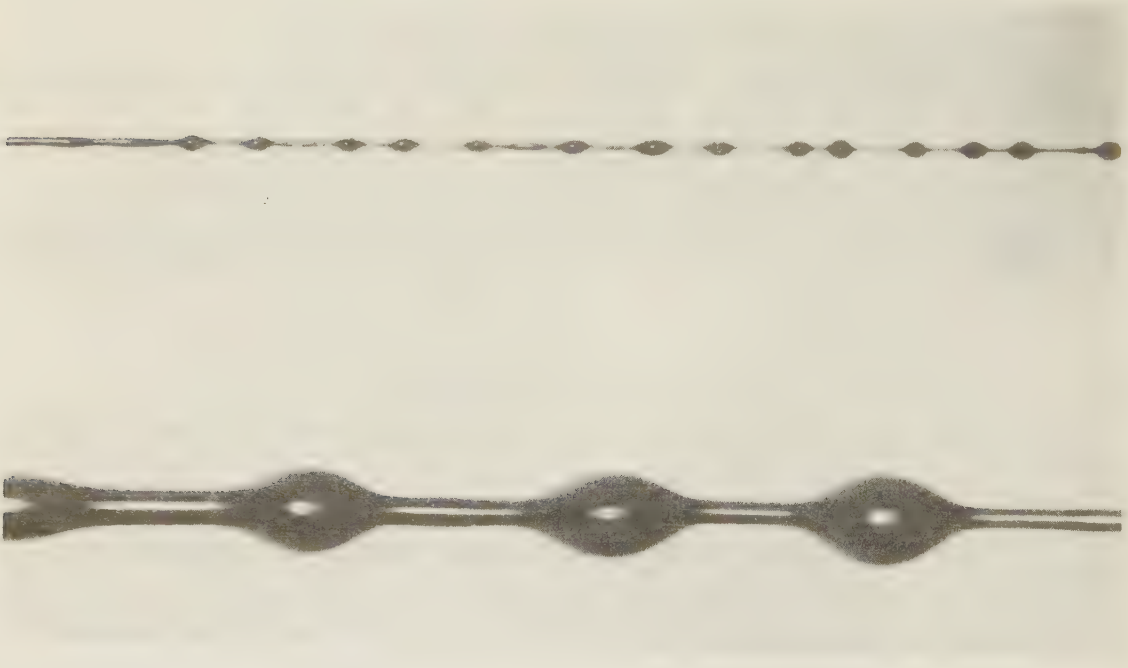

Figure 5.3. Polyethylene oxide (MW 300 000) added to the secondary fluid causes the varicose drop formation to be elongated and link the drops together. Polyox concentration is 0.2% by weight in water. Primary jet diameter is 75 μm and velocity 7 m/s. Primary fluid is 20% glycerine and 80% water.

5.2.3.2 Influence of particles in the secondary fluid

Inhomogenities in the liquids in the form of particles cause disturbances and instability. Since large particles will clog the primary nozzle, experiments have only been made with particles in the secondary fluid. In Figure 5.4 a round Sephadex pellet is locally disturbing the compound jet which, however, resumes stability immediately after the pellet has passed. Thereafter the normal varicose instability dominates again and the jet resumes its stable condition.

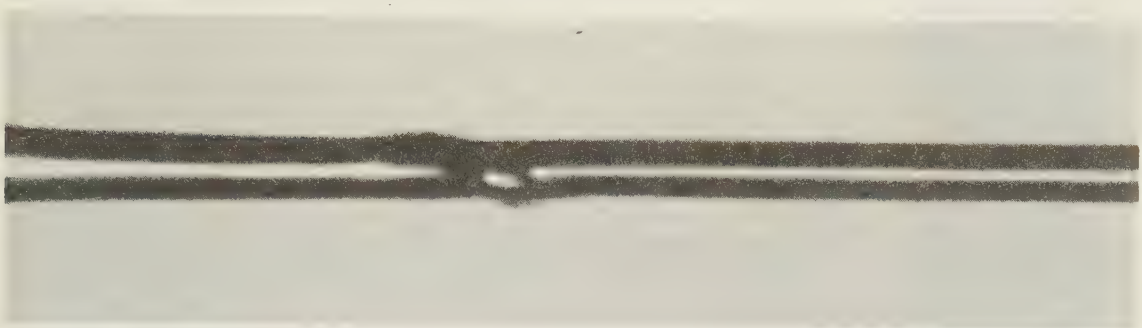

Figure 5.4. Sephadex pellet with diameter = 30 μm causing a disturbance in a compound jet with a diameter of 100 μm. The instability is local and the jet resumes stability immediately. Primary jet diameter is 75 μm and velocity 7.9 m/s. Primary and secondary fluids are 20% glycerine and 80% water.

5.3. Sinous instability

5.3.1 Examples of sinous instability

It has been mentioned earlier that the appearance of different types of instabilities depend on jet parameters. This is demonstrated in Figure 5.5 where a compound jet generated with the same primary jet is shown when the secondary flow is increased. At low secondary flow the jet is "stable" and breaks up into droplets in the varicose way described earlier. An increase of the secondary fluid flow causes the spontaneous appearance of

sinous instabilities on the jet as seen in Figure 5.5.b.

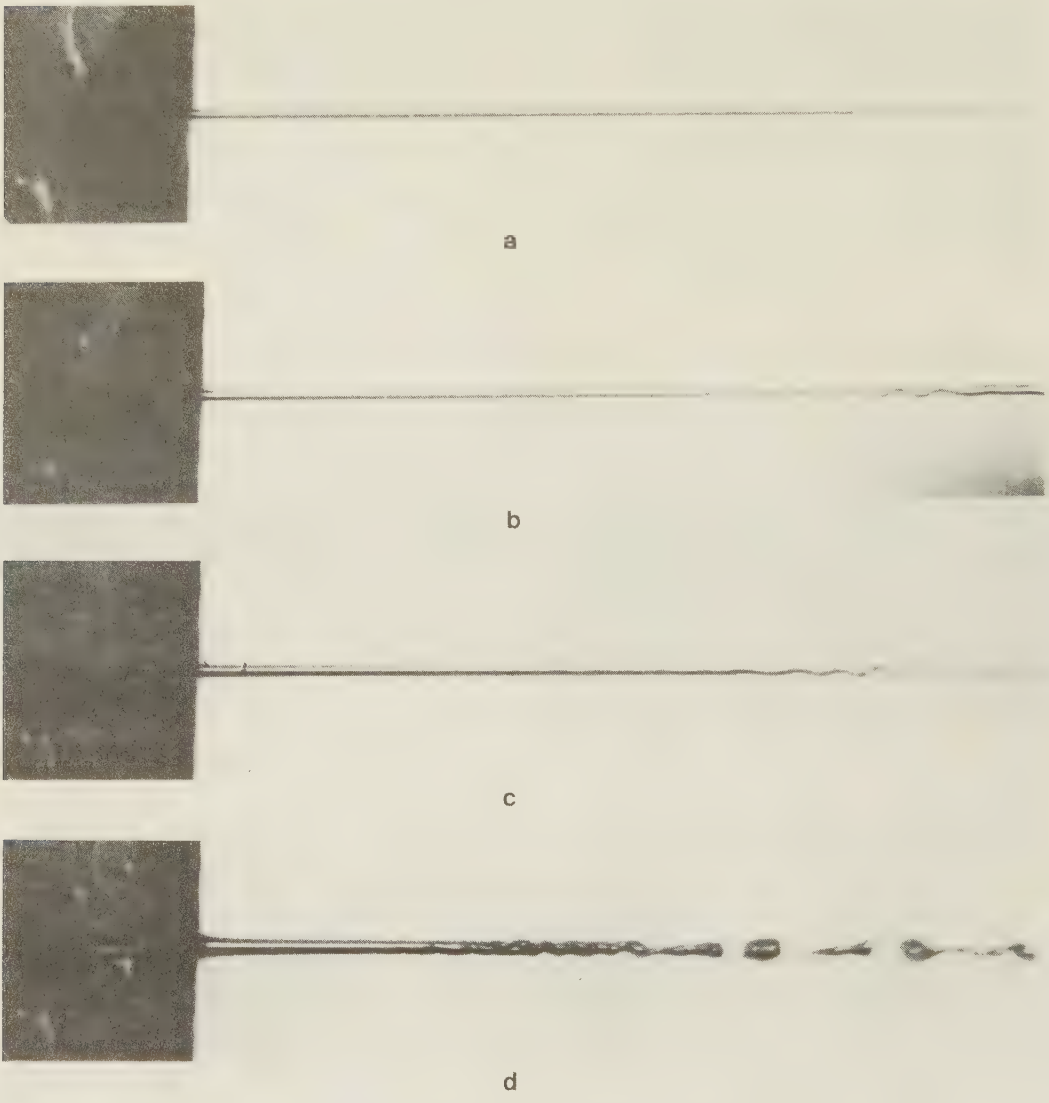

Figure 5.5. Compound jet with varying secondary fluid flow. Primary jet H_2O, secondary fluid 80% H_2O + 20% glycerine with viscosity 1.9 cP. Primary jet diameter 75 µm, velocity 11.1 m/s and flow 49 µl/s is the same in all pictures. Re_p = 875.

5.5.a Secondary fluid flow 5 µl/s
b " " " 10 µl/s
c " " " 15 µl/s
d " " " 28 µl/s

Further increase of secondary flow generates a continuous sinous instability (Figure 5.5.c). Finally, at high secondary flows (Figure 5.5.d) a random instability grows faster than the sinous instability thereby obscuring the latter. The series shown in Figure 5.5 demonstrate a general experimental fact found in all compound jets: independent of choice of viscosity and other properties of the primary and secondary fluid a stable jet can always be obtained if primary jet velocity and/or secondary fluid is decreased below a certain limit.

Figure 5.6.a and b show the drop formation point caused by sinous instability. From this example it is evident that the resulting drops leave in different directions and the jet therefore turns into a spray.

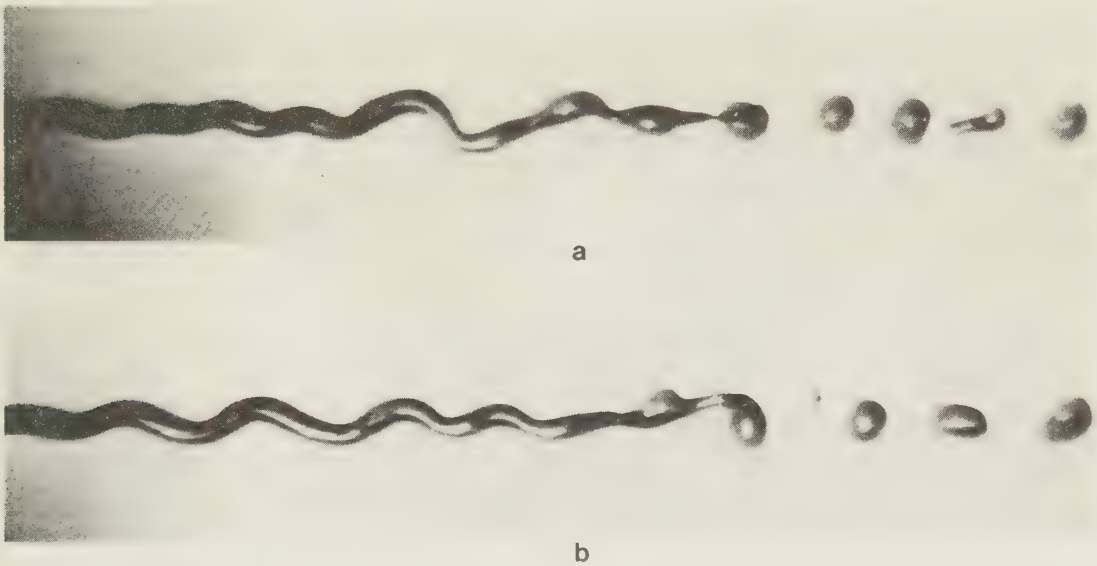

Figure 5.6. Compound jet drop formation caused by sinous instability resulting in drops travelling in different directions. Primary jet velocity 14 m/s and secondary fluid flow 30 µl/s. All other jet parameters equal to those in Figure 5.5.

5.3.2 Discussion

The series shown in Figure 5.5 has been obtained by a careful choice of the velocity of the primary jet as well as viscosities of the fluids used. It has not been possible to obtain pictures of the primary fluid column inside the compound jet when it is subject to sinous instability as in the stable jet shown in Figure 4.8. Therefore we do not know if the flow in the primary fluid column is still laminar. However, this is probably true since the surface of the compound jet is smooth, has a constant diameter and finally the jet often turns into a stable one after a moment of sinous instability. If instabilities would occur in the primary fluid column, these would at least be reflected by irregularities on the surface of the secondary fluid of the compound jet as shown below.

The helical instability in the secondary fluid forming an eddy inside the meniscus shown in Figure 4.4 and 4.5 can be expected to initiate a sinous instability (Batchelor & Gill 1962, Reynolds 1962). This instability is amplified after the primary jet has entered the funnel formed by the secondary fluid. At medium and large amplitudes of sinous instability the effect of the ambient air tends to amplify the undulations as demonstrated in Figure 5.5.c (Weber 1931, Haenlein 1932, Phinney 1973).

5.4 Random instability

5.4.1 Examples of random instability

As shown in Figure 5.5.d an irregular random instability can be induced in the compound jet. The appearance of the semi-turbulent flow pattern caused by this instability is very similar to that observed in conventional fluid jets in air having large Reynolds numbers (>500-3000). The stability and break down of these conventional jets has been investigated by among others Haenlein (1932) and Phinney (1973).

Figure 5.7 shows examples of the random instability in compound jets caused by visible instabilities in the primary jet already before reaching the meniscus. This instability is very similar to that reported by McNaughton and Sinclair(1966) for liquid-in-liquid jets with Reynolds numbers of about 1000. The instability of the primary jet is not damped after passing the meniscus but carried into the compound jet where the instabili-

ty grows and distorts the flow in the jet and causes an irregular jet break-up into drops. As momentum is transferred more effectively to the secondary fluid by the irregular surface of the primary jet, secondary fluid is picked up faster than normal. This results in an appreciable shortening of the distance from the primary jet nozzle to the secondary fluid surface if the secondary fluid is supplied with a constant flow.

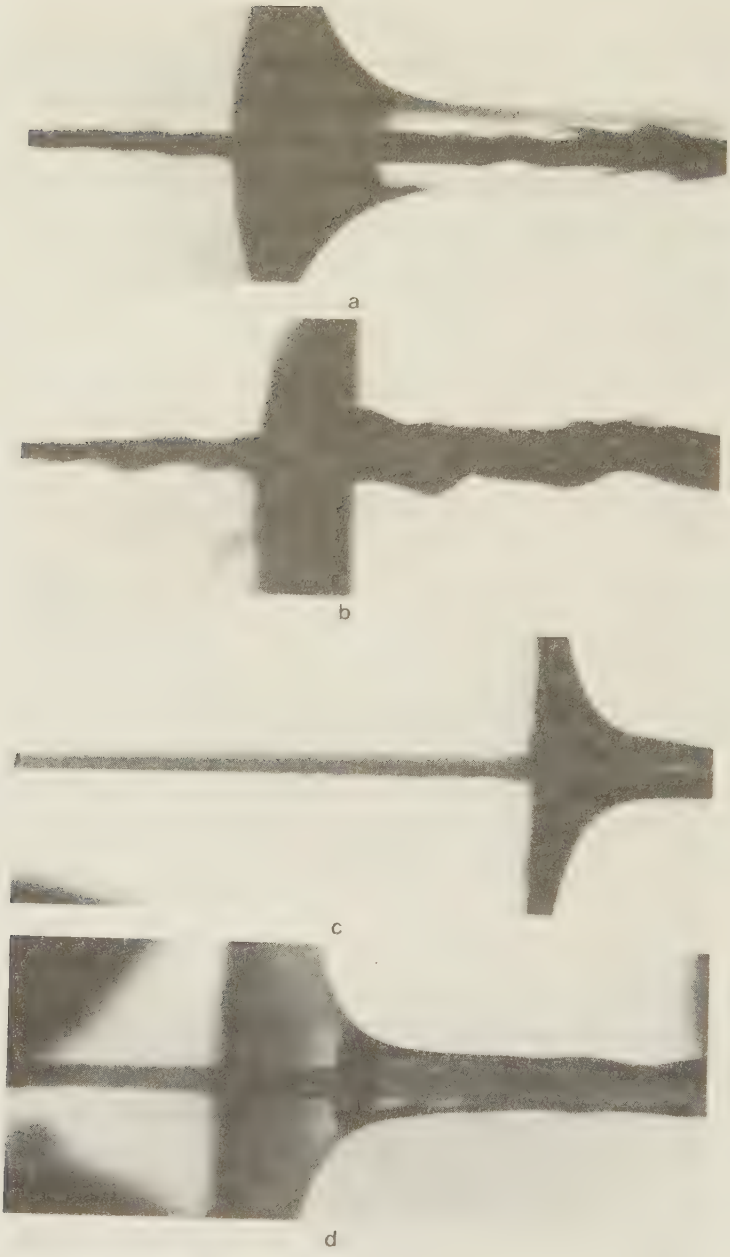

Figure 5.7. Random instability in compound jet. Instability caused by distorted flow in the semi-turbulent primary jet.
Primary jet diameter 75 μm. Primary fluid 20% glycerine + 80% water + dye. Secondary fluid 5% glycerine + 95% water (5.7.a and b), 100% water (5.7.c and d). Primary jet velocity 8.1 m/s (5.7.a), 12 m/s (5.7.b), 8 m/s (5.7.c and d). Secondary fluid flow 115 μl/s (5.7.a and b), 75 μl/s (5.7.c and d).

Figure 5.8 shows examples of the random instability in compound jets caused by disturbances in the secondary fluid close to the base of the compound jet. Here a stable primary jet is disturbed in the vicinity of the meniscus and an instable compound jet emerges. These disturbances in the secondary fluid are similar to those causing the sinous instability. The sinous instability is, however, believed to exist in a laminar flow compound jet whereas the random instability always is associated with a turbulent-like random flow.

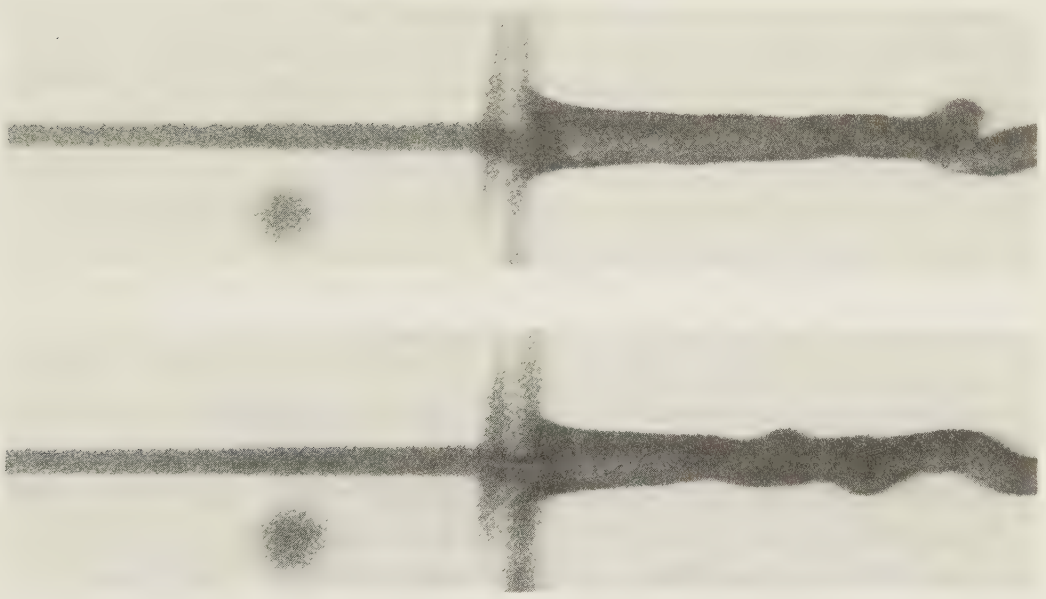

Figure 5.8. Random instability in compound jet. Instability caused by irregular flow in secondary fluid close to the entrance funnel to the compound jet (at compound jet base). Primary jet diameter 75 µm. Primary fluid 20% glycerine + 80% water + dye. Secondary fluid water. Primary jet velocity 7.5 m/s. Secondary fluid flow 40 µl/s.

5.4.2 Discussion

The random instabilities observed in Figure 5.7 and 5.8 obviously result in compound jets not suitable for high resolution ink jet printing. The origins for the instabilities are, however, different. Therefore instability in a specific compound jet can be avoided by means different from those used in another one.

The different instabilities observed in fluid jets are partly due to the physical properties of the jet and surroundings, absolute velocity of the jet and velocity profile of the jet, but depend also strongly on nozzle design. A qualitative correlation between the nozzle shape and the issuing jet shape of conventional jets has been described by McCarthy and Molloy (1974). They pointed out that the nozzle should convert potential energy to kinetic energy as effectively as possible. This is best achieved by a sudden, smooth contraction of the flow area from the supply line to the desired nozzle diameter. However, the question of the angle of convergence appears uncertain. There would seem to be an optimum somewhere between 15° and 100°! Also the nozzle aspect ratio length/diameter has a highly significant effect on the initial jet velocity profile and thus, also subsequent instabilities. For example a long straight nozzle delivers a jet with an initial parabolic velocity profile and a short nozzle a jet with plug flow distributions.

The analysis of the dependence of nozzle shapes and surfaces for the stability of ordinary fluid jets also has significance for the generation of compound jets. Firstly a stable primary jet obviously is essential for a stable compound jet. Secondly the compound jet assembly also represents a nozzle for the compound jet where the kinetic energy of the primary jet is transferred to the secondary fluid. Since also this mechanism is quite fast, it should be as regular and smooth as the conversion of potential energy to kinetic energy in the primary jet nozzle. Therefore the study of an ordinary jet can be of significant value for the understanding of the compound jet and vice versa.

The experiments have substantiated the importance of the form of the primary jet nozzle. Nozzles with ragged edges cause random instabilities in

the compound jet at much lower primary jet velocities than nozzles which are carefully ground and polished (cf. Figure 3.2 and 3.3). On the other hand the flow profile of the primary jet at the nozzle seems to be of less importance since stable compound jets have been obtained easily with primary jets having parabolic flow profile or plug flow profile.

Ordinary laminar fluid jets emerging from long tubes and therefore representing a parabolic flow profile will in the course of the passage through the gaseous ambient atmosphere distribute the velocity profile to a nearly flat plug profile (cf. chapter 6.32). Therefore this energy redistribution must play a significant role in the disintegration of the jet in some cases. Eisenklam and Hooper (1958) noted and explained a bursting break-up caused by the violent energy redistribution in high speed laminar jets. Therefore jets with initial parabolic velocity profiles are potentially the most unstable jets. On the other hand jets with plug flow are the most stable since they exhibit no velocity profile relaxation effects.

5.4.3 Influence of polyethyleneoxide on random instability

Drag reducing additives in both primary and/or secondary fluid effectively counteracts the instabilities described above. Small concentrations of Polyox (0.0005 to 0.1 % in weight depending on molecular length) have been used successfully. The higher concentrations stabilize the jet more effectively but cause problems when used in practical printing applications. The liquid threads connecting the drops after drop formation (cf. Figure 5.3) represent high electrical resistors. In ink jet printing each drop is charged to a predetermined value by a charging electrode situated around the point of drop formation. However, if the R-C time constant increases, because of the high resistance threads between the drops, the charging time increases so much that the charges cannot be controlled well enough. Therefore a compromise has to be reached between hydrodynamic and electrical aspects in printing applications.

Since most of the instabilities observed here are initiated when the primary jet transverses the secondary fluid the reason for the stabilizing effect of polyox should be similar to the effect of polyox on liquid-in-liquid jets described by Filipsson et al. (1977/78).

5.5 Development of the instabilities

5.5.1 Instabilities caused by increase of secondary fluid

Figure 5.9 shows the development of instabilities when increasing the flow of secondary fluid. Here the secondary fluid is a 20% glycerine-water mixture. The flow of primary fluid is kept constant (49 µl/s) and the primary jet velocity is 11.1 m/s. The primary fluid is water.

5.9.a shows the primary jet without secondary fluid. In Figure 5.9.b a compound jet with primary to secondary flow ratio = 10 is shown. Here a sinous instability is apparent. When increasing the secondary fluid flow the instability increases until in 5.9.h with primary to secondary flow ratio = 1.8 a random instability grows faster than the sinous instability therefore obscuring it. With further increased secondary fluid flow the sinous instability is entirely obscured.

Similar to Figure 5.9, Figure 5.10 shows the development of instabilities when increasing the flow of secondary fluid. However, the secondary fluid here is water. The flow of primary fluid (water) is kept constant at 49 µl/s as in Figure 5.9.

Figure 5.10 shows no sinous instability when increasing the secondary fluid flow. In Figure 5.10.h with primary to secondary flow ratio = 1.8 a random instability occurs as in Figure 5.9. This random instability grows with increasing secondary fluid flow.

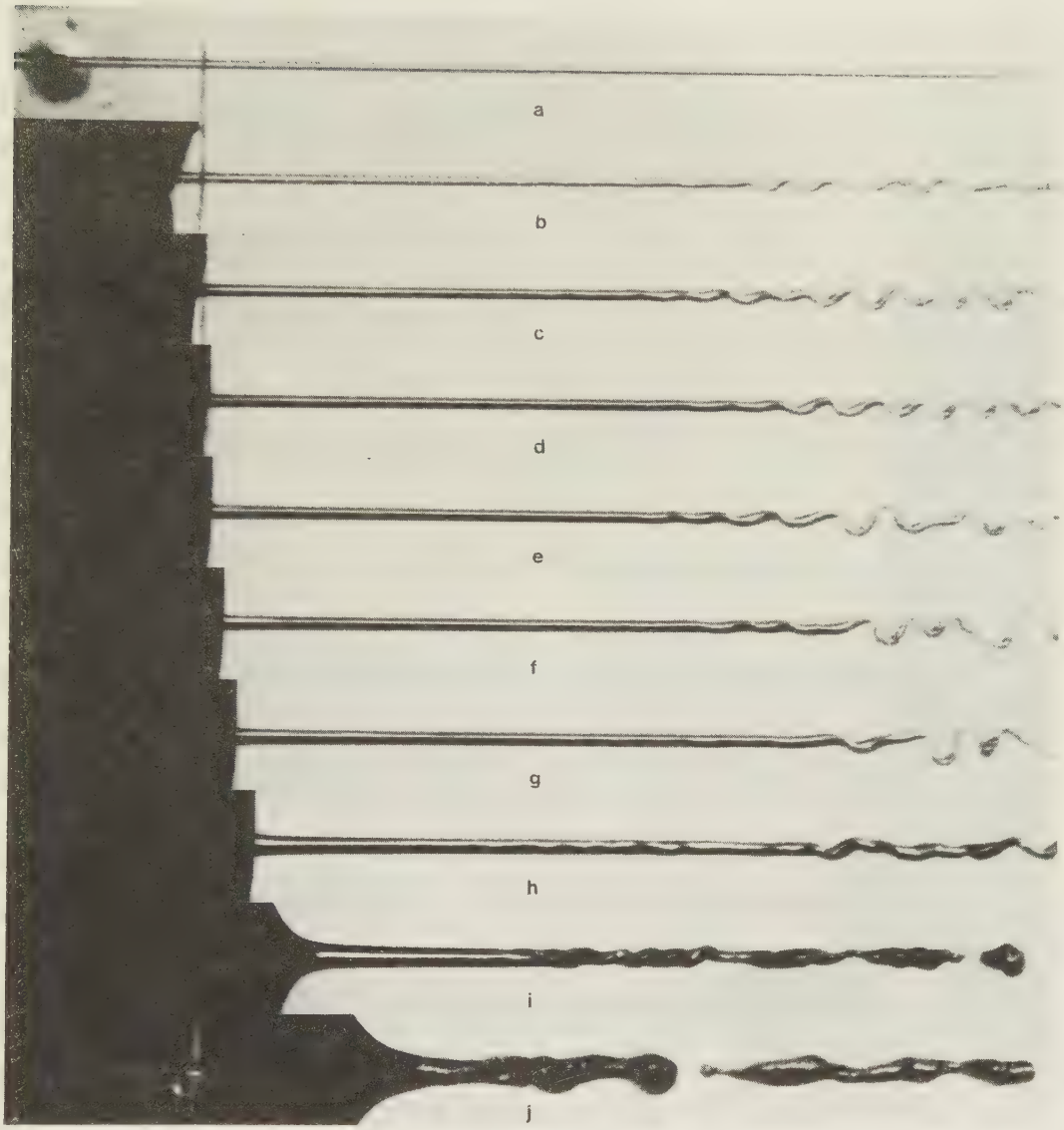

Figure 5.9. Primary jet: 75 μm, viscosity 0.95 cP, velocity 11.1 m/s and flow 49 μl/s. Secondary fluid viscosity 1.9 cP. Secondary fluid flow:
5.9.a: 0 μl/s
b: 5 μl/s
c: 10 μl/s
d: 12 μl/s
e: 15 μl/s
f: 17 μl/s
g: 20 μl/s
h: 28 μl/s
i: 43 μl/s
j: 85 μl/s

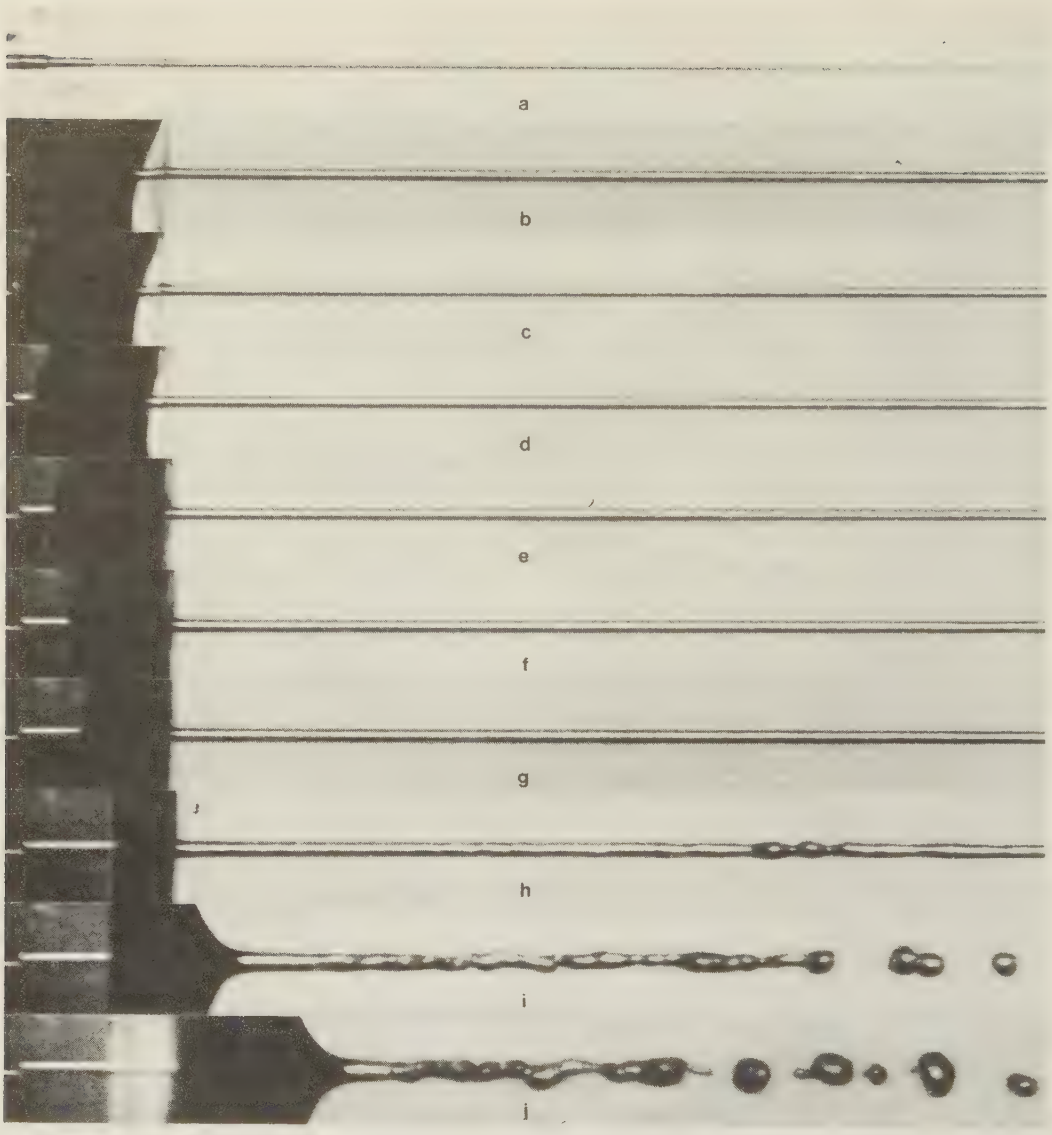

Figure 5.10. Primary jet: 75 μm, viscosity 1.9 cP, velocity 11.1 m/s and flow 49 μl/s. Secondary fluid viscosity 0.95 cP. Secondary fluid flow:

5.10.a: 0 μl/s
b: 5 μl/s
c: 10 μl/s
d: 12 μl/s
e: 15 μl/s
f: 17 μl/s
g: 20 μl/s
h: 28 μl/s
i: 43 μl/s
j: 58 μl/s

5.5.2 Instabilities caused by increase in primary fluid flow

Figure 5.11 shows the development of instabilities when increasing the flow of the primary jet. The primary fluid is 20% glycerine-water mixture. The secondary fluid is pure water with constant flow rate 28 µl/s except in the first and the last picture where the flow is 0 µl/s and 43 µl/s respectively.

In Figure 5.11b a thick compound jet is produced due to the low velocity of the primary jet (5 m/s). Only varicose instability is observed when increasing the primary jet velocity to 7.9 m/s. In Figure 5.11.e small random instabilities are noticeable where primary jet velocity is 9.7 m/s. This random instability increases further with increasing primary jet velocity. Finally Figure 5.11h shows a jet with increased secondary fluid flow. Here the random instabilities develop even faster than in Figure 5.11.g and earlier figures.

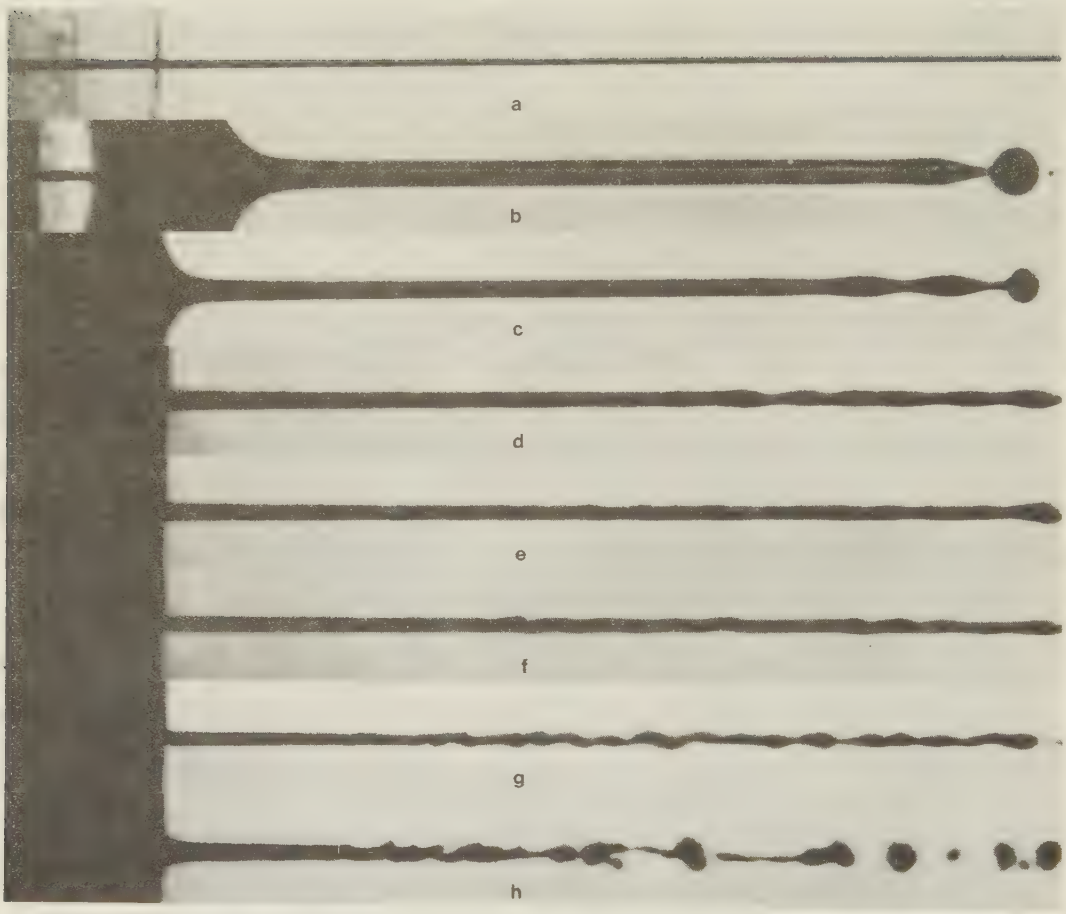

Figure 5.11. Primary jet: 75 μm, viscosity 1.9cP,
increasing velocity.
Secondary fluid viscosity 0.95 cP.
Primary jet velocity and secondary fluid flow:
5.11.a: 5 m/s 0 μl/s
b: 5 m/s 28 μl/s
c: 5.9 m/s, 28 μl/s
d: 7.9 m/s, 28 μl/s
e: 9.7 m/s, 28 μl/s
f: 12.5 m/s, 28 μl/s
g: 15.5 m/s, 28 μl/s
h: 15.5 m/s, 43 μl/s

5.5.3 Discussion

It has been shown above that three types of instabilities can be generated in the compound jet. These instabilities are due to different causes which are dependent on a combination of jet parameters. The reasons for different instabilities are complex since they are determined by many parameters as e.g. viscosity, surface tension, speed and diameter of primary jet, ratio between primary and secondary fluid etc. The following statements can be deduced from 5.5.1 - 5.5.3.

a. All three instabilities are always present in each jet. Which of the three becomes finally visible depends on the rate at which they grow. The instability whose rate of growth is largest will develop first into a visible disturbance and thus domnate over the others.

b. A stable jet condition (Rayleigh varicose instability dominates) can always be obtained if speed of primary jet is reduced sufficiently.

5.6 Pumping action of primary jet

5.6.1 Description of the pumping action

When the secondary fluid is supplied at sufficiently high and constant flow rate the primary jet will continuously entrain the amount of fluid offered, thus generating a stable compound jet. If, however, the secondary fluid flow rate is decreased too much, there exists a minimum limit under which the secondary fluid is not continuously entrained any more. This is most easily explained by the events that take place when the compound jet is turned on. If the primary jet is emerging from the nozzle and the secondary fluid meniscus is situated behind the primary jet nozzle, no secondary fluid will be entrained. Now, if the pump delivering the secondary fluid is turned on, the meniscus will approach the primary jet nozzle. When the secondary fluid reaches the primary jet it will suddenly be entrained. If, however, the secondary fluid flow is set too low, more fluid will be entrained per unit time than is delivered by the pump. Due to viscous forces so much secondary fluid will be carried along that the meniscus moves behind the nozzle again. Due to surface tension the

secondary fluid will wet the outside walls of the primary jet nozzle also when the meniscus moves back. This represents a fluid bridge between the backward moving secondary fluid and the emerging primary jet and allows the primary jet to entrain secondary fluid even if the nozzle is no longer submerged in the secondary fluid. At last this fluid bridge grows too long and the connection breaks. No more secondary fluid can be entrained at this stage. However, since the secondary fluid is continuously supplied the meniscus moves forward again until it covers the nozzle, after which the process is repeated over and over again. This looks as if the meniscus is rapidly moving back and forth and the primary jet is pumping discrete volumes from the secondary fluid at a constant rate.

The frequency of the pumping action is increased when the secondary fluid flow rate is increased since then the forward movement of the meniscus is faster. Decreasing the surface tension of the secondary fluid makes the fluid bridge shorter and thus also increases the frequency of the pumping action. Increasing the viscosity of the secondary fluid causes more fluid to be entrained in each pumping "stroke" and therefore decreases the pumping frequency.

The pumping action is of no importance for most applications since it only occurs at very low secondary fluid flow rate. However, the pumping action represents the lowest useful limit of secondary fluid flow rate for each compound jet. The specific limit is depending on both secondary fluid parameters and on physical construction of the primary and the compound jet nozzle. As a rule no pumping occurs when the ratio primary to secondary fluid flow is 10 or more.

5.6.2 Pumping induced by Polyox in secondary fluid

If the secondary fluid is non-Newtonian due to Polyox addition the viscous forces in the fluid bridge between primary and secondary fluids during pumping action will be much increased. Therefore in this case the pumping phenomenon is much more apparent. Sometimes, however, the fluid bridge will not break at all (cf. drop formation with Polyox addition). In this case the meniscus moves backward until the viscous entraining force from the primary jet equals the flow resistance of the thin fluid

bridge on the walls of the primary jet nozzle. Then the meniscus may be steadily situated at some distance behind the primary jet nozzle, supplying secondary fluid over the fluid bridge to the compound jet which will be continuous. However, the flow in the fluid bridge may vary along the different sides of the nozzle. Therefore the direction of the compound jet is unstable and not suitable for high resolution printing purposes.

Since it is sometimes desirable to use Polyox addition in order to counteract instabilities, this addition should be made to the primary fluid. No fluid bridge like the one described above results from additions to primary fluid. However, the pumping action described at very low flow rates in 5.6.1 still occurs.

6 DISCUSSION OF THE FLUID DYNAMICS OF COMPOUND JETS

6.1 Introduction

Most of the experiments in the present investigation are aimed at revealing physical properties of the compound jet. In order to explain these properties theoretically calculations are made in this chapter using approximative models. The calculated results are compared with the experiments in order to strengthen the model used. Difficulties arise, however, when the approximations in the model are large and the results therefore ambiguous. Since no analytical solution of the flow in a compound jet is known and the approximations used are rough, only quantitative comparison between experiments and theory has been possible.

The theoretical investigation of the compound jet given in this chapter is divided into two parts. The first part deals with the liquid-in-liquid jet up to the meniscus of the secondary fluid. The second part discusses the compound jet in air.

List of symbols

a	acceleration or retardation of a fluid
C	concentration
d	diameter
D	diffusion coefficient
f	spontaneous drop formation frequency
$K = M/\rho$	kinematic momentum flux
l	distance from origin of a conventional jet until plug flow profile is developed
L	distance from origin of a jet to point of drop formation
M	flux of momentum
p	pressure
Q	flow of fluid
r	radial coordinate or radius
r_D	diffusion length
R	radius of jet
Re	Reynolds number
s	distance

t	time
v	velocity
$\hat{v}$	maximum axial velocity
$\bar{v}$	mean axial velocity
z	axial coordinate
z_o	axial distance from point source to orifice of primary jet capillary
z_m	axial distance measured between the orifice of primary jet capillary and surface of secondary fluid
$z' = z-z_o$	calculated axial distance reaching from the orifice of primary jet.
δ	infinitesimal disturbance to jet
η	viscosity of fluid
ρ	density of fluid
$\nu = \eta/\rho$	kinematic viscosity of fluid
σ	surface tension

Indici used

c	compound jet
o	at the orifice of primary jet capillary
p	primary jet or fluid
r	radial direction
s	secondary fluid
z	axial direction
∞	far from the origin of the jet when plug flow profile is attained

Examples:

$\bar{v}_{zo}$	mean axial velocity at the orifice of primary jet capillary
R_∞	radius of a jet far from the orifice
$R_{p\infty}$	radius of the primary jet inside the secondary fluid far from the orifice.

6.2 Liquid-in-liquid jets

6.2.1 Introduction

The flow in a turbulent liquid-into-liquid jet was theoretically studied by Tollmien (1926). The analog problem for laminar flow was studied by Schlichting (1933). Since the present investigation deals mostly with laminar liquid-in-liquid jets the results from Schlichting are used.

Using the approximation that a fluid jet emerges from a point source in a flat wall into a large container filled with the same fluid Schlichting calculated the distribution of velocity in the container in cylindrical coordinates. He also neglected the radial accelerations in the sense of boundary layer theory. The longitudinal flow velocity v_z and the radial velocity v_r were calculated from the expression

$$v_z \frac{\partial v_z}{\partial z} + v_r \frac{\partial v_z}{\partial r} = \frac{1}{\rho r} \frac{\partial}{\partial r} \left(r\eta \frac{\partial v_z}{\partial r} \right) \qquad (6.1)$$

which is derived from the Navier Stokes' equations in cylindrical coordinates if the pressure is regarded as constant. Here ρ is the density of the fluid, and z and r the longitudinal and radial coordinates using the point source as the origin. Schlichting found

$$v_z = \frac{3K}{8\pi\nu z} \cdot \left(1 + \frac{\xi^2}{4}\right)^{-2} \qquad (6.2)$$

$$v_r = \frac{1}{4z} \left(\frac{3K}{\pi}\right)^{1/2} \left(\xi - \frac{\xi^3}{4}\right) \left(1 + \frac{\xi^2}{4}\right)^{-2} \qquad (6.3)$$

where

$$\xi = \frac{r}{\nu z} \left(\frac{3K}{16\pi}\right)^{1/2}$$

$$K = \frac{M}{\rho}$$

M being the momentum crossing a plane normal to the axis of the jet per second, called the momentum flux in the following, and ν the kinematic viscosity of the fluid.

6.2.2 Velocity and momentum measurements in real jets

Since Schlichting assumes the jet origin to be a point source the theore-

tically calculated velocities show singularities for z = 0. This simplifying assumption is the most serious one of the theory, since he assumes an infinite velocity at the origin. Andrade and Tsien (1937), however, showed that the theory could successfully be applied to an actual jet with a slight modification only. They made experiments with a jet, issuing from a circular aperture of finite size, measuring the velocity of the jet and the surrounding fluid. The measurements were carried out by means of photographing aluminium particles added to the fluid as they were carried along with the jet and afterwards measuring the tracks formed on the film. Since the exposure time was carefully controlled, the length of each track was proportional to the velocity at the position of the track.

The theory of Schlichting proved to be successful in interpreting the results of the measurements of Andrade and Tsien when an additional assumption was made. They found that if the jet was to issue from a point source as assumed in the calculations, then that point must not be situated at the orifice of the nozzle producing the actual jet but within it. Also the distance z_o of this imagined point source from the orifice must increase as the momentum flux increases and the angle of the jet becomes smaller.

The necessity of assuming the point source to be situated within the nozzle comes from the difference between the calculated volume flow from a point source and the measured results. The volume flow per second Q through a plane normal to the z-axis increases according to Schlichting with the distance z as:

$$Q = 2\pi \int_0^\infty v_z \, r \, dr = 8\pi \nu z \qquad (6.4)$$

Therefore the volume flow at a certain distance from the point source is believed to be independent of the velocity of the jet at the orifice. According to Schlichting a faster jet causes a more narrow area of the surrounding fluid to be accelerated than a slower one, resulting in the same volume flow through a plane if the kinematic viscosity is the same for both jet and surrounding fluid.

This calculated volume flow does not agree with measured results. The experiments showed that the flow increases with the momentum flux of the jet and the simplest assumption which could be justified by considerations of the kinetic energy was that the distance z_0 from the imagined point source to the real orifice was proportional to the flow Q. This assumption resulted in a rough agreement between theory and experiments where discrepancies of 10 to 20 per cent were accepted in the calculated value of z_0. The theory therefore could be made to give velocity everywhere except in the immediate neighbourhood of the orifice. Therefore these results will be used below.

A further difference between the theoretical calculations of Schlichting and the experiments of Andrade and Tsien is the surroundings of the orifice. Schlichting assumed a point source in a flat wall whereas the experiments were carried out with a glass capillary inside a tank of fluid. Later theoretical work by Landau (1959) describes a flow field around a point source situated in a container far from all walls thus better resembling the experimental arrangements described. Since, however, the calculations of Landau do not offer appreciably better agreement with the experimental results of Andrade and Tsien they will not be used in the following.

The momentum flux of the jet

$$M = 2\pi\rho \int_0^\infty v_z^2 \, r \, dr \qquad (6.5)$$

depends on the velocity profile of the jet. From measurements of the volume flow Q per second from the orifice the momentum, therefore, can be calculated for different velocity distributions. For a parabolic distribution the momentum is 4/3 times the momentum of a plug formed distribution if the mean velocity and thus the volume flow are the same. From the velocity distribution measurements mentioned earlier the momentum flux can be deduced and thus compared to the calculated momentum of different flow profiles. The best agreement with experimental results is obtained by the assumption of a plug flow profile when Reynolds number $Re > 180$

and that the parabolic distribution ceases when $Re \approx 80$ for the specific glass capillary used by Andrade and Tsien. The geometry of the capillaries used in the present investigation indicates a parabolic distribution for still larger Reynolds numbers since the internal walls are only slightly convergent. The geometry differs, however, from one capillary to another.

The calculated distance z_o from the point source within the capillary to the orifice depends on the assumed velocity distribution. Andrade suggests that

$$z_o = 0.160 \cdot \frac{r^2 \bar{v}_{zo}}{\nu} \qquad (6.6)$$

where r is the radius of the orifice and $\bar{v}_{zo}$ is the mean axial flow velocity at the orifice of the capillary. A somewhat different value for z_o is obtained from a comparison between the kinetic energy for the flow profile at the orifice calculated from the measured flow volume and the velocity distribution measured outside the orifice, cf. Andrade et al. (1937).

6.2.3 Velocity profiles in compound jets

Before reachting the surface of the secondary fluid the primary jet resembles strongly the liquid-in-liquid jets theoretically studied by Schlichting (1933) and Landau (1959). They assume, however, identical liquids in both the jet issuing from the point source and in the fluid surrounding it. This is not always the fact in compound jets, but can be experimentally arranged for better agreement with the assumptions of the model.

In the following experimental proof is presented that the velocity distribution calculated by Schlichting (1933) constitutes a good approximation of the actual flow lines which develop between the nozzle and the surface of the secondary fluid. It will be shown that the experimentally determined distance z_m between the nozzle and the surface of the secondary fluid of a compound jet can be calculated using Schlichtings theory with satisfactory accuracy using a reasonable hypothesis. Also the dependence

of z_m on the viscosity of the fluid follows roughly Schlichtings predictions.

According to Schlichting the total flow Q transversing a plane normal to the axis of the linear jet situated at the distance z from the jet origin is given by

$$Q(z) = 8 \pi \nu z \qquad (6.4)$$

While Schlichting derived his results for a jet having an infinitesimal diameter, Andrade et al. (1937) showed that these results closely resembled the experimentally obtained velocity distributions in front of a submerged jet having a finite diameter, if the distance z in Schlichting's equations was replaced by $z' + z_o$, z_o being a constant depending on jet diameter, jet velocity and kinematic viscosity of the fluid. Thus according to Andrade

$$Q(z) = 8 \pi \nu (z' + z_o) \qquad (6.7)$$

where $z' = z - z_o$ is the distance from the nozzle.

Now, in a compound jet all of the primary and nearly all of the secondary fluid flow enters the compound jet the flow of which is Q_c. Thus, at the entrance funnel of the compound jet, i.e. at the surface of the secondary fluid, practically the entire flow crossing the plane constituted by the secondary fluid surface is equal to Q_c. Thus, if the results of Schlichting and Andrade can be used to describe the flow distribution of a compound jet, we should have

$$Q(z) = Q(z_m + z_o) = Q_c \qquad (6.8)$$

Using the equations (6.6), (6.7) and (6.8) we find for the distance z_m

$$z_m = z - z_o = \frac{Q_c}{8\pi\nu} - 0.160 \frac{r^2 \overline{v}_{zo}}{\nu} = \frac{Q_c - 1.28\, Q_p}{8\pi\nu} \qquad (6.9)$$

Agreement between equation (6.9) and the experimental result is demonstrat-

ed in Figure 6.1 where the measured length z_m is plotted against corresponding calculated values $z - z_o$ for different primary and secondary flow Q_p and Q_s respectively. The theoretical distance $z - z_o$ in Figure 6.1 was calculated for each combination of primary and secondary fluid flow from equation (6.9).

Figure 6.1. Measured distances between the orifice of the primary jet nozzle and the surface of the secondary fluid at different primary and secondary fluid flows. The experimental results are plotted against theoretically calculated values.
△ Q_p = 20.0 µl/s
○ Q_p = 31.5 µl/s
□ Q_p = 45.3 µl/s

The three different graphs plotted in Figure 6.1 correspond to three different primary fluid flow volumes. Since the same primary jet nozzle was used (75 µm diameter) the flow is directly related to the primary jet mean velocity. For different secondary fluid flows the distance from the orifice of the primary jet capillary to the meniscus of the secondary fluid was measured. The primary and secondary fluids used are the same in the experiments (viscosity = 1.7 cP, density 10^3 kg/m^3).

Agreement between measured lengths z_m and calculated distances $z - z_o$ is satisfactory for the two graphs with the highest primary fluid flow except for the slope of the lines. Since the slope of the plotted graphs is dependent on the value used for viscosity in equation (6.9) a correction of the viscosity would adjust the disagreement in slope. The viscosity was measured with a viscosimeter formed from a capillary glass tube through which a certain amount of fluid was allowed to flow. The time for the passage of the fluid was measured and compared to the time for the same amount of water to pass. The quotient was then calculated and since the viscosity of water was known for the actual temperature the viscosity for the unknown fluid could be determined. Since, however, much higher shear forces exist in the jet, the measured value for viscosity may not immediately be used for the calculations of jet parameters. This would explain that the calculated distances $z - z_o$ in Figure 6.1 have to be increased with 0.1 mm and multiplied with a factor = 1.1 to obtain total agreement between theory and experimental results. This fact seems to indicate that Schlichting's velocity distribution can be applied also to the fluid space between the nozzle and the meniscus of a compound jet, the primary and secondary fluids of which are the same.

After a single calibration measurement in order to remove the discrepancy between calculated and measured distances $z - z_o$ it is thus possible to predict the distance z_m from the primary jet orifice to the surface of the secondary fluid with the formula (6.9).

6.2.4 Dependence of viscosity

Since a reasonably good agreement exists between measured results and from (6.4) calculated flow volumes, also effects due to changes in viscosity should be theoretically predictable.

When keeping the primary and secondary fluid flows constant in a compound jet a change in viscosity in one and/or the other fluid will cause a change in flow pattern inside the meniscus. Also the distance between the primary jet orifice and the meniscus will change. In order to demonstrate this dependence of viscosity a series of different compound jets were photographed. In all pictures the primary and secondary fluid flows were kept constant while primary or secondary fluid viscosity was varied. The experimental results obtained by this variation of the viscosity was then compared with the theoretically calculated axial and radial velocity distributions of a submerged point source (6.2) and (6.3). Only the experiments using the same viscosity in both the primary and secondary fluid could be used in this comparison since this is an assumption made in the theory.

The calculated axial flow field from a point source with viscosity 0.95 cP is shown in Figure 6.2. Different velocity profiles at increasing distance from the point source are plotted. The radial scale is 4 times the axial one. In Figure 6.2 the orifice of a primary jet nozzle with 75 μm diameter is depicted. It is situated at a distance z_o from the point source (cf. (6.6)). Also the meniscus of the secondary fluid and the compound jet are introduced in the figure. The position of the meniscus is obtained from measurements on a photograph of a real compound jet having the same parameters as the theoretical one. The base line of the first flow velocity profile is situated exactly at the orifice of the primary jet and the following profiles are spaced axially 200 μm from each other.

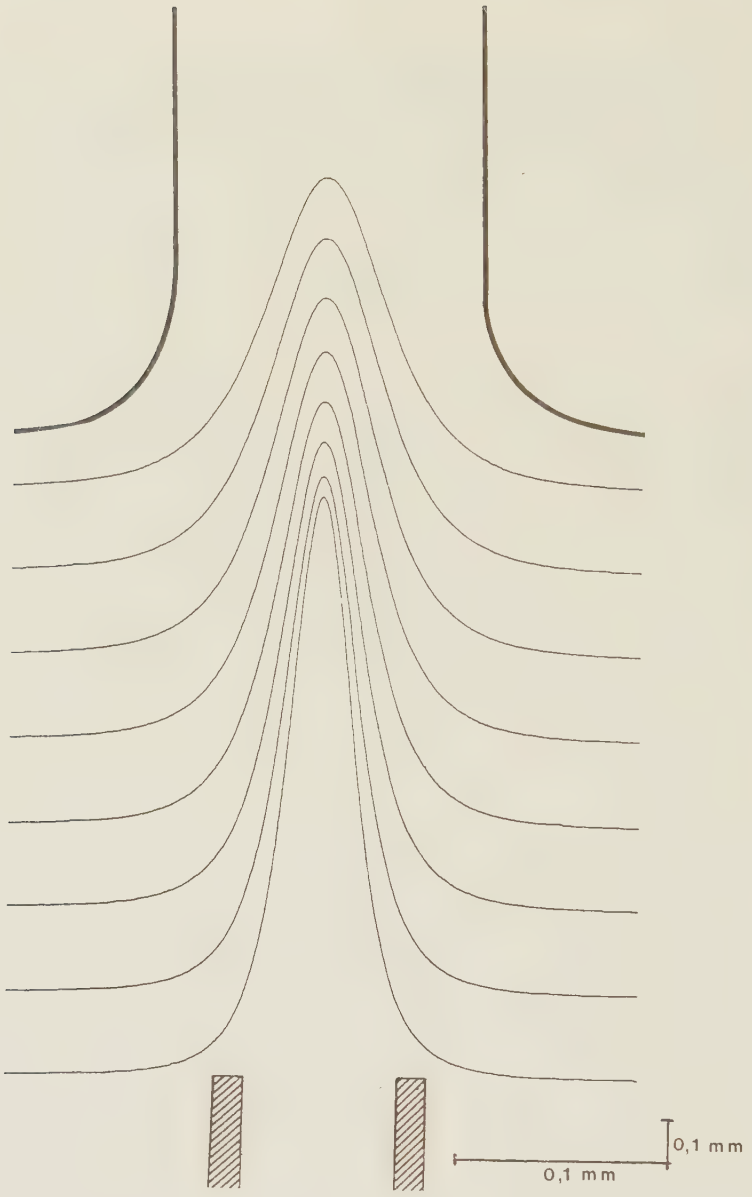

Figure 6.2. Calculated flow velocity profiles from a submerged point source. Superimposed 75 µm primary jet nozzle and secondary fluid meniscus with indicated compound jet obtained from photograph of actual jet.

$\eta_p = \eta_s$ 0.95 cP

Q_p = 33 µl/s

Q_s = 42 µl/s

As can be seen from Figure 6.2 the theoretical axial velocity decreases rapidly with increasing radius and is almost zero outside the compound jet radius.

A series of pictures similar to Figure 6.2 are shown in Figure 6.3 in order to demonstrate the effect of a change in viscosity. Compared with Figure 6.2 the scale of the calculated axial velocity is reduced somewhat in order to avoid overlapping velocity profiles at hicher viscosities.

From (6.7) and Figure 6.3 it is apparent that a change in viscosity causes the surface of the secondary fluid to move if other parameters are kept constant. However, the primary and the secondary fluid do not necessarily have the same viscosity as assumed in (6.9) and in Figure 6.3. The dependence of different viscosities is demonstrated in Figure 6.4. Here the measured distance z_m from the primary jet orifice to the surface of the secondary fluid is plotted against the viscosity of the secondary fluid which is supplied at the same flow rate in all experiments. Four different graphs representing different primary jet viscosities are shown.

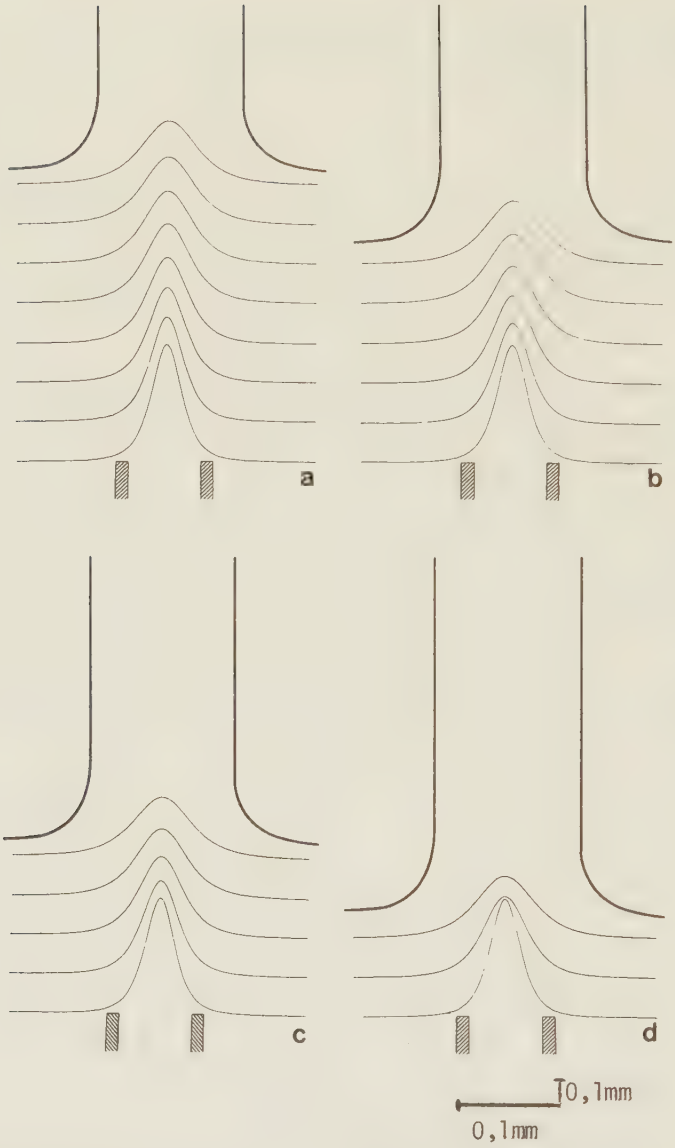

Figure 6.3. Calculated flow velocity profiles from a submerged point source with superimposed pictures of real compound jets with primary jet nozzles obtained from photographs.

Q_p = 32.7 µl/s, Q_s = 42.4 µl/s

6.3.a $\eta_p = \eta_s$ = 1.0 cP

6.3.b $\eta_p = \eta_s$ = 1.4 cP

6.3.c $\eta_p = \eta_s$ = 1.9 cP

6.3.d $\eta_p = \eta_s$ = 3.7 cP

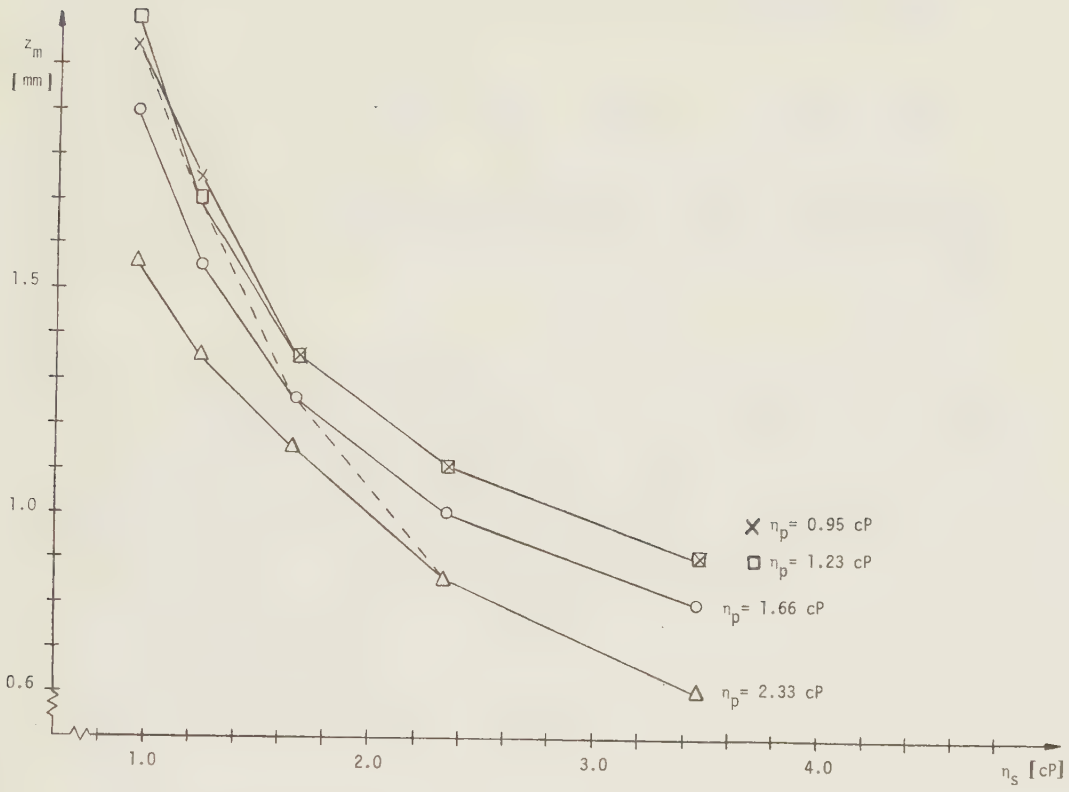

Figure 6.4. Measured distance between the orifice of the primary jet nozzle and the surface of the secondary fluid at different primary and secondary fluid viscosities. The distances are plotted against secondary fluid viscosity.

The different graphs are similar and somewhat spaced from each other except for the one representing the lowest primary fluid viscosity. As seen in both Figure 6.3 and 6.4 an increase in viscosity results in a decreasing distance between primary jet nozzle and secondary fluid surface. According to (6.9) it is expected that the distance should be inversely proportional to the viscosity if other parameters are kept constant. This is demonstrated in Figure 6.4 if plotted points on the different graphs with similar viscosity in both primary and secondary fluid are connected with each other (dotted line).

The curve in Figure 6.4 representing primary fluid viscosity = 0.95 cP is situated too low compared to the other curves. This is caused by a random instability in the primary jet when travelling through the secondary fluid causing the jet to entrain the surrounding liquid faster. Therefore the distances measured are comparatively shorter than with the other primary fluids.

When using the same primary fluid at a constant flow rate it is thus possible to determine experimentally the distance for some secondary fluids with known viscosities. From this a calibration diagram can be drawn. Using this diagram the viscosity of an unknown liquid can be found by measuring the distance between the primary jet nozzle and the secondary fluid surface. This kind of viscosimeter has special properties since the shear rate occuring in the instrument can be made very high with a high velocity jet. Therefore non-Newtonian properties of the fluids used will strongly influence the measurements. Also the amount of fluid necessary for the measurement is small.

An example of the usefulness of the method is the characterization of elastic fluids, e.g. water containing Polyox or similar additive in low concentrations. The determination of such concentrations is often difficult. With the method described above an 0.01 per cent concentration of Polyox with MW 300 000 in water can readily be demonstrated. Since the secondary fluid supplied to the compound jet is always fresh no successive breakdown of the long molecules will take place.

6.2.5 Velocity profile at primary-secondary fluid interface

Using primary and secondary fluids with identical viscosities results in the smooth looking velocity distributions shown in Figure 6.2 and 6.3. If the viscosities η_p and η_s of the primary and secondary fluid are different a more complicated velocity profile results. Two qualitatively different velocity profiles of the liquid-in-liquid jet are distinguishable. Since the shear forces and the velocity $v_z(r)$ in the fluids are continuous at the boundary between the primary jet and the secondary fluid we find

$$\eta_p \left[\frac{\partial v_{zp}(r)}{\partial r}\right]_{R_p} = \eta_s \left[\frac{\partial v_{zs}(r)}{\partial r}\right]_{R_p} \qquad (6.10)$$

where $v_{zp}(r)$ and $v_{zs}(r)$ are the velocities of the primary and secondary fluid in the jet direction respectively and R_p the radius of the primary jet.

Thus, if $\eta_p \neq \eta_s$ a discontinuity in the derivative of the axial velocity function (acceleration) exists at this boundary. A qualitative picture of this function is given in Figure 6.5 for $\eta_p < \eta_s$ and $\eta_p > \eta_s$. These profiles show an inflection point at the very boundary between the two fluids if $\eta_p < \eta_s$, suggesting that instabilities should develop more easily in this case. This is also confirmed by the experiments (cf. Figure 6.4).

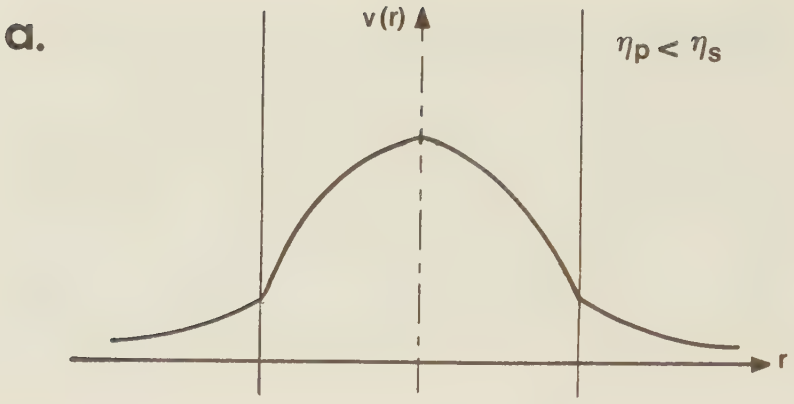

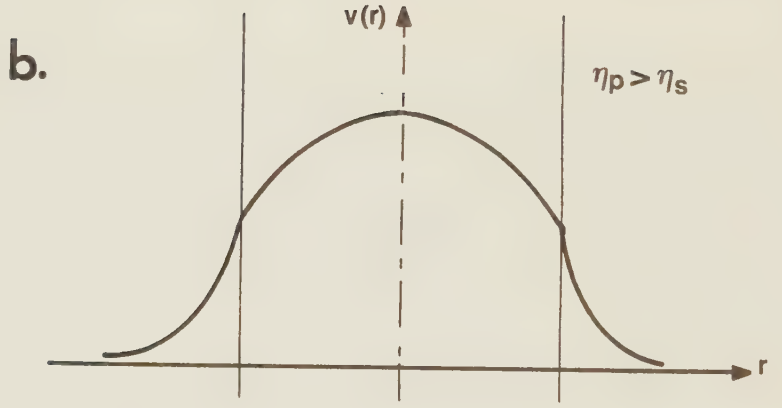

Figure 6.5. Axial velocity distribution if a) $\eta_p < \eta_s$ and b) $\eta_p > \eta_s$.

6.3 Compound jet in air

6.3.1 Introduction

After breaking the surface of the secondary fluid the primary jet emerges into air enclosed in a sheath of secondary fluid. The microphotographs in Figure 4.8 show clearly that the jet consists of a central primary fluid column coaxially enclosed by the secondary fluid. Since also the varicose instability causing drop formation is quite symmetric it can be concluded that the flow in the jet is essentially laminar.

When generating a compound jet the secondary fluid is accelerated while the velocity of the primary jet decreases. A successive relaxation of the flow velocity profile into a flattened plug flow profile takes place inside the compound jet.

In the following different parameters will be calculated for the compound jet. These parameters will be used in estimating the change of velocity of primary and secondary fluid as well as final velocity and minimum velocity of the compound jet. Also the effect of molecular diffusion and surface tension will be discussed. The distance to the point of drop formation will be calculated in terms of the distance to drop formation for the primary jet alone and secondary to primary fluid flow ratio.

6.3.2 Development of plug flow profile in a conventional jet

Shortly after entering the compound jet funnel the velocity distribution in the jet assumes a plug flow profile. This happens due to viscous forces independently of the actual initial velocity profile. The length l for this transition can be estimated in a conventional jet according to (4.1).

The change of velocity profile results in a change of jet diameter since the flow volume per second in the jet is constant. Assuming an initial parabolic velocity profile

$$v(r) = \hat{v}_o \left(1 - \frac{r^2}{R_o^2}\right)$$

where $\hat{v}_o$ is the maximum axial velocity on the axis of a conventional jet

with radius R_o. Since the flow in a jet is constant along the jet axis we find for a jet with plug flow profile

$$2\pi \int_0^{R_o} r\, v(r)dr = \pi R_\infty^2\, v_\infty \qquad (6.11)$$

Here R_∞ is the radius and v_∞ the velocity of the plug flow jet. From (6.11) follows

$$R_\infty = R_o \left(\frac{\hat{v}_o}{2\, v_\infty}\right)^{1/2} \qquad (6.12)$$

Since the momentum flux of a conventional jet is constant during the velocity redistribution we have

$$2\pi\rho \int_0^{R_o} r\, v^2(r)dr = \pi\rho\, R_\infty^2\, v_\infty^2 \qquad (6.13)$$

resulting in

$$R_\infty = R_o \frac{\hat{v}_o}{v_\infty\, 3^{1/2}} \qquad (6.14)$$

From (6.12) and (6.14) therefore follows

$$v_\infty = \frac{2}{3}\hat{v}_o \qquad (6.15)$$

and $$R_\infty = \left(\frac{3}{4}\right)^{1/2} R_o \qquad (6.16)$$

6.3.3 Calculations of compound jet parameters

6.3.3.1 Momentum flux of the compound jet

Since the secondary fluid is initially almost at rest, the momentum flux of the compound jet is practically equal to the momentum flux of the primary jet when emerging from the nozzle. This is supported by the assumption that in low-viscosity fluids the boundary layer theory is applicable (Schlichting 1968).

Let Q_p be the volume flow of the primary jet emerging with an average speed $\bar{v}_{po}$ from a nozzle with a diameter $2\, R_{po}$. Since the nozzle is a

glass tube, the length of which is more than 200 times its diameter, the jet can in most cases be assumed to have a parabolic velocity profile when leaving the nozzle. Therefore $\hat{v}_{po} = 2\,\bar{v}_{po}$ is the maximum speed in the jet and $\bar{v}_{po} = Q_p/\pi\,R_{po}^2$. Then the momentum flux M_p of the primary jet is (Batchelor and Gill 1962)

$$M_p = \frac{4}{3}\frac{\rho_p\,Q_p^2}{\pi\,R_{po}^2} \qquad (6.17)$$

Now, the coaxial geometry of the compound jet allows calculation of its momentum flux M_c. If ρ_p and ρ_s are the densities and R_p and R_c the radii of the primary fluid column and the compound jet, respectively, then

$$M_c = 2\pi\int_0^{R_{p\infty}} \rho_p\,v^2(r)\,r\,dr + 2\pi\int_{R_{p\infty}}^{R_c} \rho_s\,v^2(r)\,r\,dr \qquad (6.18)$$

where the first term is the flux of momentum of the primary fluid column and the second that of the secondary fluid sheath under the assumption of a constant pressure. $v(r)$ is the unknown function of the velocity component parallel to the jet axis z.

The plug flow profile assumed by the compound jet shortly after emerging from the secondary fluid means that $v(r) = v_c$ = constant. Therefore equation (6.18) can be integrated. Using the relation

$$Q_c = Q_p + Q_s = \pi\,R_c^2\,v_c \qquad (6.19)$$

where Q_c, Q_p and Q_s are the volume flows of the compound jet and the primary and secondary fluids, the flux of momentum of the compound jet is

$$M_c = \pi\rho_p\,v_c^2\,R_{p\infty}^2 + \pi\,\rho_s\,v_c^2\,(R_c^2 - R_{p\infty}^2) =$$

$$= v_c\,(Q_p(\rho_p - \rho_s) + Q_c\,\rho_s) \qquad (6.20)$$

6.3.3.2 Velocity of the compound jet

Assuming an initially parabolic velocity profile for the primary jet and that the momentum flux of the primary jet is equal to that of the compound jet (6.15) and (6.18) imply

$$v_c = \frac{4}{3} \frac{\rho_p Q_p^2}{\pi R_{po}^2} \frac{1}{Q_p (\rho_p - \rho_s) + Q_c \rho_s} \qquad (6.21)$$

If $\rho_p = \rho_s$ then

$$v_c = \frac{4}{3} \frac{Q_p^2}{\pi R_{po}^2 Q_c} = \frac{4}{3} \bar{v}_{po} \frac{Q_p}{Q_c} \qquad (6.22)$$

Since v_c is the velocity of the compound jet at some distance from the surface of the secondary fluid, a comparison can also be made with the velocity of the primary jet at the same place. Since plug flow profile is assumed for both jets from the equality of momentum flux follows

$$v_c = v_p \frac{Q_p}{Q_c} \qquad (6.23)$$

where v_p is the final velocity the primary jet would assume in air (cf. 6.15).

Further, since

$$Q_p = \pi R_{p\infty}^2 v_c = \frac{3}{4} \pi R_p^2 \bar{v}_{po}$$

from (6.21) follows

$$R_{p\infty} = \left(\frac{3}{4} \frac{\rho_p Q_p + \rho_s Q_s}{\rho_p Q_p}\right)^{1/2} R_{po} \qquad (6.24)$$

i.e. the radius $R_{p\infty}$ of the primary fluid in the compound jet is larger than the radius the primary jet would assume in air some distance from the nozzle, i.e. $(3/4)^{1/2} R_{po}$, R_{po} being the nozzle radius.

6.3.3.3 Acceleration of compound jet

The magnitude of the acceleration of the secondary fluid and the deceleration of the primary fluid during the formation of the compound jet can only be estimated since the flow line distribution for the fluid-in-fluid jet preceding the compound jet is not known.

The maximum speed of the primary jet $\hat{v}_{po} = 2\,\bar{v}_{po}$ in the center of the nozzle decreases to v_c when the primary jet has entered the compound jet and plug flow distribution is attained. Thus the velocity change is $\hat{v}_{po} - v_c$ along the jet axis. Therefore the average deceleration is

$$a_p = \frac{v_{po}^2 - v_c^2}{2\,s} \qquad (6.25)$$

where s is the distance from the nozzle to the secondary fluid surface plus the relaxation length l necessary to establish plug flow in the compound jet (cf. equation 4.1). Using equations (6.22) and (6.25) the average deceleration along the axis of the jet shown in Figure 4.1 is found to be $a = 1.3 \cdot 10^5$ m/s^2 (cf. 4.2).

Since the secondary fluid initially is essentially at rest the average acceleration of the secondary fluid layers at the surface of the primary jet is given by

$$a_s = \frac{v_c^2}{2\,s} \qquad (6.26)$$

Using this equation for the jet in Figure 4.1 gives $a = 1.4 \cdot 10^4$ m/s^2.

Obviously the acceleration is not uniform along the jet axis as assumed above. Therefore the maximum acceleration occuring during the generation of the compound jet shown in Figure 4.1 must be appreciably higher. Using primary jets having a diameter of 10 µm and a velocity of 40 m/s average accelerations as high as $10^5 - 10^6$ m/s^2 have been observed in laminar and stable compound jets. It is obvious that these large accelerations are associated with high shear forces in the fluids. Therefore instabilities may be generated as shown in chapter 5.

6.3.3.4 Reynolds number of compound jet

If the kinematic viscosities of the primary and secondary fluid are not too different it is reasonable to define Reynolds number for the compound jet as

$$Re_c = \frac{2 v_c R_c}{\nu} \qquad (6.27)$$

where the value of ν lies somewhere between the values of the kinematic viscosity of the primary and the secondary fluid.

Assuming that the viscosities and densities of the primary and secondary fluids are very similar, i.e. $\eta_p \simeq \eta_s \simeq \eta$ and $\rho_p \simeq \rho_s \simeq \rho$, then the momentum flux of the compound jet is

$$M_c = \rho \pi R_c^2 v_c^2 \qquad (6.28)$$

Thus for the Reynolds number

$$Re_c = \frac{2}{\nu} \left(\frac{M_c}{\rho\pi}\right)^{1/2} \qquad (6.29$$

By the same reasoning the Reynolds number of the primary jet

$$Re_p = \frac{2 \bar{v}_p R_p}{\nu_p} = \frac{2}{\nu_p} \left(\frac{M_p}{\rho_p \pi}\right)^{1/2} \qquad (6.30)$$

Comparing equations (6.29) and (6.30) shows that

$$Re_c \simeq Re_p \qquad (6.31)$$

under the assumption that $\rho_p \simeq \rho_c$ and $\eta_p \simeq \eta_s$.

Thus, since the densities and viscosities of the fluids in the compound jet nearly always are very similar, it is found that the Reynolds number of the compound jet is approximately equal to that of the primary jet. Batchelor and Gill (1962) found that the Reynolds number for a liquid-in-liquid jet is constant along the jet axis which is very similar to the present results.

6.3.3.5 Minimum fluid flow in primary jet

If the momentum fluid of the primary jet is too small no compound jet can be formed. Assuming the secondary fluid surface to be situated at rest in front of the primary jet nozzle the surface represents a certain resistance against penetration by the primary jet when this jet is turned on. The secondary fluid surface will bend outwards, thereby increasing the surface tension resistance against penetration when the velocity of the primary fluid is increased. There exists, however, a maximum surface tension resistance when the secondary fluid is formed like a halfsphere at the point where the primary fluid jet is directed. The pressure inside this halfsphere due to surface tension σ_s of the secondary fluid is

$$p = \frac{2\,\sigma_s}{r_s} \qquad (6.32)$$

where r_s is the radius of this halfsphere.

The surface of the secondary fluid has to withstand the force of the momentum flux of the primary jet

$$M_p = \frac{4}{3}\,\frac{\rho_p\,Q_p^{\,2}}{\pi\,R_{po}^2} \qquad (6.17)$$

This momentum flux represents a force on the halfsphere causing a pressure which must be greater than the pressure caused by surface tension to generate a compound jet. Therefore

$$\frac{M_p}{\pi r_s^{\,2}} > \frac{2\,\sigma_s}{r_s} \qquad (6.33)$$

The radius r_s can be estimated as the radius of the compound jet R_c if the compound jet would emerge from the secondary fluid. Assuming identical momentum flux and densities of the primary and compound jet

$$M_p = Q_c\,v_c\,\rho \simeq \pi R_c^{\,2}\,v_c^{\,2}\,\rho \qquad (6.34)$$

and therefore

$$R_c = Q_c \left(\frac{\rho}{\pi M_p}\right)^{1/2} \qquad (6.35)$$

It follows from (6.33) and (6.35)

$$M_p > (4 \sigma_s^2 Q_c^2 \pi\rho)^{1/3} \qquad (6.36)$$

From (6.17) and (6.36) follows

$$Q_p > \left(\frac{27}{16} \frac{\sigma_s^2 \pi^4 R_{po}}{\rho^2} Q_c^2\right)^{1/6} \qquad (6.37)$$

Thus, for example, for a secondary fluid of water with a flow Q_s = 65 µl/s the minimum flow of the primary jet from a 75 µm nozzle is 15 µl/s or about 4.5 m/s average nozzle velocity $\bar{v}_{po}$.

6.4 Molecular diffusion in a stable compound jet

Since no visible mixing occurs between the primary and secondary fluids in the stable compound jet the two fluids can mix only by molecular diffusion across the boundary between them.

Following from the diffusion equation

$$\frac{dC}{dt} = D \nabla^2 C \qquad (6.38)$$

where C is the concentration of one fluid in an other and D the coefficient of diffusion the diffusion length can be estimated. Assuming that the radius of the primary fluid column is large compared to the diffusion length r_D a solution representing a diffusion through a plane can be used. From equation (6.38) it can be derived that (Joos 1964)

$$r_D = (2 D t)^{1/2} \qquad (6.39)$$

where t is the time of the flight of the primary jet from the nozzle to the point of drop formation and r_D the distance from the boundary where the concentration has dropped to 1/e. Since for fluids D is of the order of 10^{-9} m^2/s and t about 3 milliseconds in many of the photographed jets,

then r_D = 2.5 µm. Thus the mixing due to molecular diffusion is not detectable in the photographs. For all practical purposes except when the primary and secondary fluid react chemically with each other this effect can be neglected.

6.5 Surface tension effects in a compound jet

6.5.1 Distance to compound jet drop formation

The varicose instability leading to a stable point of drop formation is caused by surface tension. In the compound jet with two mixable fluids the surface tension of the secondary fluid determines the place for drop formation. According to Weber (1931) the disintegration into droplets occurs at a distance L from the nozzle for a low viscosity jet where

$$L = 12.0 \cdot \bar{v} \left(\frac{d^3 \rho}{\sigma}\right)^{1/2} \qquad (6.40)$$

$\bar{v}$ being the mean velocity of the jet and d the diameter of the nozzle. In comparing the compound jet with the primary jet in air alone c and p are used as indici. From (6.23) and (6.40) follows if the surface tension of the secondary fluid is the same as that of the primary fluid

$$L_c = 12\, \bar{v}_c \left(\frac{d_c^3}{\sigma}\right)^{1/2} = 12\, \bar{v}_p \frac{Q_p}{Q_c} \left(\frac{d_p^3\, Q_c^3\, \rho}{\sigma\, Q_p^3}\right)^{1/2} = L_p \cdot \left(\frac{Q_c}{Q_p}\right)^{1/2} \qquad (6.41)$$

Therefore the distance to the point of drop formation for the compound jet increases compared to the distance of the primary jet alone. In a conventional jet for ink jet printing applications L_p may be 2 mm. If the same jet is converted into a compound jet with $Q_c/Q_p = 2$, this length would increase to L_c = 2.8 mm according to (6.41). This increase is, however, smaller in reality which may depend on the fact that the compound jet is more unstable than the primary jet alone, thereby causing the jet to disintegrate somewhat earlier than expected from equation (6.40).

6.5.2 Pressure caused by surface tension

The pressure inside a liquid thread with radius r caused by surface tension is

$$p = \frac{\sigma}{r} \qquad (6.42)$$

Inside a 110 μm diameter compound jet with water as secondary fluid the pressure above ambiant atmosphere is thus $1.3 \cdot 10^3$ N/m^2 = 0.014 kp/cm^2. Since this pressure is so low it will not play any important part compared to mass forces. Also for a small 10 μm diameter compound jet the pressure is only 0.15 kp/cm^2 and can therefore be disregarded.

6.5.3 Surface tension between two non-mixable fluids

Experiments with water solution as primary fluid and silicon fluid as secondary fluid have shown notable influence of the surface formed between the two fluids (cf. chapter 4). The interfacial surface tension causes the primary fluid column to disintegrate within the secondary fluid column, thereby forming the primary fluid drops shown in Figure 4.9.

The interfacial surface tension between silicon fluid and water cannot be calculated simply by subtraction of the surface tensions of each of the two fluids against air. This can be demonstrated by the fact that a drop of olive oil will spread on a water surface until a monolayer $\approx 10^{-9}$ m thickness exists. This happens since the surface tension between air and water ($73 \cdot 10^{-3}$ N/m) is larger than the sum of the surface tension between air and olive oil ($32 \cdot 10^{-3}$ N/m) and the interfacial surface tension between olive oil and water ($18.5 \cdot 10^{-3}$ N/m). Therefore the edge of the drop of olive oil will be drawn outwards with a force per unit length $\approx 73 \cdot 10^{-3} - 32 \cdot 10^{-3} - 18.5 \cdot 10^{-3} = 22.5 \cdot 10^{-3}$ N/m (Bergmann-Schaefer 1965).

A rough estimation of the interfacial surface tension is, however, possible as is shown in chapter 4.4. This estimation becomes empirically true if the surface tension between the fluids and air are measured on the liquids when they are mutually saturated with each other according to Antonoff's relationship (Davies 1963). This mutual saturation often occurs slowly and cannot be expected to be attained in the compound jets described here. The saturation causes the surface tension to decrease for both fluids against air since the saturating fluid contaminates the surface against air. Since preliminary experiments show that drops of silicon fluid only slowly spread on the surface of water the spreading coefficient is small and therefore the estimation in chapter 4.4 must be reasonably good according to Davies (1963).

7 PRACTICAL APPLICATIONS

7.1 Compound jet in copying devices

7.1.1 Introduction

In order to compare the compound jet with conventional jets in ink jet printing applications with respect to printing speed, resolution and stability, several experiments have been performed on a copying device. This apparatus is essentially a facsimile machine and consists of two rotating drums D_1 and D_2 on a common axis driven by a motor (cf. Figure 7.1).

For comparison of the copying ability of both ordinary and compound jets an original was fastened to drum D_1 and scanned by an optoelectrical device. The output signal of this device was then used to on-off modulate the ink jet which copied the original on ordinary paper fastened to drum D_2.

For testing the upper frequency limit of on-off printing with both types of jets the same apparatus was used. However, in that case the electrical signal controlling the ink jet was generated by a separate pulse generator, the pulse length of which could be varied. As will be shown below this testing device allowed the determination of upper frequency limit of the compound jet.

7.1.2 Experimental apparatus

To intensity modulate the compound jet in the copying device the Hertz modulating method is used. The characteristics of this method is well documented for conventional jets and therefore well suited for the purpose of comparison (Månsson 1972).

The copying device used is shown in Figure 7.1. The two drums D_1 and D_2 were fixed to the same axis as a motor M, capable of turning the drums with desired velocity. Using a screw drive connected by cog wheels to the drum axis the motor moved the drums simultaneously and slowly sideways in the direction of their axis at a speed of 0.1 mm for each revolution. Hence the scanning line density is 10 lines/mm. Using other screw drives other scanning line densities could be obtained.

When using the apparatus for copying purposes the original was fastened on drum D_1 while D_2 held the recording paper. When the drums were turned by the motor M the original on drum D_1 was scanned line by line by a photoelectric device consisting of a microscope lens O with an 0.1 mm aperture A fixed in the rear focal plane of the objective and a photodiode detector D (PIN 3 DP) positioned behind the aperture in a dark housing. The original was illuminated by a high intensity lamp L and a focusing lens between the lamp and the drum. The lamp illuminated the original in 45° direction. The distance between the photoelectric system and the drum was adjusted in such a way that the original was projected onto the aperture with a magnification of 1, thereby collecting all the light from an area 0.1 mm in diameter on to the photodiod.

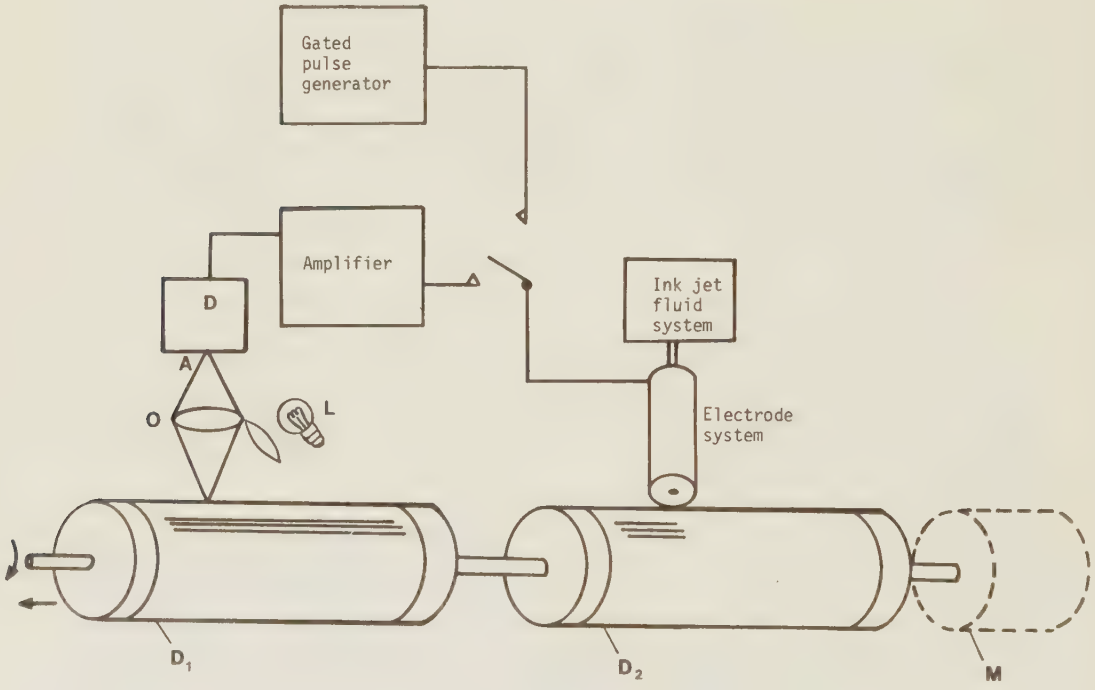

Figure 7.1. Principle of drum apparatus used for copying and test purposes.

After amplification the analog signal from the photodiode was fed to a comparator which delivered an on-off signal depending on whether the light intensity from the scanned spot was larger than a predetermined value set by a potentiometer. The electronic circuits are shown in Figure 7.2. together with the switching amplifier necessary for charging the jet during "off" periods. Adjustable hysteresis was added to the comparator in order to avoid fast oscillations when the intensity from the scanned spot slowly approached the predetermined switching value.

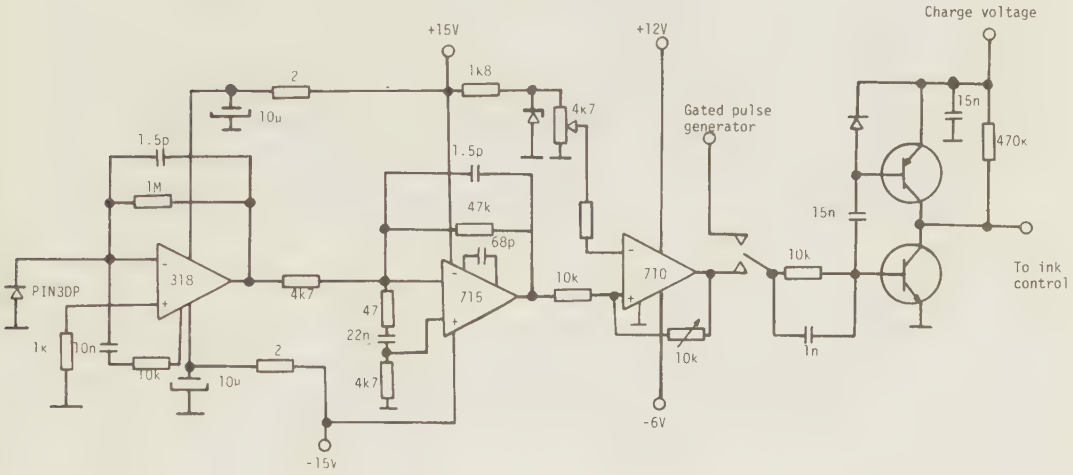

Figure 7.2. Electronic circuits used between scanner and reproducing device.

The signal from the comparator turned the ink jet on and off. Therefore no true grey shades were reproduced. Since, however, the switching speed was found to be high, an impression of grey shades was achieved as the pulse width for on-off modulation was varied due to the changing grey scale of the original. This could be adjusted by altering the hysteresis of the comparator.

When using the drum apparatus as a testing device an external pulse signal was applied to the switching amplifier instead of the signal from the scanner. The pulse generator supplying the pulses was synchronized with the mains frequency. Since the motor M was a synchronous one the pulse signals were synchronized with the drum rotation. This caused the electric pulses to produce ink jet traces parallel to the drum D_2 forming lines with a width depending on the pulse length.

The electrode system used in the investigations reported here has been described earlier by Hermanrud and Hertz (1979). Different porous materials were tested for the electrodes to prevent them from clogging when pigmented inks were used. Materials suitable for frequent use with Indian ink have, however not been found (cf. 7.2.2).

7.1.3 Results

7.1.3.1 Dependence of jet velocity

Since the copying device could be used with the compound jet as well as with conventional jets a comparison could be made. The switching from compound jet to conventional jet was achieved by switching off the peristaltic pump which supplied the secondary fluid (cf. chapter 3.2.2). The change in position of the point of drop formation when changing the secondary fluid flow was negligible (cf. chapter 6.5.1). The change in compound jet velocity due to a change in secondary fluid flow was however of greater consequence since the time of flight of the drops to the printing surface was altered. Therefore the compound jet would strike the surface at a different place compared to a conventional jet. This is shown in Figure 7.3 where an ordinary jet has printed the left part of a typewritten original and a compound jet the right part of it. The compound jet print is shifted by the distance S vertically downwards since the surface of the drum rotated upwards.

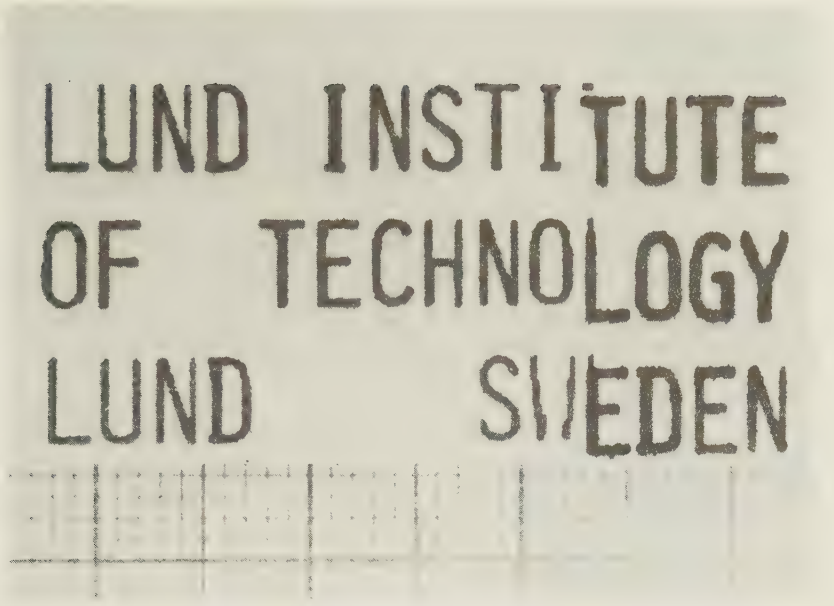

Figure 7.3. Comparison between print made with conventional (left) and compound jet (right). Primary and secondary fluid pure dye ink. Primary jet diameter 10 µm.

The vertical shift S observed on the surface caused by turning the secondary fluid on and off was measured on prints made with the drums rotating with a surface speed of 3 m/s. Afterwards the drums were manually slowly rotated. With the scanner as well as the ink jet still working a third print was made at very low speed. Now the vertical distance S' between the latter print and the ordinary jet print was measured and the quotient S'/S was calculated. Since the velocity of the drum was constant during the first two prints the quotient between the ordinary jet velocity v and the compound jet velocity v_c is

$$\frac{v}{v_c} = 1 + \frac{S}{S'} \qquad (7.1)$$

Since the surface velocity v_s of the drum and the distance z from the drop formation point to the drum surface is known we find for v:

$$v = \frac{z\, v_s}{S'} \qquad (7.2)$$

Primary jet velocities ranging from 15 m/s to 40 m/s from 10 µm and 15 µm nozzles were used with different secondary fluid flow. The changes in velocity due to addition of secondary fluid were well predicted by the formulas given in chapter 6.3.3.2.

7.1.3.2 Determination of upper frequency limit

Measurement of upper frequency limit for on-off intensity modulation of the compound jet was carried out on the testing device. A pulse generator was allowed to generate pulses of different length to control the compound jet, thereby turning the jet off and on. Since the surface velocity of the drum was known (3 m/s) the length of the recorded trace could directly be compared with the pulse length of the pulse generator. A recording showing the result obtained with a 10 µm diameter primary jet with and without secondary fluid added is reproduced in Figure 7.4. Since less ink is applied on the paper with the conventional than with the compound jet the traces from the latter have higher contrast.

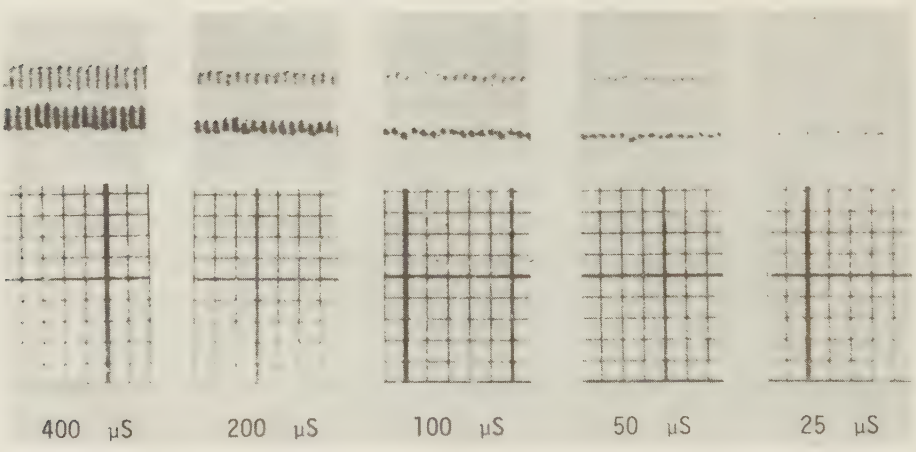

Figure 7.4. Comparison between print made with conventional (top) and compound jet (bottom). The signal source is a pulse generator. The length of the pulses used is shown under respective part of the traces. Primary and secondary fluid pure dye ink. Primary jet 10 µm.

The upper frequency limit for on-off modulation of the jet is dependent on at least six parameters which will be discussed in the following:

1. Primary jet nozzle diameter
2. Primary jet velocity (due to ink pressure)
3. Secondary fluid flow rate
4. Voltage used to charge the jet
5. Distance from point of drop formation to printing surface
6. Spontaneous or externally excited drop formation.

For conventional jets the maximum growth rate for spontaneous disturbances due to varicose instability exists when the wavelength of the disturbance is 4.51 times the diameter d of the jet (cf. chapter 1.2). Therefore the spontaneous drop frequency f is

$$f = \frac{v}{4.51\ d} \tag{7.3}$$

where v is the velocity of the jet. For a compound jet the velocity is decreased as the secondary fluid flow is increased. Assuming equal densities in the primary and secondary fluid it follows from (6.23) and (7.3)

$$f_c = \frac{v_p}{4.51\ d_p} \cdot \left(\frac{Q_p}{Q_c}\right)^2 \tag{7.4}$$

where f_c is the spontaneous drop frequency of the compound jet, v_p and d_p are the velocity and diameter of the primary jet and Q_p and Q_c the primary and secondary fluid flow.

If no external disturbance is superimposed on the compound jet and if varicose instability prevails over other instabilities, equation (7.4) determines the drop formation frequency of the compound jet. Since the quotient Q_p/Q_c is often in the range of 1/2 the drop formation frequency is reduced to one fourth of the drop formation frequency of the primary jet alone. The upper frequency limit for the jet modulation is also reduced accordingly.

The voltage used to charge the jet has influence on the maximum modulation frequency since a higher charge voltage causes the uncharged drops to merge faster. Due to this merging the minimum amount of liquid in each pulse cannot be less than about 5 original drops according to Månsson (1972).

The distance from point of drop formation to printing surface should be as short as possible since the merging of uncharged drops increases with distance. The minimum length of the necessary electrode system, however, is dependent on other parameters, i.e. jet velocity, jet diameter and charge voltage (cf. Månsson 1972). Normally an electrode system with a size appropriate for the primary jet alone was used also for the compound jet. The increase in mass to charge ratio when changing from primary jet to compound jet was found to be of no importance since the velocity of the jet was decreased at the same time.

Only spontaneous drop formation compound jet was used for printing purposes. However, it should be pointed out that increased drop formation frequency is readily obtainable with compound jets when excited by mechanical vibrations with frequencies higher than the spontaneous drop formation frequency. In scaled up experiments (75 μm primary jets) vibrations from magnetostrictive material were added to the secondary fluid, thereby providing good acoustical coupling to the compound jet. When using mechanical vibration frequencies above the spontaneous drop formation frequency a corresponding higher frequency of drop formation was achieved. The highest drop formation frequency obtained was about 30 per cent higher than the spontaneous drop formation frequency which is in agreement with the results obtained by Schneider and Hendricks (1964).

Experimental results from the testing device demonstrate good agreement with theory concerning upper modulation frequency. A 10 μm diameter primary jet with 40 m/s velocity generates together with an equal flow of secondary fluid a compound jet that disintegrates into $220 \cdot 10^3$ droplets per second according to (7.4). Since no less than 5 drops can be expected to generate a separate trace on the recording surface using spontaneous drop formation the shortest expected trace represents a 23 μs pulse.

The shortest traces actually measured under the conditions mentioned above are obtained with 25 μs pulses. Using pigmented secondary fluid results in a lower upper frequency. Common Indian ink used as secondary fluid under the conditions mentioned above produces no well defined compound jet traces shorter than 35 μs. This result can possibly be improved by the use of specially manufactured Indian ink with smaller pigment particles. Two results from the copying device using Indian ink as secondary fluid are shown in Figure 7.6.

Figure 7.5. Compound jet prints made on the copying device using common Indian ink as secondary fluid. Primary jet emerges at 40 m/s from a 10 μm diameter nozzle. Primary fluid is 20% glycerine, 80% water.

Since the quality of the recordings was found to be dependent on the quality of the recording paper a high quality baryte coated paper was used for most of the experiments. This type of paper with low ink absorption and barium sulfate coating has proved to be superior to other materials in many ink jet applications due to the higher contrast that can be attained. Using Indian ink on this type of paper a reflection density equal to 1.8 was measured. A reflection densitometer of the type McBeth QuantaLog RD-107 R was used for the density measurements.

7.2 Use of compound jet in computer controlled drafting machines

7.2.1 Introduction

Computer controlled drafting machines are used increasingly in many applications. In many cases high quality drafting at low speed with Indian ink is required. The pens used for Indian ink drawing, however, suffer from frequent clogging. Therefore the computer controlled drafting process must be continuously supervised and the benefits of automatic paper feed and computer night work are lessened since a person still has to be present. Also different line widths demand different pens and these must, therefore, be exchanged during a draft if other line widths are needed in the draft. Some drafting machines carry 3 or 4 pens for different line widths at the same time but this might still not be enough for a specific draft.

The second area of increasing use of drafting machines concerns high speed drafting. This means comparatively low quality drafting. However, this part has already become more frequent than high quality drafting (measured in machine hours) and its importance is growing as the number of applications grows. High speed drafting is used in clothing industry for pattern drafts and in many other applications. The drafting speed of the machines is, however, limited by three factors which will be discussed in the following:

1. Maximum writing velocity of the drafting pens
2. Maximum acceleration and velocity of the drafting machines
3. The time necessary to raise and lower the drafting pens with respect to the drafting surface.

The maximum writing velocity possible with conventional floating ball pens and high pressure ball point pens is about 1 m/s. The use of non-impact ink jets offers higher drafting speed and should therefore be considered when the need for higher drafting velocity makes the ball pens unsatisfactory.

Maximum acceleration of the drafting machine is important for the over all time to make a draft. Most drafts consist of short lines and small details with few long straight lines. The drafts therefore often consist of a series of accelerations and decelerations with few maximum velocity lines. Therefore the time to make a draft is highly dependent on the maximum acceleration of the drafting machine. During recent years the maximum acceleration obtained by new machines has been increased but the mechanical difficulties are large. Since, however, the need for high accelerations is due to the need for the machine to stop completely at the beginning of a line to be drafted and then again completely stop at the end of the line, the need for high accelerations would decrease if the stops could be omitted during a draft. The use of electrically on-off modulated ink jets offers the possibility to start and stop a drafted line while the printing head is continuously moving, thereby avoiding the necessity of stops. Therefore a drafting machine can be faster with an ink jet than with a pen if only the stops are omitted.

The shortest time to raise and lower the drafting pen in present machines is in the range of 1 - 3 ms. When screening or shading areas of a draft with many very short lines the total time spent moving the pen up and down during a draft amounts to a considerable portion of the total drafting time. This time spent to move the pen vertically is not necessary for non-impact ink jets. Therefore this time can be saved too when using ink jet technology.

7.2.2 Electrode systems

Different electrode systems for achieving the intensity modulation of the compound jet are used, one of which is shown in Figure 7.3. Compared to earlier constructions two new requirements were met by the new system (cf. Månsson 1972 and Smeds 1973). First of all a system for the control of a compound jet should be able to remove pigmented and fast drying ink

without clogging. Secondly a system should be easily and safely interchangeable by unskilled persons for cleaning.

The electrode system shown in Figure 7.6 is intended for vertical use only. The housing is symmetric and coaxially situated around the ink jet. The drop formation point of the jet is adjusted to lie within the entrance E at the top of the housing. The housing is conductive and kept at ground potential. During "off" periods a positive voltage is applied to the ink, thereby causing the drops formed within E to be charged and form a spray within the housing (cf. Figure 1.3). The charged spray is deflected by an electrostatic field maintained between two thread-formed electrodes, where G is kept at ground and H at positive potential. The deflected drops are collected at the internal walls of the housing or at the electrodes from which the ink drops down to the bottom of the housing. Since the bottom is formed like a fosse around the exit hole the unused ink will be collected there from which it is continuously removed through P by means of a suction pump. The uncharged drops travel through the exit hole to the recording paper.

Since no porous material is used in this electrode system it will not be clogged by pigmented ink. If it eventually clogs anyhow, it can easily be removed for cleaing and reinstalled thereafter. The removal can also be safely performed since the housing is kept at ground potential. A further benefit with this electrode system is the wind shielding properties of the housing, making the system independent of any movements of either the printing surface or the system itself. The suction through P must, however, be carefully adjusted at a low level in order not to disturb the flight of the uncharged drops inside the housing.

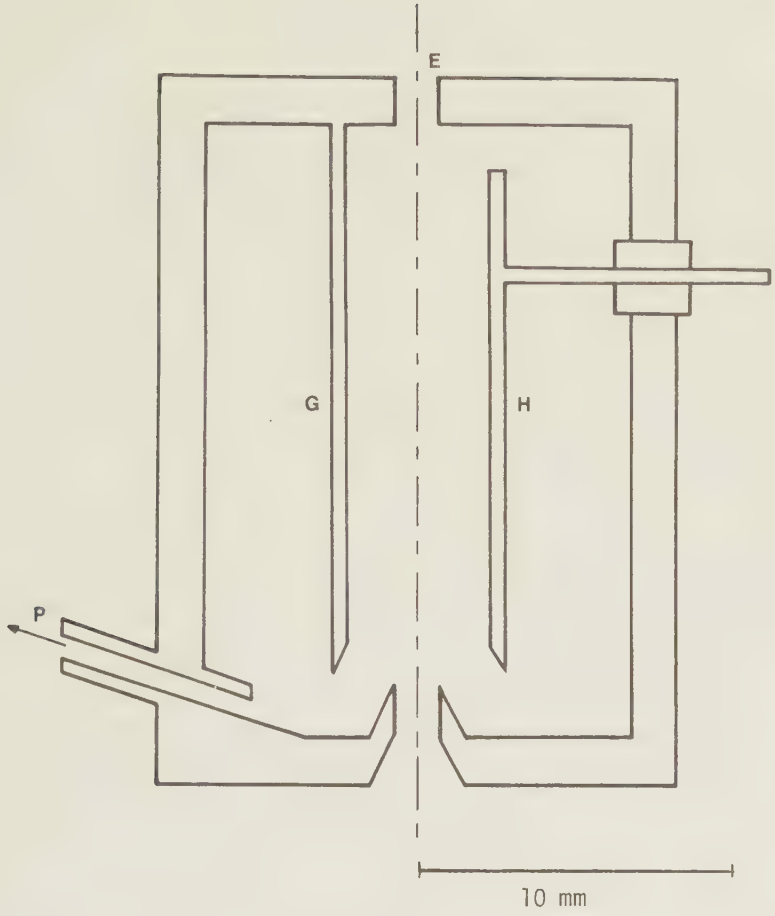

Figure 7.6. Electrode system used for intensity modulation of the compound jet.

7.2.3 Principle of controlling ink jet line width

The method most commonly used to change line width in drafting machines is changing the ink pen used. This method cannot be used in high speed drafting since such pens must work at low speed. The method for controlling ink jet line width described below can be adapted also for high speed drafting where other methods of drafting fail to attain acceptable results.

When a continually squirting ink jet in a printhead is moved along a printing surface a line is drafted. The amount of ink applied on each milli-

meter of the line is inversely proportional to the velocity of the printhead. If the printhead velocity is low the amount of ink applied per unit length of the surface will be large and the ink will spontaneously spread on both sides of the line. The spreading of the ink is depending on both the amount of ink applied and on the absorbing properties of the surface. At high speeds of the print head, less spreading will occur for similar reasons.

Since the spreading of the ink around the line is dependent on the velocity of the printhead, the line width will, therefore, vary according to changes in drafting speed. This effect is commonly observed with conventional drawing pens and ball point pens.

With the Hertz ink jet modulating system an ink jet can rapidly be switched on and off. Using a certain "on" pulse width, each pulse will squirt a certain amount of ink on the printing surface. In a continuously pulsed modulation of the ink jet the flow of ink from the printhead is proportional to the frequency of the pulses. If this frequency is chosen proportional to the velocity of the printhead the amount of ink applied per unit length of the printed line will be kept constant. Therefore, also the line width will be constant and independent of velocity variations of the printhead (Hertz and Welinder 1977).

A practical way to obtain the necessary pulses from a drafting machine is to use the distance pulses generated by the machine when the printhead moves along the x- and y-axis. The distance between the pulses depends on the resolution obtainable with the drafting machine. Normally one pulse is generated per 10 μm increment. Using electrical interpolation of these pulses, actually 4 pulses per 10 μm or one pulse per 2.5 μm are obtained with good accuracy.

From the pulses generated in the drafting machine for the x and y directions the actual distance travelled by the printhead can be calculated. Therefore pulses can be generated the number of which is proportional to the distance travelled by the printhead, e.g. 1 pulse every 100 μm. If these "distance" pulses are used to modulate the ink jet, a constant line

width trace will be obtained independent of drafting speed for the following reason.

Each ink jet "on" pulse produces a dot on the printing surface. If the distance between the dots is small enough they will form an unbroken line. Dots spaced 100 μm from each other must therefore be larger than 100 μm to form a line. Indepdent of the velocity of the printhead these dots will be placed at equal distance from each other, thus forming a line with constant line width.

Increasing the amount of ink generated by each "on" pulse causes the dots to be larger. If the distance between the dots is unaltered the line width will grow according to the increasing diameter of the dots.

The increased amount of ink in every "on" pulse can be obtained in two ways. First the duration of the pulse can be increased up to a certain limit when a new pulse must be generated since the printhead has moved to the position of the new pulse, i.e. 100 per cent duty-cycle. Secondly the flow of ink from the ink jet can be increased. This can be obtained with the compound jet since the flow of secondary fluid can easily be controlled.

Since the distance between two pulses should not be longer than the width of the line drawn, an upper limit exists for the "on" time of the ink jet depending on the maximum velocity of the printhead. For an example let us assume that the thinnest lines to be drawn are 100 μm and the maximum velocity is 0.5 m/s. This would require an "on" pulse to the ink jet each 200 μs. Now, if the pulse length of the "on" pulses was chosen to be 400 μs the jet would be in the on-mode all the time if the drafting velocity is larger than 0.25 m/s. Thus the ink delivered to the paper is no longer proportional to the velocity above this velocity limit. The shortest "on" time for the ink jet depends on how short pulses are necessary to produce a dot with 100 μm diameter. With a 10 μm capillary 50 μs "on" pulses seem adequate since shorter pulses do not produce notably smaller spots but only less contrast.

The quotient between maximum and minimum "on" time is thus 4 in the calculated example. This also represents the possible change i flow folume per millimeter. In order to increase the maximum flow volume and thus the maximum line width secondary fluid can be added to the primary jet. Since the compound to primary fluid flow ratio can be at least 3, the maximum flow of the compound jet on the line becomes 12 times the minimum flow with the primary jet alone. Therefore a combination of a change in pulse width and a change in secondary flow represents a method to easily change the line width within a large range.

If the primary and secondary fluids are identical no change in composition of the ink in the compound jet can be detected when the volume flow of secondary fluid is changed. This restricts the choice of ink to conventional types without pigments and intended for ink jet printing. If, however, pigmented inks are desired for drafting purposes the method here described can be used without changing the compound jet. In that case a pigment-free primary fluid is used. Then the primary jet alone cannot be used for drafting and the composition of the compound jet will change when the secondary fluid flow is changed.

7.2.4 Experimental apparatus and procedures

Experiments with variable line width compound jet have been performed on drafting machines. A schematic diagram is shown in Figure 7.7 and will be described in the following.

The drafting machine is equipped with a movable carrier for penholder, ink jetprinthead or other equipment. DC motors move the carrier according to signals from a control panel situated on the drafting machine or under control of the supervising host computer. The position of the carrier is detected by optical transducers and transferred to the computer. Drafting programs are generated with all details of the draft except maximum drafting speed which is set on the control panel on the drafting machine. This arrangement is necessary since different pens allow different maximum speed. Also, the same draft can be made on different paper surfaces requiring different drafting speeds.

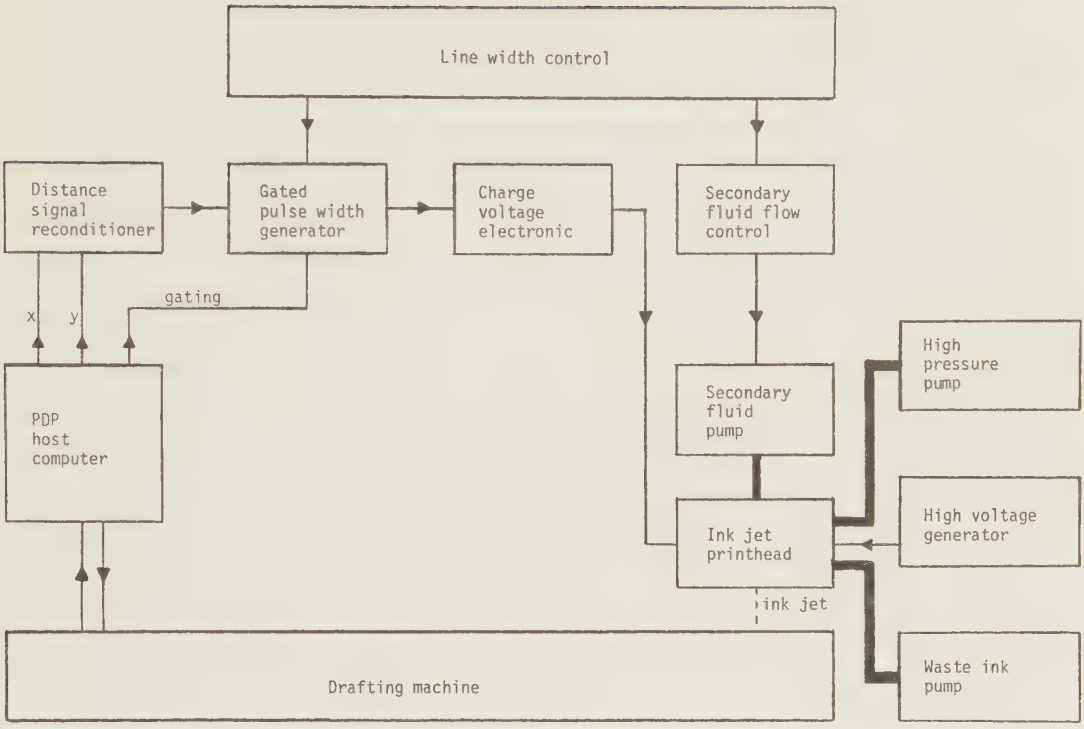

Figure 7.7. Schematic diagram showing arrangement of compound jet equipment for drafting different line widths together with necessary interface to a computer controlled drafting machine.

From the computer three signals are fetched for the ink jet control. The x and y signals delivering pulses at 2.5 μm increment movement of the carrier and a gating signal telling if the actual movement of the carrier shall be drafted or if the movement is a transportation of the carrier to the starting point of a new line. The x and y signals are reconditioned

to generate a distance pulse at appropriate increments. This increment can be chosen and is 170 µs in the results demonstrated below if not otherwise mentioned. The distance pulse triggers the "on" pulse for the ink jet. The pulse width of the "on" pulse determines how long the ink jet will apply ink on each spot along the drafted line and is controlled by the line width control. The pulse width generator is gated by the host computer to keep the ink from the printing surface during carrier transportation when the "on" pulses are still generated but no line is expected. The charging voltage electronics generates charging voltage to the ink during "off" periods and ground voltage during "on" pulses, thereby allowing the ink to pass the electrode system in the ink jet printhead and hit the printing surface. When larger ink flow is desired in order to produce broader lines the secondary fluid flow is started and increased (cf. 7.2.2).

The flow from the secondary fluid pump is determined by the secondary fluid flow control. This pump is situated together with the ink jet printhead on the carrier of the drafting machine. The ink jet printhead consists of a capillary holder with compound jet assembly and electrode system arranged vertically in a row and adjusted to let the ink jet pass through the electrode system to the paper when the jet is not charged. The primary fluid is supplied to the capillary from a high pressure pump situated besides the drafting machine. A high voltage generator delivers positive high voltage for the deflection field inside the electrode system. A suction ink pump removes the deflected ink from the electrode system through a soft tubing into a waste ink container.

Since the printhead and the secondary fluid pump are situated on the carrier of the drafting machine at some distance from the primary fluid pump, control electronics and other equipment, the tubings and cables used have a length of about 3 m. No problems were experienced with this arrangement.

The drafting experiments were carried out under software control. A drafting program was loaded into the computer and run, thereby producing an ink jet or pen draft on the drafting machine, depending on which de-

vice was mounted on the carrier. Several drafts of the same figure were made with different settings of the signal conditioner, the gated pulse width generator, or the secondary fluid flow control for comparison of different pens and ink jet parameters. Also different maximum velocity settings on the drafting machine were tested. Further, different ink formulas were studied as well as additives to the ink in various concentrations. Finally, several drafting surfaces were used with ink jets and compared with draftings made with Indian ink pens and ball point pens.

7.2.5 Results

Since no drafting machine capable of higher drafting speed than 24 m/min = = 0.4 m/s was available for test purposes, no drafts of higher velocity could be made. It should, however, be pointed out that velocities up to at least 3 m/s present no ink jet problems other than those encountered at lower speed.

The ability of ink jets to draft lines with constant linewidth independent of velocity is demonstrated in Figure 7.8. A 10 μm primary jet alone is producing a line consisting of spots at 170 μm distance from each other. The jet is issuing ink 200 μs at each spot. The velocity ranges from zero in the corners of the figure to 24 m/min. The different maximum velocities are noted in the figure. The linewidth is constantly kept at 0.25 mm. Some ink spatter is observed around the drafted line. The soluble dye black ink used was manufactured by Pelikan for experimental purposes only.

Different linewidths produced by a primary jet alone and compound jets are demonstrated in Figure 7.9. The thinnest line in this experiment is about 0.2 mm generated from a primary jet alone pulsated with 50 μs at 170 μm interval. The broadest line is about 0.6 mm generated by a compound jet with 240 μs at 170 μm interval. In other experiments line widths down to 0.15 mm and up to 0.8 mm are obtained due to other surfaces and/or inks used. The black ink used is the same as the experimental one shown in Figure 7.8.

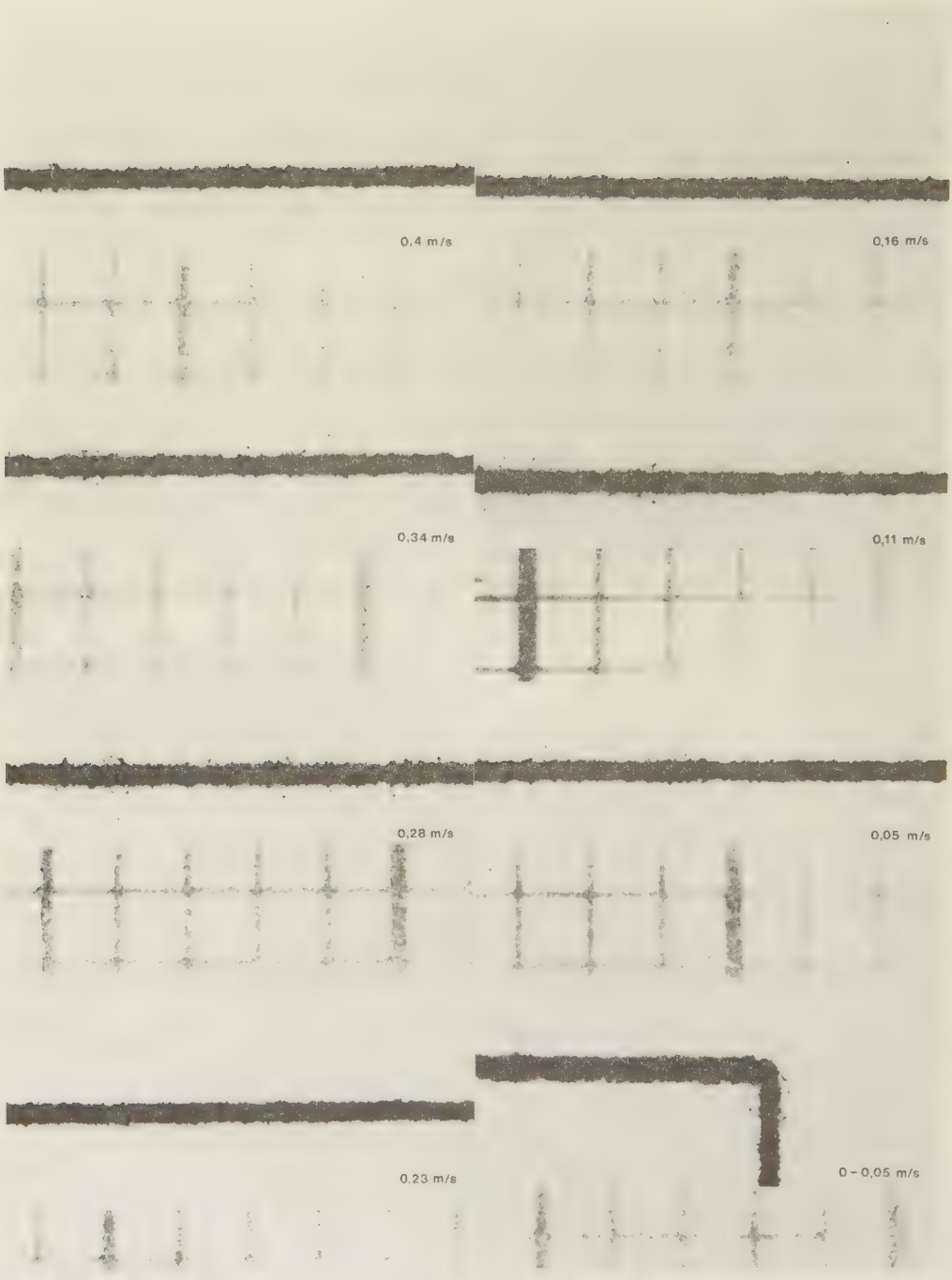

Figure 7.8. Ink jet drafts showing constant linewidth independent of drafting velocity. 10 µm jet pulsed 200 µs at 170 µm increments. For comparison between photographed millimeter paper and original, see attached leaf at the end of this report.

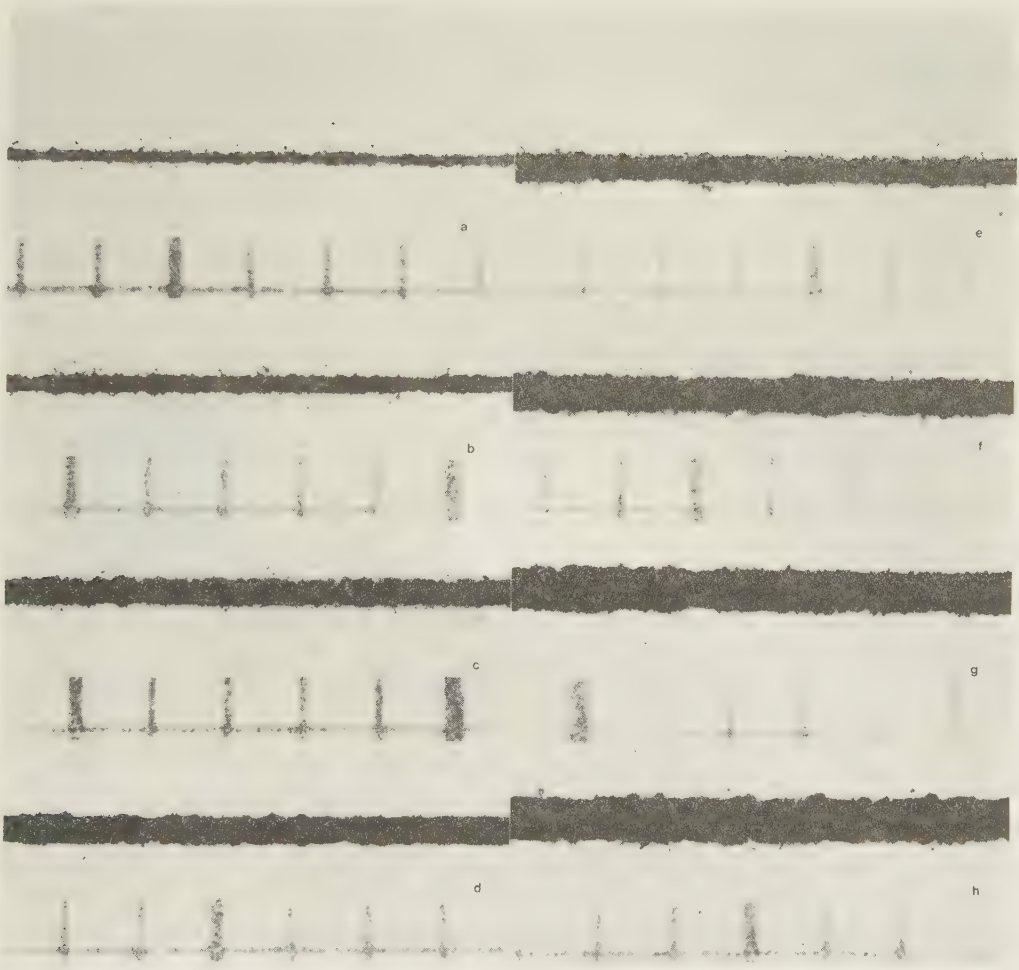

Figure 7.9. In jet drafts showing different linewidths due to different ink flow. In Figure 7.9.a - - 8.9.d only the 10 µm primary jet was used. Figure 7.9.e - 7.9.h were produced by compound jets having different secondary fluid flow.

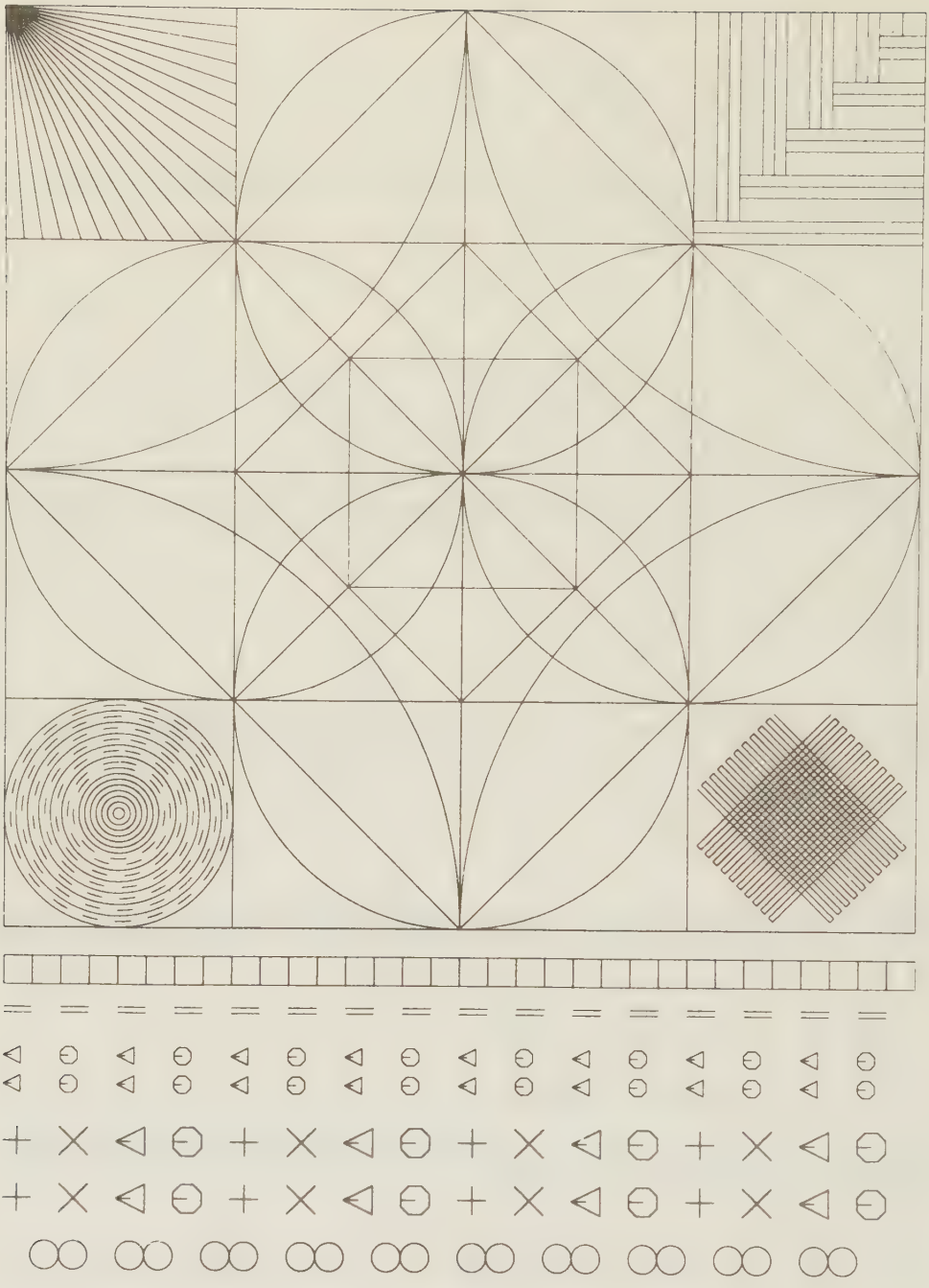

Figure 7.10. Pattern used for test drafts. Actual size of the draft is 220 x 160 mm.

Many types of ink usable for ink jet printing were tested. The test draft used to compare different inks and surfaces is shown in Figure 7.10. Since the details of the drafts have to be studied in order to compare contrast, linewidth and bordersharpness, enlargements of the lines will be demonstrated below.

Enlarged pictures showing details of 6 different drafts made with different inks are demonstrated in Figure 7.11. Ordinary thin drawing paper is used as printing surface. The width of the lines photographed is about 0.3 mm. Each dot is separated 100 µm from the next and produced by 300 µs "on" pulses controlling a 10 µm jet.

For comparison Figure 7.12 was prepared. Lines drafted with ink jet on high quality baryte coated paper are shown. Ink jets from Pelikan, Koh-I-Noor and Siemens-Elema inks are used as well as Indian ink pens and ball point pens.

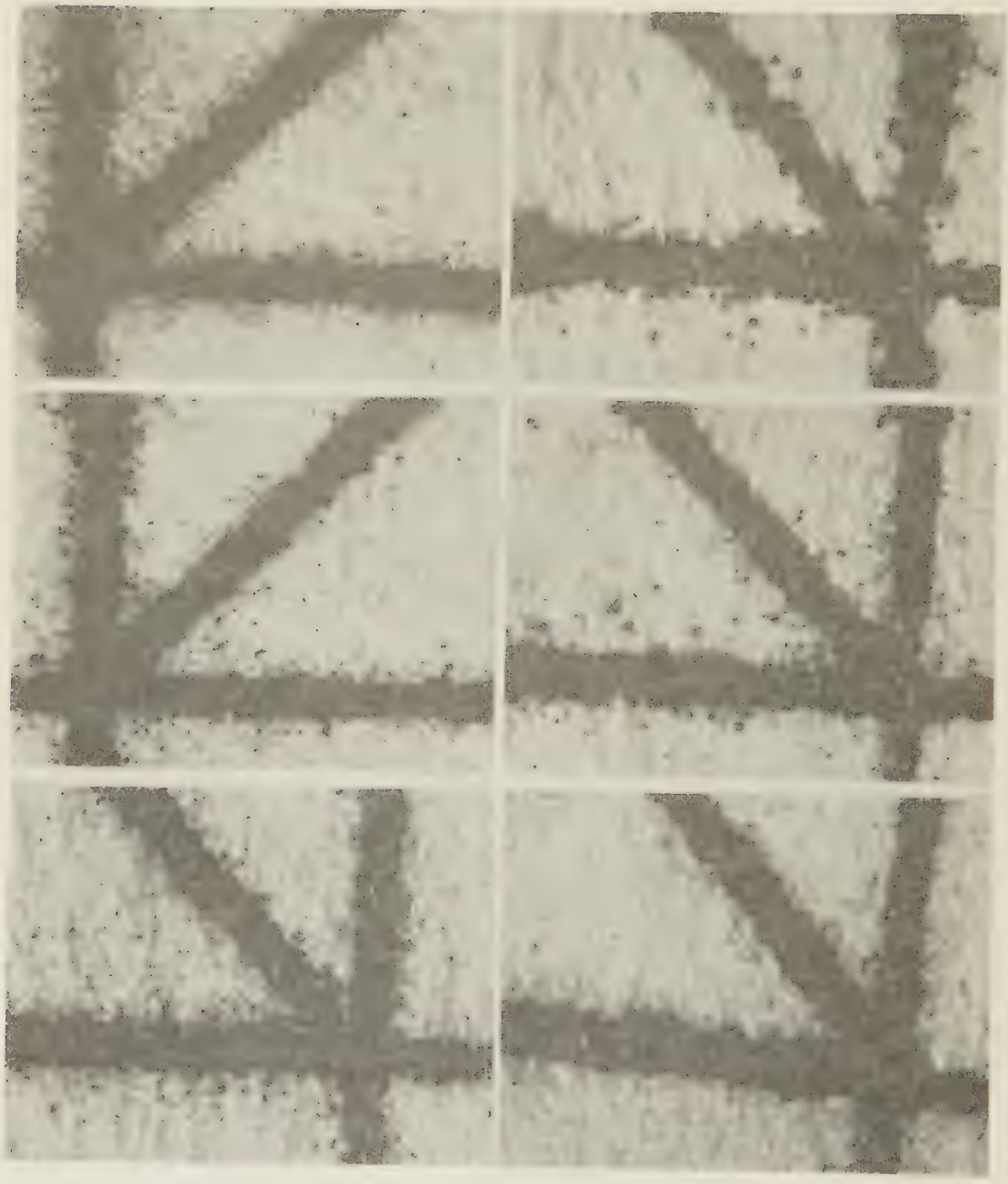

Figure 7.11. Details of test drafts produced with different Pelikan experimental inks. A 10 µm ink jet was used on ordinary drawing paper in all drafts shown.

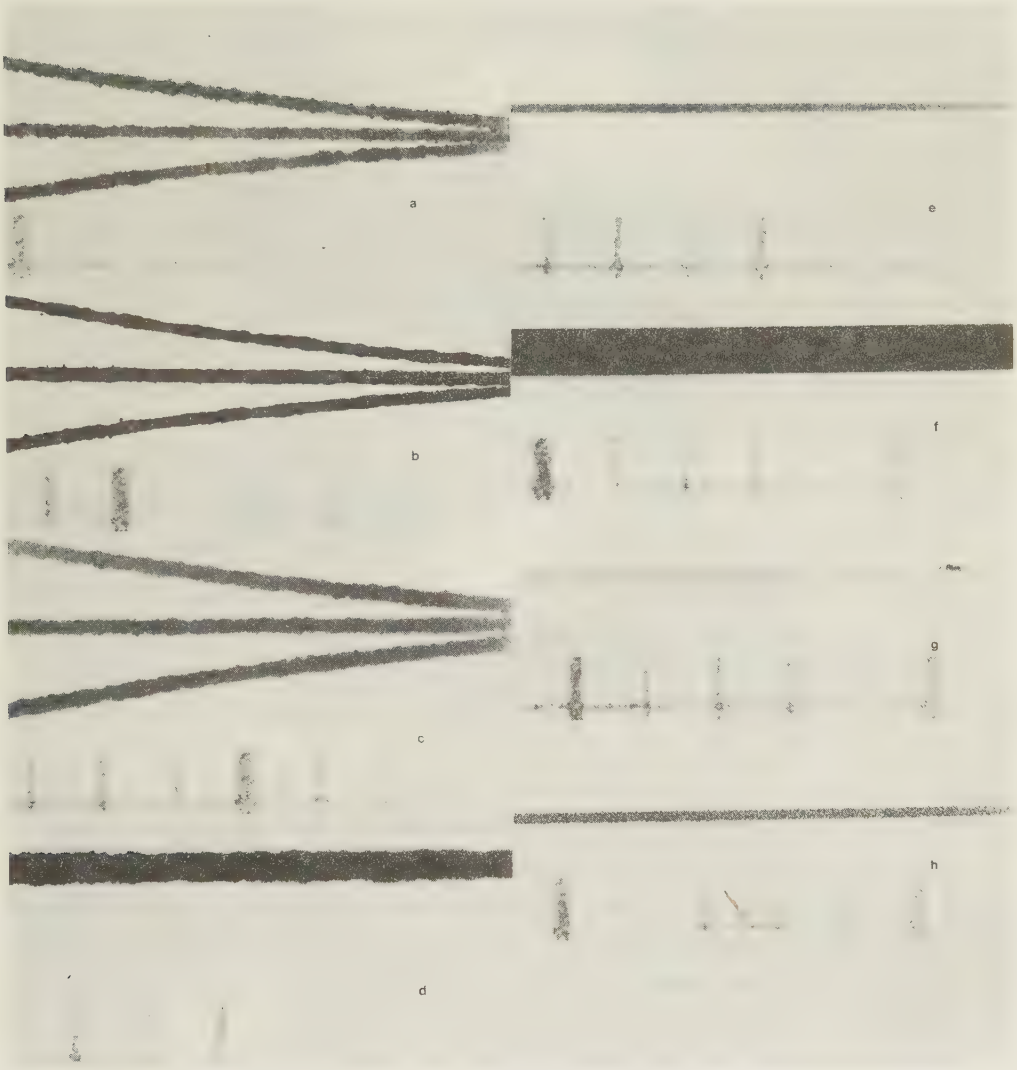

Figure 7.12. Lines drawn with different techniques reproduced with the same enlargement. 7.12.a - 7.12.d show ink jet lines on high

quality baryte coated paper, 7.12.e - 7.12.h show pen drawn lines on high quality "Cronaflex" drafting paper.

7.12.a.	Black Pelikan experimental ink 30.1. Primary jet only.
7.12.b.	Black Koh-I-Noor plotting ink (diluted). - " -
7.12.c.	Blue Siemens-Elema ink.
7.12.d.	Black Pelikan experimental ink 30.1. Compound jet.
7.12.e.	Indian ink pen (0.13 mm).
7.12.f.	Indian ink pen (0.6 mm).
7.12.g.	Ball point pen.
7.12.h.	Gas filled ball point pen.

7.2.6 Spatter reducing technique

The viscoelastic properties of long polyethylene oxide molecules (Polyox) can be beneficial in many ways. The drag reducing effect in turbulent flow as well as the stabilizing effect in unstable flow is well known (Landahl 1972, Bark 1978). The viscoelastic property can, however, be used to reduce ink jet spatter as well.

When ink jet drops at high speed hit the printing surface they are almost immediately absorbed into the material. If, however, further drops hit the same spot before the first drop is sucked away the drops will hit a wet surface, thereby causing splashing of small drops to the neighbourhood. This is almost always the case with ink jets and causes reduced quality in the drawn line, since spattered drops appear along and close to the line (cf. Figure 7.11).

The addition of Polyox in low concentrations to the ink does not reduce the formation of small drops when an ink drop hits on the previous one already deposited on the paper surface. However, shortly after the generation of these small drops they are still connected to the main drop by threads of fluid, which have to rupture before the small drops can leave the paper (are free). If this rupture is prevented by the elastic properties of the ink due to the addition of Polyox, the small drops are not able to leave the paper surface. Instead they are pulled back into the main drop of ink on the paper (Bark 1978). Therefore no traces of small drops are visible on both sides of the drafted line. This effect is demonstrated in Figure 7.13 where a comparison is made with a 10 μm diameter ink jet with and without Polyox addition to the ink.

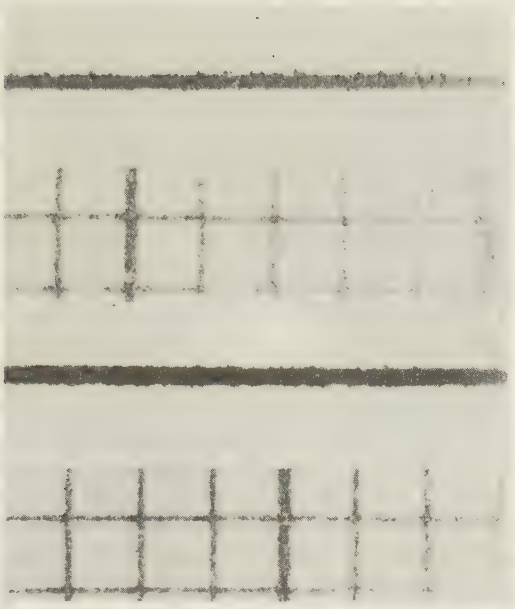

Figure 7.13. Ink jet drafted lines. Blue Siemens-Elema ink without (top) and with 0.01% addition of Polyox with MW = $4 \cdot 10^6$. 10 µm diameter jet pulsed 250 µs at 170 µm increment. Linewidth is 0.25 mm.

Increasing concentration of Polyox causes the distance to the point of drop formation to increase as well, thereby causing the switching properties of intensity modulating systems to deteriorate (cf. 5.4.3). If, however, the switching speed is of minor importance only, higher concentrations can be utilized, thereby completely avoiding ink mist and spatter.

ACKNOWLEDGEMENTS

I wish to express my sincere gratitude to professor Hellmuth Hertz, Head of the Department of Electrical Measurements, Lund Institute of Technology, for initiating this study as well as for his stimulating guidance throughout the work. His helpful direction and support have been invaluable during my years at his Department.

The keen interest in my work shown by all colleagues has created an inspiring atmosphere at the Department and I especially wish to thank Dr. Lennart Grahm for his goodhearted criticism. The assistance given by Mr. Lennart Nilsson and his collaborators in the workshop has made the experiments possible and is very much appreciated. Further, the concern shown by Mr. Gunnar Tilly in helping me with the photographs as well as with laboratory equipment is thankfully acknowledged.

I am also greatly indebted to Mrs. Anita Borné and Mrs. Elly Schlyter for preparing the drafts.

Finally I wish to thank Mrs. Margaret Jansson for typing and retyping the manuscript and for her ever encouraging enthusiasm.

REFERENCES

Andrade, E.N. and Tsien, L.C. (1937) Proc. Phys. Soc. Lond., Vol. 49, 381.

Bark, F.H. (1978) Svensk papperstidning, Vol. 81, 367.

Batchelor, G.K. (1973) An Introduction to Fluid Dynamics, Cambridge University Press.

Batchelor, G.K. and Gill, A.E. (1962) J. Fluid Mech., Vol. 14, 529.

Bergmann, L. and Schaefer, Cl. (1965) Lehrbuch der Experimentalphysik I, Walter de Gruyter & Co.

Bruce, C.A. (1976) IBM J. Res. Develop. May 1976, 258.

Brun, R.F. and Leinhard, J.H. (1968) Behavior of Free Laminar Jets Leaving Poiseuille Tubes, ASME paper 68-FE-44.

Chaudhary, K.C. and Redekopp, L.G. (1980) J. Fluid Mech., Vol. 96:2, 257.

Davies, J.T. (1963) Interfacial Phenomena, Academic Press.

Eisenklam, P. and Hooper, P.C. (1958) Min. of Supply D66W Rept. EMR/58/JRL/42.

Filipsson, L.G.R., Lagerstedt, J.H.T. and Bark, F.H. (1977/78) J. Non-Newtonian Fluid Mech., Vol. 3, 97.

Haenlein, A. (1932) NACA Tech. Memo No. 659.

Hermanrud, B. and Hertz, C.H. (1979) J. Appl. Photogr. Eng., Vol. 5, 220.

Hertz, C.H. and Månsson, Å. (1972) Rev. Sci. Instr., Vol. 43, 413.

Hertz, C.H. and Welinder, J.B. (1977) U.S.patent 4.050.075.

Hertz, C.H. et al. (1967) Acta Univ. Lundensis, Sec. II, Vol. 15, 1.

Hoyt, J.W. et al. (1974) J. Fluid Mech., Vol. 63, 635.

Joos, G. (1964) Lehrbuch der Theoretischen Physik, Geest & Portig, Leipzig, 558.

Kamphoefner, F.J. (1972) IEEE Trans. Electron. Dev., Vol. ED-19, 584.

Landahl, M.T. (1972) Proc. of Thirteenth Int. Congr. of Theor. and Appl. Mech., Moscow, Springer Verlag, 177.

Landau, L.D. and Lifschitz, E.M. (1959) Fluid Mechanics, Pergamon Press, 86.

Lennox, S.C. and Pack, D.C. (1962) J. Fluid Mech., Vol. 33:2, 513.

Lessen, M. and Singh, P.J. (1973) J. Fluid Mech., Vol. 60, 433.

McCarthy, M.J. and Molloy, N.A. (1974) Chem. Eng. J., Vol. 7, 1.

McNaughton, K.J. and Sinclair, C.G. (1966) J. Fluid Mech., Vol. 25, 367.

Månsson, A. (1972) Electric Control of Fluid Jets, Theory and Application to Image Generation, Report 1/1972, Dept El. Measurem., Lund Institute of Technology.

Phinney, R.E. (1973) J. Fluid Mech., Vol. 60, 689.

Plateau (1856) Phil. Mag., Vol. 12, 286.

Prandtl, L. and Tietjens, O.G. (1934) Applied Hydro- and Aeromechanics, McGraw-Hill.

Reynolds, A.J. (1962) J. Fluid Mech., Vol. 14, 552.

Rayleigh, J.W.S. (1878) Proc. London Math. Soc., Vol. 10, 4.

Rayleigh, J.W.S. (1892) Phil. Mag., Vol. 34, 145.

Savart (1833) Ann. Chim. Phys., Vol. 53, 337.

Schlichting, H. (1968) Boundary-Layer Theory, McGraw-Hill.

Schlichting, L. (1933) Z. f. angew. Math. u. Mech., Vol. 13, 260.

Schneider, J.M. and Hendricks, C.D. (1964) Rev. Scient. Instr., Vol. 35, 1349.

Smeds, B. (1973) Bit, vol. 13, No. 2, 181.

Stemme, E. et al. (1973) IEEE Trans. Electron Dev., Vol. ED-20, January 1973, 14.

Sweet, R.G. (1964) High-Frequency Oscillography with Electrostatically Deflected Ink Jets, Technical Report No. 1722-1, Stanford Electronics Laboratories, Stanford University.

Sweet, R.G. (1965) Rev. Sci. Instr. 36, 131.

Tollmien, W. (1926) Z. f. angew. Match. u. Mech., Vol. 6, 468.

Tomotika, W. (1935) Proc. Roy. Soc., Vol. A 150, 322.

Weber, C. (1931) Z. f. angew.Math.u. Mech., Vol. 11:2, 136.

Winston, C.R. (1962) "Method and apparatus for transferring ink", U.S. patent 3.060.429.